

Climatic and glacial impact on erosion patterns and sediment provenance in the Himalayan rain shadow, Zanskar River, NW India

Tara N. Jonell^{1*}, Andrew Carter², Philipp Böning³, Katharina Pahnke³, and Peter D. Clift^{1,4},

¹*Department of Geology and Geophysics, Louisiana State University, Baton Rouge, LA 70803, USA*

²*Department of Earth and Planetary Sciences, Birkbeck College, London, WC1E 7HX, United Kingdom*

³*Max Planck Research Group for Marine Isotope Geochemistry, Institute for Chemistry and Biology of the Marine Environment (ICBM), University of Oldenburg, 26129 Oldenburg, Germany*

⁴*School of Geography Science, Nanjing Normal University, Nanjing 210023, China*

ABSTRACT

Erosion is a key step in the destruction and recycling of the continental crust yet its primary drivers continue to be debated. The relative balance between climatic and solid Earth

forces in determining erosion patterns and rates, and in turn orogenic architecture, is unresolved. The monsoon-dominated frontal Himalaya is a classic example of how surface processes may drive focused denudation and potentially control structural evolution. We investigate whether there is a clear relationship between climate and erosion in the drier Himalayan rain shadow of northwest India where a coupled climate-erosion relationship is less clear. We present a new integrated dataset combining bulk petrography, geomorphometric analysis, detrital U-Pb zircon geochronology, and bulk Nd and Sr isotope geochemistry from modern river sediments that provides constraints on spatial patterns of sediment production and transport in the Zanskar River. Zanskar River sands are dominated by Greater Himalayan detritus sourced from the glaciated Stod River catchment that represents only 13% of the total basin area. Prevalent zircon peaks from the Cambro-Ordovician (440–500 Ma) and Mississippian-Permian (245–380 Ma) indicate more abundant pre-Himalayan granitoids in the northwest Himalaya than in the central and eastern Himalaya. Erosion from the widely-exposed Tethyan Himalaya, however, appears modest. Spatial patterns of erosion do not correlate with highest channel steepness. Our data demonstrate that Zanskar differs from the monsoon-soaked frontal Himalaya and the arid, extremely slow-eroding orogenic interior in that focused erosion and sediment production are driven by glaciers. Subsequent remobilization of glacially-derived sediments is likely controlled by monsoonal rainfall and we suggest sediment reworking plays an important role. These data support strong climatic control on modern orogenic erosion on the periphery of the Himalayan rain shadow.

INTRODUCTION

The growth and destruction of orogenic systems are governed by the distribution and pace of tectonically driven rock uplift and surface processes. Solid Earth and climatic forces together facilitate denudation that in turn regulates the flux and composition of sediments recycled through rivers to the oceans. How the magnitude of these forces and their resultant erosion shape orogens is debated. Many studies argue for strongly linked climate-precipitation and focused erosion (e.g., Beaumont et al., 2001; Clift et al., 2008; Hodges et al., 2004; Kirby and Ouimet, 2011; Thiede et al., 2004) while others favor a decisive solid Earth control (Burbank et al., 2003; Wallis et al., 2016). Constraining the roles of these processes is crucial in quantifying how sedimentation reflects tectonic and climatic conditions. If we are to relate exhumation and paleoenvironmental histories from long denuded mountain belts then analysis of the sedimentary record provides the only method to reconstruct these processes in relative continuity over long periods of geologic time.

The dramatic topographic and climatic gradients of the Himalaya-Tibetan orogen provide the opportunity to assess the interdependency between tectonics, climate, and surface processes. Intense summer monsoonal rainfall on the southern flank of the Himalaya produces extreme erosion, steep topographic relief (Bookhagen and Burbank, 2006; Bookhagen et al., 2005b; Gabet et al., 2008) and some of the highest riverine fluxes of sediment to the ocean (Milliman and Meade, 1983). Erosion patterns in river basins across the wet, frontal Himalaya, like the Marsyandi (e.g., Attal and Lavé, 2006; Garzanti et al., 2007), Sutlej (Bookhagen and Burbank, 2006), and Alaknanda Rivers (Srivastava et al., 2008) tightly correlate with the distribution and intensity of monsoon precipitation (Fig. 1). Moreover, focused erosion on the Himalayan front has been proposed to control the distribution of deep exhumation and tectonic strain (e.g., Beaumont et al., 2001; Thiede et al., 2004).

How erosion is facilitated by climatic processes is less clear farther north in the Himalayan rain shadow, where high topography impedes northward advection of monsoonal moisture onto the Tibetan Plateau. Arid regions north of the Indus River in Ladakh and the Karakorum show exhumation rates scale with tectonically generated topography and glacial cover rather than with precipitation as found along the Himalayan front (Dortch et al., 2011a; Munack et al., 2014; Wallis et al., 2016). Despite this apparent lack of correlation between precipitation and erosion, some observations suggest the Himalayan rain shadow may be especially sensitive to climatic perturbations. Intense summer rainstorms have resulted in modern day examples of extreme erosion (i.e., (Hobley et al., 2012) and suggest that volumetrically large sediment signals (>60% total flux) can be produced by only a few events (Bookhagen et al., 2005a; Wulf et al., 2010; Wulf et al., 2012). However, whether this is geologically important was questioned by Munack et al. (2014) who showed that the long-term denudation derived from ^{10}Be cosmogenic isotopes is consistent amongst samples both before and after the intensive climatic events of the summer 2010 in Ladakh.

Here we examine whether precipitation, glaciation, or rock uplift dominate in controlling modern erosion on the western margin of the Tibetan Plateau in the Zanskar River basin. This river is ideally situated for evaluating coupling between climate and erosion because it is the largest river basin in the Himalayan rain shadow draining the High Himalaya towards the north, directly into the trunk Indus River. Our investigation sets out to quantify sediment provenance in the Zanskar River basin to establish the modern relative spatial distributions of erosion, or erosion patterns. We further explore whether climate modulates sediment production and transport in the rain shadow as it does in the frontal ranges, or if present-day erosion instead reflects strong, underlying tectonic control.

BACKGROUND

Climatic and Geographic Setting

The Zanskar River basin lies directly north of the Himalayan topographic divide on the southern edge of the Tibetan Plateau and occupies a modern drainage area of 14,939 km² (Fig. 1). All material sourced from the Zanskar River basin transmits to the Indus River, the main river system routing water and sediment from the western Himalaya into the Arabian Sea for roughly the last ~45 m.y. (Clift et al., 2001). The broader Zanskar River basin can be subdivided into five catchments of the main tributaries: the Tsarap, Stod, Khurna, Markha, and Oma Rivers (Fig. 1C).

Glaciers occupy 8% of the Zanskar River basin, with some glacial tongues extending as low as ~4100 m (Owen, 2011; Taylor and Mitchell, 2000). Recessional and terminal moraines are preserved throughout Zanskar. Although glaciers were not much more widespread at the Last Glacial Maximum (~20 ka), older glaciations were quite extensive (Dortch et al., 2011a; Dortch et al., 2013; Hedrick et al., 2011; Owen et al., 2005). One terminal moraine dated to ~78 ka extended as low as ~3400 m to create the Padum Basin, which is a key confluence within the Zanskar catchment (Owen et al., 2002; Taylor and Mitchell, 2000).

Precipitation is delivered by the Summer Monsoon and Winter Western Disturbances (Westerlies) as rainfall in the summer (Jun–Aug) and snowfall in the winter, respectively (Owen and Benn, 2005). Dramatic attenuation of monsoonal precipitation across the topographic barrier of the High Himalaya produces a rain shadow to the north in the orogenic interior (Fig. 2). Likewise, a gradient is observed for Westerly-derived precipitation that decreases considerably to the southeast across this region (Leipe et al., 2014). Sutlej River basin weather station and hydrologic modelling data imply that 30–50% of the total annual precipitation to upper Indus

River tributaries is received as winter snowfall, and contributes as much as ~66% of the total yearly discharge as snow or glacial meltwater (Bookhagen and Burbank, 2010; Burbank et al., 2012).

Modern erosion rates in the frontal Himalaya are tightly coupled with monsoonal rainfall and discharge (e.g., Bookhagen, 2010; Gabet et al., 2008; Goodbred, 2003). Overall annual sediment fluxes from arid rain shadow regions, like the drier upper drainages of the Indus, Sutlej, and Marsyandi River basins (Fig. 1B), are lower because of lower runoff. In the upper Marsyandi and Sutlej Rivers, highest suspended sediment yields occur during late summer when temperatures are highest rather than at the onset of monsoon season (Burbank et al., 2012; Wulf et al., 2012). This suggests that subglacial drainage channels provide the initial flux, with progressively increasing contributions from hillslopes and river channels as summer monsoon rainfall arrives (e.g., Bookhagen and Burbank, 2010). Despite lower annual precipitation, high intensity monsoonal rainstorms can produce extreme erosion and, in only a few events, produce 30–50% of the total annual sediment flux in semi-arid to arid regions (Wulf et al., 2010; Wulf et al., 2012). These observations suggest, that at least under modern day climatic conditions, regions directly adjacent to the present rainfall maxima shadow potentially produce disproportionate sediment signals during such events (Bookhagen, 2010).

Geologic Setting

Basement rocks exposed in Zanskar can be divided into three lithotectonic groups: (1) the Tethyan Sedimentary Sequence, or Tethyan Himalaya; (2) the High Himalayan Crystalline Sequence, or Greater Himalaya; and (3) the Indus Suture Zone (Fig. 3). Exposures of these groups are structurally controlled by orogen parallel structures related to SW-verging thrust

nappes and the Zanskar Shear Zone (ZSZ) (Dèzes et al., 1999). The ZSZ represents a ~150 km long strand of the South Tibetan Detachment (Herren, 1987), the major tectonic boundary that separates the Greater and Tethyan Himalaya in this part of the orogen (Burchfiel et al., 1992; Burchfiel and Royden, 1985).

The Tethyan Himalaya is a package of Neoproterozoic to early Paleocene sandstones, limestones, dolostones, and shales classically considered to have been deposited as a passive margin sequence on the northern margin of Greater India (Gaetani et al., 1986; Gaetani et al., 1983; Garzanti et al., 1986; Green et al., 2008). Tethyan Himalayan rocks are very low- to low-grade metasedimentary rocks, although parallel to the ZSZ and Nyimaling-Tso Morari gneiss dome Neoproterozoic-Ordovician formations locally reach lower amphibolite facies (e.g., Dèzes et al., 1999; Fuchs, 1987; Gaetani et al., 1986; Steck, 1993).

Paleozoic magmatism produced two igneous suites observed in the Zanskar region: (1) Pan-African Cambro-Ordovician granitic plutons and (2) Mississippian-Permian granitic plutons associated with Panjal Traps flood basalts. U-Pb zircon ages constrain Pan-African (or Bhimphedian) Orogeny plutonism from ~435 to ~483 Ma (Cawood et al., 2007; Girard and Bussy, 1999; Godin, 2001; Horton and Leech, 2013; Noble and Searle, 1995; Pognante et al., 1990). Later Gondwanan rifting produced isolated granitic plutons dating 268–305 Ma (Horton and Leech, 2013; Noble et al., 2001; Spring et al., 1993) as well as Panjal Traps flood basalts at ~289 Ma (Shellnutt et al., 2011; Shellnutt et al., 2014; Singh et al., 1976).

Structurally below the Tethyan Himalaya and forming the core of the High Himalaya in Zanskar are the exhumed high-grade equivalents of the Neoproterozoic-Ordovician Tethyan Himalaya and late Paleozoic granitic intrusions, collectively referred to as the Greater Himalaya (Dèzes et al., 1999; Honegger, 1983; Horton and Leech, 2013; Pognante et al., 1990; Pognante

and Lombardo, 1989; Schlup et al., 2003; Schlup et al., 2011; Searle et al., 1992; Walker et al., 2001). The Greater Himalaya in Zanskar consists of amphibolite to lower granulite facies Neoproterozoic-early Cambrian paragneiss and metapelitic (Herren, 1987), Cambro-Ordovician orthogneiss (Frank et al., 1977; Horton et al., 2015; Mehta, 1977; Noble and Searle, 1995; Pognante et al., 1990; Stutz and Thöni, 1987; Walker et al., 1999) and Mississippian-Permian orthogneiss (Honegger et al., 1982; Horton and Leech, 2013; Noble et al., 2001; Spring et al., 1993).

Rapid exhumation of the Greater Himalaya between the Main Central Thrust (MCT) and ZSZ from 26 Ma (Robyr et al., 2006) to ~17 Ma (Leloup et al., 2010) induced partial melting and injection of leucogranitic melts into the Greater and lower Tethyan Himalayan series (Dèzes et al., 1999; Noble and Searle, 1995; Robyr et al., 2006). Exhumation of Greater Himalayan material continued until ~16 Ma in the south of Zanskar to ~8 Ma around the Nyimaling-Tso Morari gneiss dome (Schlup et al., 2003; Schlup et al., 2011). No significant neotectonic activity in the Zanskar region is observed (Jade et al., 2010).

Sedimentation related to the collision of Greater India and Eurasia is documented in the third lithotectonic group, the Indus Suture Zone (e.g., Searle, 1983; Searle et al., 1990). Thrust slices of ophiolitic mélange, Indus Molasse sandstones, and Cretaceous-Eocene forearc basin strata are exposed near the Zanskar-Indus confluence (Clift et al., 2002a; Henderson et al., 2010; Pedersen et al., 2001; Searle et al., 1990).

METHODS

We use several complementary methods to constrain the provenance of modern sediment in the Zanskar River and understand how bulk sediment compositions evolve downstream before

reaching the Indus River confluence. Sediment samples from the Zanskar River and its major tributaries were collected from 2012 to 2014 during monsoon seasons from active channel beds and point bars (Table 1). We preferentially sampled very fine- to medium sand ($>63 \mu\text{m}$) because this size fraction is commonly targeted for single-grain mineral provenance techniques that often limit evaluation of finer grain sizes owing to analytical spot size. By only targeting the bedload we cannot consider how suspended load contributes to provenance and this introduce biases to our analyses (Garzanti et al., 2011; Garzanti et al., 2009). However, we argue that our selected size fraction can be considered representative of the bulk zircon provenance (Yang et al., 2012) and provide important initial constraints on patterns of erosion in the Zanskar River basin.

Basin Morphology

We evaluated basin-wide and river channel morphology by extracting topographic parameters and longitudinal river profile data from digital elevation models. Topographic parameters were generated from the void-filled Shuttle Radar Topography Mission (SRTM) V4 90-m digital elevation model (Jarvis et al., 2008) provided by the Consultative Group on International Agricultural Research (<http://srtm.csi.cgiar.org>) and post-processed with an iterative fill routine (Whipple et al., 2007). Slope values were calculated using a 1 km-radius circular moving window. Local relief, expressed as maximum elevation difference, was calculated using a 5 km-radius circular moving window. Mean annual rainfall values were generated from the 1998–2009 Tropical Rainfall Measuring Mission (TRMM) 2B31 and 2B42 data products for the Himalaya (Bookhagen and Burbank, 2010). Extent of modern glaciers in the Zanskar River basin were derived from the Global Land Ice Measurements from Space (GLIMS) Version 1 data (Shrestha et al., 2014).

Longitudinal river profiles were generated from digital elevation model (DEM) and smoothed every 2 km to remove elevation spikes. Under topographic steady-state, local channel slopes (S) follow a simple power-law scaling relationship with upstream drainage area (A):

$$k_s = S/A^{-\theta} \quad (1)$$

where k_s is the channel steepness index and θ is the concavity index (Flint, 1974; Hack, 1957).

Channel steepness is often dependent on uplift rate but other pertinent factors, such as rock strength, precipitation, sediment flux, channel width, and channel hydraulic geometry, commonly influence this relationship (e.g., Craddock et al., 2007; Lavé and Avouac, 2001; Roe et al., 2002; Sklar and Dietrich, 1998; Tucker and Whipple, 2002; Whipple and Tucker, 2002). Discrimination of abrupt breaks in channel steepness can help identify factors perturbing model channel morphologies Application of this index to longitudinal river profiles has become a powerful quantitative tool for extracting information about the relationship between regional tectonics, topography and erosion in fluvial systems (e.g., DiBiase et al., 2010; Kirby and Whipple, 2001; Whipple and Tucker, 2002).

In this study we applied a fixed reference concavity, $\theta_{ref} = 0.45$, to facilitate comparison of data between river basins (Wobus et al., 2006) and generate a normalized channel steepness index, k_{sn} . Following a methodology similar to Ouimet et al. (2009), we used the freely available MatLab and ArcMap scripts (<http://www.geomorphotools.org>) to generate k_{sn} values every 2 km for all major tributaries draining $>100 \text{ km}^2$.

Bulk Sediment Petrography

Bulk, unsieved sediments were counted in thin section with at least 200 points following the Gazzi-Dickinson method (Ingersoll et al., 1984) with lithic fragments classified after

Garzanti and Vezzoli (2003) by noting the composition and metamorphic rank of rock fragments (MI Index). Thin sections were stained with alizarin red-S to distinguish calcite from dolomite. Sands were classified according to the relative proportion of quartz, feldspar, and lithic material in each sample exceeding 10%.

Hydrodynamic processes can produce significant variability in the composition of sediments with identical provenance (Frihy et al., 1995; Garzanti et al., 2009; Gazzi et al., 1973). We can correct for this environmental bias and limit intrasample variability by applying a “Source Rock Density” (SRD) correction to our petrographic data (Garzanti and Andò, 2007a; Vermeesch et al., 2016). The relative abundance of mineral phases are adjusted according to their densities for each sample and corrected to a suitable SRD value appropriate for provenance type and erosion level (Garzanti and Andò, 2007a, b). We corrected our data using a SRD of 2.71 g/cm³. Bulk petrographic data are reported in Table 2.

Major and Trace Element Geochemistry

Samples were analyzed for major and trace elements to provide a base characterization of the composition and the degree of chemical alteration. Carbonate was not removed prior to total digestion. All samples were freeze-dried and ground before mixing 600 mg of sample with 3600 mg of lithium tetraborate (LiB₄O₇; Spectromelt). Samples were pre-oxidized at 500°C with NH₄NO₃ and fused to glass beads. Samples were analyzed by X-Ray Fluorescence for Si, Al, Ti, Fe, Na, Ca, K, P and Rb using a Philips PW 2400 X-ray spectrometer at the Institut für Chemie und Biologie des Meeres (ICBM) at the Carl von Ossietzky Universität, Oldenburg, Germany. Measurements on the XRF were followed after Böning et al. (2009). To assure accuracy and

precision, several in-house standards and the certified standard of GSD-12 were analyzed, and results were better than 3%. Data are presented in Table 3.

Isotope Geochemistry

All sediments were analyzed for Sr and Nd isotopes as these isotopic systems can provide complementary insight on chemical weathering and provenance in sedimentary systems. Sr isotopic compositions are largely a function of the age and composition of silicate bedrock but chemical weathering is known to elevate $^{87}\text{Sr}/^{86}\text{Sr}$ values (Derry and France-Lanord, 1996). However, when provenance can be constrained by a system unaffected by transport or diagenetic processes, such as the largely immobile Sm-Nd system (Goldstein et al., 1984), the paired Rb-Sr and Sm-Nd isotopic systems make a powerful provenance proxy for siliciclastic sediments that has a proven track record in the NW Himalaya (e.g., Clift et al., 2002b). The bulk silicate sediment fraction was analyzed for most samples, but a few samples only allowed analysis of the $<300\text{ }\mu\text{m}$ fraction.

Samples were first leached using buffered acetic acid to remove any carbonate-bound Sr prior to total digestion. Mn-Fe oxides containing authigenic Sr, and potentially any material bearing authigenic Nd, were removed with a leach of 25% (v/v) acetic acid and 0.02 M hydroxylamine hydrochloride (HH). All Sr and Nd signatures measured are therefore assumed to originate from the silicate fraction, perhaps with minor fractions of dolomite. Leached sediments were digested in closed PTFE-vessels following the procedure described in Böning et al. (2004). Briefly, organic matter was oxidized from all samples by treatment with concentrated HNO_3 overnight. Subsequently, HF and HClO_4 were added and the vessels were heated for 12 h at 180°C . After digestion, solutions were evaporated on a heated metal block (180°C) and residues

were redissolved, fumed three times with 6N HCl, and dissolved finally in 1N HNO₃. All acids were of ultrapure quality.

To isolate rare earth elements (REEs) and Sr, the remaining solutions were put through two-step column chemistry using Eichrom TRU-Spec resin. Nd was separated from interfering REEs using Eichrom LN-Spec resin with 0.23–0.25 N HCl as eluant. The fraction containing Rb and Sr was loaded on Eichrom Sr-Spec columns using HNO₃, Rb was washed out with HNO₃, and Sr was eluted with Milli-Q water.

Isotopic compositions of Nd and Sr were analyzed using a Thermo Neptune Plus Multicollector ICP-MS at the ICBM in Oldenburg. Samples for Nd were analyzed using the Nd standard JNd-1. The ¹⁴³Nd/¹⁴⁴Nd values of all samples were corrected for internal mass fractionation using ¹⁴⁶Nd/¹⁴⁴Nd = 0.7219 and normalized to the reported JNd-1 value of ¹⁴³Nd/¹⁴⁴Nd = 0.51215 (Tanaka et al., 2000). Internal mass fractionation for Nd was corrected for using ¹⁴⁶Nd/¹⁴⁴Nd = 0.7219. Nd isotopic compositions are expressed in ε_{Nd} notation:

$$\varepsilon_{\text{Nd}} = [(\text{Nd}^{143}/\text{Nd}^{144})_{\text{sample}} / (\text{Nd}^{143}/\text{Nd}^{144})_{\text{CHUR}} - 1] * 10^4 \quad (2)$$

(¹⁴³Nd/¹⁴⁴Nd)_{CHUR} is the Chondritic Uniform Reservoir with a value of 0.512638 (Jacobsen and Wasserburg, 1980). The external reproducibility is calculated for each session separately using the analyses of JNd-1 and was generally better than ±0.000015 or ± 0.3 ε_{Nd} units (2σ). The BCR-2 standard (n = 4) had an ε_{Nd} value of 0.1 (± 0.3, 2σ) and was well within the reported ε_{Nd} value of 0.0 ± 0.2 (Raczek et al., 2003). The procedural blank was ≤ 30 pg Nd.

Samples for Sr were analyzed using standard-sample bracketing techniques using NBS987 and normalized to the reported value of 0.710248 (Thirlwall, 1991). Mass fractionation for Sr was corrected using ⁸⁶Sr/⁸⁸Sr = 0.1194. Contents of Kr, Rb, and Ba were monitored and found to be negligible. The external reproducibility is calculated using the analyses of NBS987

and was generally better than 80 ppm (2σ). The BCR-2 standard ($n = 4$) had a $^{87}\text{Sr}/^{86}\text{Sr}$ ratio of 0.70502 ± 0.00004 (2σ) and was within the reported $^{87}\text{Sr}/^{86}\text{Sr}$ ratio of 0.70496 ± 0.00002 (Raczek et al., 2003). The procedural blanks were negligible throughout. Results are reported in Table 4.

Detrital Zircon U-Pb Geochronology

Detrital zircon U-Pb dating has an established history of resolving questions on sediment provenance within Himalayan river systems (e.g., Alizai et al., 2011; Amidon et al., 2005) and in other drainage basins in Asia (e.g., He et al., 2013; Robinson et al., 2014). Zircon is a common mineral and is chemically and mechanically resistant to erosion, such that several cycles of erosion and sedimentation do not significantly alter U and Pb compositions (Gehrels, 2014). In this study we target the 63–250 μm size fraction because this range can effectively yield the same distribution of all significant age populations present in the bulk zircon population (Yang et al., 2012).

The use of U-Pb zircon dating for the Zanskar River is especially appropriate because there are a significant number of existing U-Pb zircon bedrock analyses from Himalaya bedrock. Although lithostratigraphic units in the western Himalaya have zircon populations that overlap, strong preferential occurrence of certain age groups can aid in identifying regions of sediment yield. (e.g., Bernet et al., 2006; Clift et al., 2004; DeCelles et al., 2004; Gehrels et al., 2011; Hu et al., 2015; Shellnutt et al., 2014; White et al., 2011; Wu et al., 2007).

Samples were separated for zircon using standard magnetic and heavy liquid separation techniques. A rare-earth element hand magnet was passed several times over the sample to remove extremely magnetic material and sieved again to 63–250 μm before magnetic separation. All samples were pre-treated using hydrogen peroxide, acetic acid, and oxalic acid to remove

organic material, carbonate, and Fe-oxides, respectively. Zircons were mounted in epoxy, polished, and imaged by reflected light and cathodoluminescence.

U-Th-Pb isotopic compositions were determined at the London Geochronology Centre facilities at University College London using a New Wave 193 nm aperture-imaged frequency-quintupled laser ablation system, coupled to an Agilent 7700 quadrupole-based ICP-MS. An energy density of ~ 2.5 J/cm² and a repetition rate of 10 Hz were used during laser operation. Laser spot diameter was ~ 30 μm with sampling depth of ~ 5 μm . Sample-standard bracketing by measurement of external zircon standard PLESOVIC (Sláma et al., 2008) and NIST 612 silicate glass (Pearce et al., 1997) were used to correct for instrumental mass bias and depth-dependent intra-element fractionation of Pb, Th and U. Temora (Black et al., 2003) and 91500 (Wiedenbeck et al., 2004) were used as secondary zircon age standards. Over 100 grains were analyzed for each sample to provide a statistically robust dataset for lithologically diverse units (Vermeesch, 2004). Age data were filtered using a $\pm 15\%$ discordance cut-off. For grains with ages less than 1000 Ma, the $^{206}\text{Pb}/^{238}\text{U}$ ratio was used and the $^{207}\text{Pb}/^{206}\text{Pb}$ ratio for grains older than 1000 Ma. All measurements were processed using GLITTER 4.4 data reduction software (Griffin et al., 2008). Sample-standard bracketing by measurement of external zircon standard PLESOVIC (Sláma et al., 2008) and NIST 612 silicate glass (Pearce et al., 1997) were used to correct for instrumental mass bias and depth-dependent intra-element fractionation of Pb, Th and U. Temora (Black et al., 2003) and 91500 (Wiedenbeck et al., 2004) were used as secondary zircon age standards. Over 100 grains were analyzed for each sample to provide a statistically robust dataset for lithologically diverse units (Vermeesch, 2004). Age data were filtered using a $\pm 15\%$ discordance cut-off. For grains with ages less than 1000 Ma, the $^{206}\text{Pb}/^{238}\text{U}$ ratio was used and the $^{207}\text{Pb}/^{206}\text{Pb}$ ratio for grains older than 1000 Ma. All measurements were processed using

GLITTER 4.4 data reduction software (Griffin et al., 2008). Time-resolved signals recording isotopic ratios with depth in each crystal enabled filtering to remove signatures owing to overgrowth boundaries, inclusions and/or fractures. Individual U-Pb ages are reported at 1σ .

Kernel density estimations (KDE) provide robust age distributions and are presented in the text for visual analysis of age population distributions and abundance. Traditional probability density functions may smooth older age populations that inherently have a greater age error than younger populations at 1σ , therefore KDEs are favored in this study to prevent this bias (Vermeesch, 2012). Multidimensional scaling (MDS) was performed using R.info Version 3.1.1 programming codes modified after Vermeesch (2013) to quantitatively compare zircon spectra.

RESULTS

Basin Morphology

A large-scale rainfall gradient exists across Zanskar from the southwest to the northeast (Fig. 2, 4A), with highest mean annual rainfall ($>650 \text{ mm}\cdot\text{yr}^{-1}$) values observed in the northwest inside the Stod River catchment. Lowest values ($<150 \text{ mm}\cdot\text{yr}^{-1}$) occur around Tso Kar (Fig. 1C). Steepest slopes are in the Stod and Khurna catchments, as well as the Zanskar Gorge, (Fig. 4B), that correspondingly also indicate regions of highest local relief (Fig. 4C).

Zanskar channel profile geometries (Figure 5) indicate strong glacial modification. Remnants of multiple recessional moraines exist in the lower Tsarap River, the overdeepened Stod and Khurna Rivers, and the steep, headwater Tsarap tributaries. The broad, alluviated Padum Basin ends with a terminal moraine at Hanumil (Fig. 1C). The Zanskar Gorge can be characterized in general as a large knickzone. Reworking of a recessional moraine results in a

small knickzone in the lower Tsarap River, although the knickzone is likely enhanced in part by a remaining artifact in the DEM data.

Normalized channel steepness values (Fig. 4D) correspond to several locations for recessional moraines in small, headwater tributaries, and in the lower Tsarap, Khurna and Markha Rivers (Fig. 5). The highest k_{sn} values (>500) occur in the upper Zanskar Gorge and in short segments in the middle reaches of the Tsarap River containing bedrock gorges. We do not include k_{sn} values for the presently endorheic Tso Kar basin (Fig. 4D) but do include other morphometric parameters for this region for reference.

Bulk Sediment Petrography

The Zanskar River transports an incredible diversity of sands that range from lithic carbonaticlastic to feldspatho-quartzolithic metamorphiclastic compositions (Table 2). Framework petrography indicates abundant quartz, feldspar, low rank metacarbonate, high-rank fibrolite-bearing metafelsite fragments, with minor chert, epidote-bearing metabasite, and serpentinized ultramafic rock fragments. Abundant mineral grains include calcite and dolomite spar, mica, sillimanite, green amphibole, and ultrastable minerals such as zircon, blue-green tourmaline, rutile, and titanite. Minor kyanite, garnet, staurolite, and brown amphibole are noted. Most sands contain moderate amounts of mica and/or dense minerals but most carbonaticlastic sands are poor in both micaceous and dense phases.

Zanskar River sediments roughly divide into two petrographic groups (Fig. 6). Samples containing slightly more lithic fragments, predominantly more carbonate and lesser volcanic fragments, fall within rocks of Tethyan Himalayan affinity (Fig. 6A). Samples that are slightly more quartzofeldspathic lie closer to rocks with Greater Himalayan affinity. Similarly, samples

with higher grade metamorphic minerals fall nearer rocks of known Greater Himalayan affinity (Fig. 6B).

Major and Trace Element Geochemistry

Major element geochemistry can be effective in assessing the intensity of chemical weathering. The “Chemical Index of Alteration” proxy expressed as:

$$\text{CIA} = ((\text{Al}_2\text{O}_3 / (\text{Al}_2\text{O}_3 + \text{Na}_2\text{O} + \text{K}_2\text{O} + \text{CaO}^*)) \cdot 100 \quad (3)$$

can be used to compare the relative leaching of labile elements (K, Na, silicate-only Ca) to residual, immobile Al during feldspar weathering (Nesbitt et al., 1980). CIA values range from 50 to 100 with higher values indicating stronger chemical weathering. A correction is made to CIA values if excess CaO is present in carbonates and phosphates by assuming a reasonable Ca/Na ratio for the silicate material and correcting for CaO in phosphate (Singh et al., 2005).

Zanskar River sediments (Table 3; Fig. 7) span low to moderate CIA values (52–71). In general, higher CIA values occur in upstream tributaries and lower values, indicating less intense weathering, occur in the lower Tsarap (ID #9) and Stod (ID #7, #8) Rivers, and Padum Basin sediment samples of Pishu (#5) and Hanumil (ID #4). CIA values are poorly correlated to SiO₂, with slight negative correlation as silica contents increase.

Isotope Geochemistry

Variations in Sr and Nd isotopes for Zanskar River sediments and regional bedrock source terranes are plotted in Figure 8. Isotopic compositions for decarbonated Zanskar River sediments display a range in ϵ_{Nd} values from -10 to -17.4 and a wide range of $^{87}\text{Sr}/^{86}\text{Sr}$ isotope values from 0.713990 to 0.755070. No coherent correlation exists between the isotopic systems.

The widest variation in $^{87}\text{Sr}/^{86}\text{Sr}$ values occurs in the upstream Tsarap River tributaries (Fig. 9). The Zara (ID #10), lower Tsarap (ID #9), and Yunam (ID #13) River samples display the greatest enrichment, and Gata (ID #12) one of the least enriched. The Stod River (ID #7, #8) sediments remain remarkably consistent with a $^{87}\text{Sr}/^{86}\text{Sr}$ value of ~ 0.723 . After the confluence with the Stod River, $^{87}\text{Sr}/^{86}\text{Sr}$ values become only slightly less enriched down the Zanskar River as the Oma (ID #3) and Markha (ID #2) Rivers join the trunk river.

The Stod River, in contrast to the Sr isotopes, demonstrates a shift to more negative ε_{Nd} values downstream (Fig. 9). Similar ε_{Nd} values are seen at Yunam (ID #13) and Gata (ID #11), as well as at Toze Lungpa (ID #11) and Zara (ID #10). Curiously, the trunk sample at Pishu (ID #5) demonstrates a more negative ε_{Nd} value than either the lower Stod (ID #7) or Tsarap (ID# 9) Rivers after they join. Downstream of Pishu (ID #5), the trunk river values do not vary significantly even downstream of the more positive Markha (ID #2) and Oma (ID #3) River confluences.

Detrital U-Pb Zircon Geochronology

All dated Zanskar River samples are presented as kernel density estimate (KDE) diagrams following Vermeesch (2004) in Figure 10. All Zanskar age analyses are presented in Table S1. Most samples contain one or more peak populations at 245–380 Ma, 440–500 Ma, 500–600 Ma, and 750–850 Ma. Some samples have a composite peak from 750–1250 Ma comprised of smaller subsidiary peaks at ~ 900 Ma, ~ 1000 Ma and ~ 1100 Ma. Paleoproterozoic and Archean peaks are found from 1600–1900 Ma and at ~ 2500 Ma, with very few ages at ~ 3200 Ma and ~ 3400 Ma.

Lower Stod (ID #7), Pishu (ID #5), Hanumil (ID #4), and Zanskar-Indus (ID #1) confluence samples display similar age spectra to one another, with very prominent peaks at 750–850 Ma, and with two smaller peaks at ~350 Ma and ~450 Ma. Tsarap tributary samples populate a second group that also display the prominent ~450 Ma peak but contain older ages clustered at ~530 Ma, the broad 750–1250 Ma peak and an older, less populous peak from 1600–1900 Ma. The Zara (ID #10), Lower Tsarap (ID #9), Markha (ID #2), and to a lesser extent Yunam (ID #13), samples contain small peaks at ~2500 Ma.

Zircons less than 300 Ma were uncommon in most samples but some tributaries yielded Mesozoic and Cenozoic ages. Pishu (ID #5), Hanumil (ID#4) and the Zanskar-Indus confluence (ID #1) yield zircon with ages clustered at ~260 Ma. Toze Lungpa (ID #11) was the only sample that yielded five zircon with a latest Triassic-earliest Jurassic mean age of 209 ± 6 Ma. The Markha River yielded two late Cretaceous ages, one at 130.5 ± 3.4 Ma and 97.2 ± 2.8 Ma. One late Paleocene age at 57.7 ± 1.1 Ma was yielded from the Zanskar-Indus confluence. Three samples (Lower Stod, Hanumil, Pishu) contained Oligocene and Miocene grains with ages ranging from 18–32 Ma.

DISCUSSION

Downstream provenance evolution

Little variability in Sr and Nd isotopic compositions is observed in the trunk river downstream of Padum. The Zanskar-Indus (ID #1) confluence sample is most comparable to the Lower Stod River (ID #7; Fig. 9). Even so, Sr values decrease and Nd values increase slightly downstream of Padum suggesting minor addition of sediment from smaller (<100 km 2) Zanskar Gorge tributaries (Fig. 5). This sediment must be isotopically similar to the Oma (ID#3) and

Markha (ID#2) Rivers because of the observed decrease in $^{87}\text{Sr}/^{86}\text{Sr}$ values and increase in ε_{Nd} . Nonetheless, contribution from the Oma River is negligible as the trunk river does not change its ε_{Nd} value downstream of this confluence.

Much of the geochemical variability in Zanskar River sediments occurs upstream of Padum before the confluence of the Lower Stod (ID #7) and Tsarap (ID #9) Rivers. $^{87}\text{Sr}/^{86}\text{Sr}$ values from the Upper (ID #8) and Lower Stod are within error of each other, but the Upper Stod is marked by a more positive ε_{Nd} value. The downstream decrease in ε_{Nd} values along the Stod River likely results from contribution of felsic, less radiogenic crystalline Greater Himalaya ($\varepsilon_{\text{Nd}} = -15.2 \pm 2.2$; (Robinson et al., 2001). Sediment from Panjal Traps basalts ($\varepsilon_{\text{Nd}} = -8-0$; (Shellnutt et al., 2014) added into the Upper Stod can account for the more positive ε_{Nd} values seen.

The Tsarap River drains almost all lithologies exposed in the Zanskar River basin and this in part rationalizes the wide variability observed in Tsarap catchment isotope compositions (Lower Tsarap (ID# 9), Toze Lungpa (ID #11), Zara (ID #10), Yunam (ID #13)). We conclude that the Lower Tsarap sample is not representative of a Tsarap catchment-averaged composition. This is because the ε_{Nd} value observed at Pishu (ID #5; $\varepsilon_{\text{Nd}} = -15.5$) after mixing of the Lower Stod (ID #7; $\varepsilon_{\text{Nd}} = -14.5$) requires that the net contribution from the Tsarap be more negative than -15.5 (consistent with measurements in the upper Tsarap), in contrast to the measured Lower Tsarap sample (ID #9; $\varepsilon_{\text{Nd}} = -13.6$). This raises the possibility that the Lower Tsarap sample is locally derived. Alternatively, this sample could represent a transient pulse of sediment in the Tsarap derived from enhanced erosion sourced from similar bedrock and/or sediments further upstream, perhaps linked to older, large volume mass movements triggered by climatic events (e.g., cloud bursts, (Hobley et al., 2012)).

Bulk petrography and detrital zircon analyses suggest two models for sediment mixing downstream (Fig. 11). Framework grains indicate a continued, progressive compositional evolution of sediments downstream, with marginally greater contribution of sediment from the Stod River (ID #7, #8) than other tributaries. In contrast, detrital zircon grains demonstrate an overwhelming dominance of material sourced from the Stod River and little variation in zircon populations downstream of Padum. MDS analysis of detrital zircon samples clearly segregates sediments into two groups, whereas bulk petrography and major element compositions form slightly less discrete groups (Figs. 12A-C). Selected source bedrock U-Pb age data are plotted for comparison in Figures 12D and S1.

Below the Tsarap (ID #9) and Stod (ID #7) River confluence at Padum, each detrital zircon sample on the trunk river contains 600–850 Ma grains as the majority population (Fig. 11). A small increase in >2400 Ma ages at the Zanskar-Indus (ID #1) confluence, however, does suggest minor contribution from the Markha River (ID #2). Bulk petrography also argues for an additional contribution from the Markha and Oma (ID#3) Rivers, and likely other small Zanskar Gorge tributaries. After exiting the gorge in the lower reaches, river sediments contain more Tethyan sedimentary and low-grade metasedimentary lithics than below Hanumil (ID #4) at the gorge entrance.

Lithic grains of trunk river samples above the gorge display closest similarity to the Lower Tsarap (ID #9) River (Figs. 11 and 12). Pishu (ID #5, #6) and Hanumil (ID# 4) samples contain abundant Tethyan Himalayan metapelitic and carbonate fragments, with very few high-grade, coarsely crystalline Greater Himalayan gneiss and calc-gneiss fragments. Although these trunk river samples do not contain a lot of high-grade lithic fragments, the abundance of quartz, feldspar and fibrolite still indicate strong contribution of Greater Himalayan material. This

sediment is likely sourced in part from the Cambro-Ordovician and Mississippian-Permian granitic gneisses exposed as part of the Greater Himalaya along the ZSZ, rather than from the Zara River (Fig. 3). The abundance of quartzofeldspathic, micaceous, and schistose metamorphic clastic detritus in the Zara (ID #10) sample might suggest an overspill connection existed between Tso Kar and the Zanskar River, as proposed by Demske et al. (2009) and Wünnemann et al. (2010). Our provenance data from the Zara River neither support nor preclude sediment supply to the Zanskar River via an overspill connection (e.g., Munack et al., 2016). Potential parent bedrock sources to the Zara River are exposed immediately northeast, outside the Tso Kar basin, as well as along strike into that basin and further southeast to Tso Morari. Furthermore, we suggest the Zara River does not contribute much Nyimaling-Tso Morari gneiss dome material to trunk river samples because none is found in bulk sediments lower in the Tsarap River (Fig. 11). Similarly, the Yunam River (ID #13) carries abundant Greater Himalayan metamorphic material but is simply diluted by the Tethyan Himalayan sedimentary fragments sourced from other tributaries downstream.

Detrital zircon populations with central ages at ~350 Ma, ~450 Ma, and ~530 Ma (Fig. 10) support previous findings for abundant Cambro-Ordovician and Mississippian-Permian granites found in the Greater Himalaya in Zanskar and elsewhere in the northwest Himalaya (Fig. S2; Honegger et al., 1982; Horton and Leech, 2013; Spring et al., 1993). Detrital zircon ages clustered at ~260 Ma could be sourced from Panjal Traps but are younger than the reported ages (~289 Ma) northeast of Zanskar (Shellnutt et al., 2014; Singh et al., 1976). Permian granites are not recognized in Greater Himalaya units from the eastern and central Himalaya (Gehrels et al., 2011). The relative lack or presence of such prominent age peaks between the central/eastern

and northwest Himalaya encourages future caution when using detrital zircon compilations to correlate strata across the orogen when such heterogeneities exists (Fig. S2).

Heavy mineral fertility likely plays a role in the apparent contrast observed between bulk petrography and detrital zircon analyses. For example, detrital zircon ages at Yunam (ID #13) appear to be transmitted downstream to Gata (ID #11; Figs. 9 and 11), consistent with a stable ε_{Nd} value over that stretch of river. However, the bulk petrography and Sr isotope values change markedly between these two samples, requiring significant sediment dilution. This discrepancy requires that either the material being added has the same zircon and Nd-bearing phases but different bulk lithologic composition, or that the sediment contributed from tributaries between Yunam and Gata (ID #11) is lacking in those phases. We favor the latter as being more likely.

Controls on Erosion

While our dataset cannot quantify sediment yields, we here provide the first initial constraints on sediment provenance and the relative contributions of sources downstream in the Zanskar River. The data presented above yield a clear image of the Stod River being a significant source of sediment to the Zanskar. This influence is moderated by downstream sediment contributions from tributaries and minor, side valley tributaries. We argue that the bulk of sediment production in the Zanskar River is driven by strong glacial erosion in the Stod River valley and lesser hillslope erosion across the catchment. We favor glacial erosion as the primary process controlling erosion because westernmost Zanskar and Stod River hillslopes and valleys have been strongly modified by glaciation for at least the last 78 k.y. (Taylor and Mitchell, 2000) and continue to be conditioned by active alpine glaciers. Glaciers comprise ~28% of the modern Stod River basin versus 7-8% of the modern Tsarap and overall Zanskar River basins. Spatial

patterns of erosion in Zanskar may not correlate significantly with convexities in river profiles caused by lithologic changes or high channel steepness (Figs. 2 and 5). Instead, the highest yields come from the Stod River catchment that contains a broad, overdeepened and alluviated U-shaped valley, steep hillslopes housing north-facing glaciers, low to moderate k_{sn} values, and convexities along the river profile that reflect earlier glacial conditioning.

Hillslope processes acting at high elevation in semi-arid regions cannot be ruled out as significant producers of sediment. Soil creep, grassification, granulation, and salt weathering are known to generate sediment along the Indus River valley but are likely less influential than (peri-) glacial and fluvial processes in driving bedrock erosion and evacuating sediment in paraglacial environments (Blöthe et al., 2015; Dietsch et al., 2015; Hales and Roering, 2007; Scherler, 2014). Hillslope processes operate at slower rates and the material that is produced is not readily mobilized. Erosion in drier, unglaciated catchments in Zanskar is likely strongly driven by slow hillslope processes but unlikely operating at comparable rates or volumes as glaciated catchments.

Bookhagen et al. (2005a) indicate that mass wasting is fundamental in driving increased sediment flux and shaping landscapes in the dry Himalayan interior. Debris flows and deep-seated landslides are facilitated when intense summer rainfall destabilizes poorly vegetated hillslopes. Over the Holocene, mass wasting events correlate well with periods of enhanced monsoonal rainfall in steep rain shadow reaches (Bookhagen et al., 2005b; Dortch et al., 2009). Our findings do not support rainfall-modulated landsliding as a primary control on modern erosion in the Zanskar River. The few mass wasting deposits identified in the basin neither correlate with modern erosion patterns nor major knickzones.

Seasonal summer monsoonal precipitation, however, may provide a first-order control on sediment transport. We propose that glacial erosion drives production of unconsolidated sediments that are then later reworked during high-intensity monsoon events in the modern Zanskar River basin. Snow and glacial meltwater cause heightened discharge and suspended sediment flux in the dry Himalaya during the early summer (Anderson et al., 2004; Burbank et al., 2012), but later monsoonal storm events more effectively drive sediment transport. The magnitude of glacial sediment production and/or flux of reworked sediment from the Stod River catchment is great enough that significant dilution of this signal does not occur downstream, even after addition of mobilized hillslope sediments. This is in contrast to what has been observed in the frontal Himalaya where glacial sediment production is masked by much stronger monsoonal erosion (Godard et al., 2012). Erosion in Zanskar also contrasts to that seen in the unglaciated basins along the Indus valley that receive $<115 \text{ mm}\cdot\text{yr}^{-1}$ precipitation and have extremely slow integrated rates of erosion (Dietsch et al., 2015; Dortch et al., 2011b; Munack et al., 2014). We argue that sediment production and transport in the Zanskar River basin are modulated by the same primary drivers of erosion (i.e., glaciers and monsoon rainfall), but that these operate at different relative magnitudes compared to the frontal Himalaya, as well as the more slowly denuding regions along the Indus Valley.

Our study of modern erosion patterns in the Zanskar River naturally solicits comparisons between contemporary and Quaternary erosive conditions. While modern sediments in semi-arid to arid Ladakh and Zanskar may in part be mobilized during high intensity storm events (e.g., Hobley et al., 2012; Stolle et al., 2015), it cannot be assumed that these conditions held true in the past. Stronger Holocene monsoon phases at 8–10 ka and 30–35 ka brought enhanced precipitation onto Tibetan Plateau margins that promoted greater vegetative cover (Demske et

al., 2009; Herzschuh, 2006; Shi et al., 2001; Wünnemann et al., 2010). Increased slope stability as a result of more vegetation could reduce the erosive capability of high-intensity storm perturbations and potentially reduce erosional response (e.g., Beaumont et al., 2000). Under prolonged enhanced monsoonal conditions, it is unlikely storm events had equivalent impacts over the region, and if these events had similar recurrence, transience, and magnitude. In light of the devastating debris flows in 2010 and 2015 in Ladakh, more work is needed to understand the nature of these high intensity events and their erosional impact.

Next, our work begs the question whether the material yielded from the Stod River is eroded from bedrock or primarily reworked from glacial moraines. We cannot definitively untangle the relative contribution of reworked glacial material at least with our dataset, however, based on the present observation of abundant incised glaciofluvial terraces we prefer the idea that large-scale recycling of material generated during the Last Glacial Maximum is the primary source of sediment to the Stod River. Furthermore we recognize that longer term glacial and monsoonal phases dictating sediment generation and reworking might be disrupted by shorter duration, perhaps stochastic, climatic perturbations. However, the generally cohesive trends in our provenance data would indicate that the modern signal is not dominated by these events.

Significant dissection of Pleistocene valley-fills in the upper Tsarap catchment highlights a long history of sediment reworking into the paleo-Zanskar River (Munack et al., 2016). Although our data here do not indicate a strong contemporary contribution from these deposits to the modern Zanskar River, to what extent the provenance signal may have been distorted as a result of such recycling in the past remains open to investigation. This combined understanding of erosion in Zanskar further emphasizes that sediment buffering over millennial to even multi-

millennial timescales is likely an important process controlling sediment routing in the Himalayan rain shadow and the overall transfer of climate-erosion signals downstream.

CONCLUSIONS

We applied a suite of geochemical and geochronological techniques to establish spatial patterns of erosion in a rain shadow river system. Our findings demonstrate that modern sediment provenance in Zanskar is driven by focused glacial erosion and monsoonal rainfall along the Greater Himalaya and Zanskar Shear Zone. The Stod River catchment, representing only 13% of the total area of the Zanskar River basin, dominates in delivering sediment to the modern drainage. The distribution of erosion in Zanskar is not directly controlled by monsoonal rainfall as is the case in the frontal Himalaya, but rather the precipitation gradient promotes a concentration of permanent, north-facing glaciers that efficiently scour the High Himalaya. The Zanskar differs from its wetter neighbors to the south in being less controlled by mass wasting but also differs from drier, formerly glaciated catchments further north in having enough precipitation to regularly mobilize the sediment produced by glaciation. Dry, low relief, unglaciated regions of Zanskar contribute minimally to the total modern sediment flux. We suggest that increased flux from these arid regions may only be significant when extreme monsoon storms, or even prolonged, intense Holocene monsoon phases, mobilize sediments from unvegetated hillslopes.

Our data are broadly consistent with the glacially-dominated sediment production model of Blothe et al. (2014), but here our analyses the potential importance of monsoon precipitation in remobilizing sediment and allowing its transportation into the main Indus River system. While the majority of sediment may be fluxed during deglacial and post-glacial times, we argue that it

monsoon may control sediment transport rather than deglaciation itself (c.f., Blöthe et al., 2014). This appears to be true at least in the present day in this transitional setting between the wet frontal Himalaya and the arid orogenic interior of the Tibetan Plateau. In the absence of tectonic forcing in Zanskar, our results support climatic control on erosion in the Himalaya. If surface processes dominate over million year timescales then these would shape orogenic architecture in the way favored by critical wedge and channel flow extrusion models (Beaumont et al., 2001; Robinson et al., 2006).

ACKNOWLEDGMENTS

This work was supported by the Charles T. McCord Jr. Chair in petroleum geology at LSU and in part by the Farouk El-Baz Student Research Award, and LSU scholarships. This manuscript was greatly improved by thoughtful and constructive reviews by Jason Dortch and Jan Blöthe. TJ and PC thank Fida Hussein Mittoo with Rockland Tourism and Arundeept Aluwahlia from Panjab University for logistical support. TJ would like to thank Eduardo Garzanti for valuable discussions on sediment petrography and Jan Blöthe and Henry Munack on Zanskar geomorphology. PB and KP thank the ICBM and Max Planck Institute for Marine Microbiology for financial support.

REFERENCES CITED

- Alizai, A., Carter, A., Clift, P. D., VanLaningham, S., Williams, J. C., and Kumar, R., 2011, Sediment provenance, reworking and transport processes in the Indus River by U-Pb dating of detrital zircon grains: *Global and Planetary Change*, v. 76, no. 1-2, p. 33–55, doi:10.1016/j.gloplacha.2010.11.008.
- Amidon, W. H., Burbank, D. W., and Gehrels, G. E., 2005, U-Pb zircon ages as a sediment mixing tracer in the Nepal Himalaya: *Earth and Planetary Science Letters*, v. 235, no. 1-2, p. 244–260, doi:10.1016/j.epsl.2005.03.019.
- Anderson, J. L., and Bender, E. E., 1989, Nature and origin of Proterozoic A-type granitic magmatism in the southwestern United States of America: *Lithos*, v. 23, no. 1, p. 19–52, doi:10.1016/0024-4937(89)90021-2.
- Anderson, R. S., Anderson, S. P., MacGregor, K. R., Waddington, E. D., O'Neil, S., Riihimaki, C. A., and Loso, M. G., 2004, Strong feedbacks between hydrology and sliding of a small alpine glacier: *Journal of Geophysical Research: Earth Surface*, v. 109, no. F3, p. F03005, doi: 10.1029/2004JF000120.
- Attal, M., and Lavé, J., 2006, Changes of bedload characteristics along the Marsyandi River (central Nepal): Implications for understanding hillslope sediment supply, sediment load evolution along fluvial networks, and denudation in active orogenic belts: *Geological Society of America Special Papers*, v. 398, p. 143-171, doi: 10.1130/2006.2398(09).
- Beaumont, C., Jamieson, R. A., Nguyen, M. H., and Lee, B., 2001, Himalayan tectonics explained by extrusion of a low-viscosity crustal channel coupled to focused surface denudation: *Nature*, v. 414, no. 6865, p. 738–742, doi:10.1038/414738a.
- Beaumont, C., Kooi, H., and Willett, S., 2000, Coupled tectonic-surface process models with applications to rifted margins and collisional orogens: *Geomorphology and global tectonics*, p. 29-55,
- Bernet, M., van der Beek, P., Pik, R., Huyghe, P., Mugnier, J.-L., Labrin, E., and Szulc, A. G., 2006, Miocene to Recent exhumation of the central Himalaya determined from combined detrital zircon fission-track and U/Pb analysis of Siwalik sediments, western Nepal: *Basin Research*, v. 18, p. 393–412, 10.1111/j.1365-2117.2006.00303.x.
- Black, L. P., Kamo, S. L., Allen, C. M., Aleinikoff, J. N., Davis, D. W., Korsch, R. J., and Foudoulis, C., 2003, TEMORA 1: a new zircon standard for Phanerozoic U-Pb geochronology: *Chemical Geology*, v. 200, p. 155–170, doi:10.1016/S0009-2541(03)00165-7.
- Blöthe, J. H., Korup, O., and Schwanghart, W., 2015, Large landslides lie low: Excess topography in the Himalaya-Karakoram ranges: *Geology*, v. 43, no. 6, p. 523-526,
- Blöthe, J. H., Munack, H., Korup, O., Fülling, A., Garzanti, E., Resentini, A., and Kubik, P. W., 2014, Late Quaternary valley infill and dissection in the Indus River, western Tibetan Plateau margin: *Quaternary Science Reviews*, v. 94, p. 102–119, doi:10.1016/j.quascirev.2014.04.011.
- Böning, P., Brumsack, H.-J., Schnetger, B., and Grunwald, M., 2009, Trace metal signatures of Chilean upwelling sediments at ~36°S: *Marine Geology*, v. 259, p. 112–121, doi:10.1016/j.margeo.2009.01.004.
- Bookhagen, B., 2010, Appearance of extreme monsoonal rainfall events and their impact on erosion in the Himalaya: *Geomatics, Natural Hazards and Risk*, v. 1, no. 1, p. 37–50, doi: 10.1080/19475701003625737.

- Bookhagen, B., and Burbank, D. W., 2006, Topography, relief, and TRMM-derived rainfall variations along the Himalaya: *Geophysical Research Letters*, v. 33, no. L08405, p. L08405 doi: 10.1029/2006GL026037.
- Bookhagen, B., and Burbank, D. W., 2010, Towards a complete Himalayan hydrological budget: The spatiotemporal distribution of snow melt and rainfall and their impact on river discharge: *Journal of Geophysical Research Earth Surface (2003–2012)*, v. 115, p. F03019, doi: 10.1029/2009JF001426.
- Bookhagen, B., Thiede, R. C., and Strecker, M. R., 2005a, Abnormal monsoon years and their control on erosion and sediment flux in the high, arid northwest Himalaya: *Earth and Planetary Science Letters*, v. 231, no. 1-2, p. 131–146, doi: 10.1016/j.epsl.2004.11.014.
- Bookhagen, B., Thiede, R. C., and Strecker, M. R., 2005b, Late Quaternary intensified monsoon phases control landscape evolution in the northwest Himalaya: *Geology*, v. 33, no. 2, p. 149–152, doi: 10.1130/G20982.1.
- Burbank, D., and Fort, M., 1985, Bedrock control on glacial limits: examples from the Ladakh and Zanskar ranges: north-western Himalaya, India: *Journal of Glaciology*, v. 31, no. 108, p. 143–149,
- Burbank, D. W., Blythe, A. E., Putkonen, J., Pratt-Sitaula, B., Gabet, E. J., Oskin, M., Barros, A., and Ojha, T., 2003, Decoupling of erosion and precipitation in the Himalayas: *Nature*, v. 426, p. 652–655, doi: 10.1038/nature02187.
- Burbank, D. W., Bookhagen, B., Gabet, E. J., and Putkonen, J., 2012, Modern climate and erosion in the Himalaya: *Comptes Rendus Geoscience*, v. 344, no. 11-12, p. 610–626, doi: 10.1016/j.crte.2012.10.010.
- Burchfiel, B. C., Chen, Z., Hodges, K. V., Liu, Y., Royden, L. H., Deng, C., and Xu, J., 1992, The South Tibetan Detachment System, Himalayan Orogen: Extension Contemporaneous With and Parallel to Shortening in a Collisional Mountain Belt, Special Paper - Geological Society of America, Volume 269: Boulder, CO, Geological Society of America, p. 1–41, doi: 10.1130/SPE269-p1.
- Burchfiel, B. C., and Royden, L., 1985, North-south extension within the convergent Himalayan region: *Geology*, v. 13, no. 10, p. 679–682, doi: 10.1130/0091-7613(1985)13<679:NEWTCH>2.0.CO;2
- Cawood, P. A., Johnson, M. R., and Nemchin, A. A., 2007, Early Palaeozoic orogenesis along the Indian margin of Gondwana: tectonic response to Gondwana assembly: *Earth and Planetary Science Letters*, v. 255, no. 1–2, p. 70–84, doi: 10.1016/j.epsl.2006.12.006.
- Clift, P. D., Campbell, I. H., Pringle, M. S., Carter, A., Zhang, X., Hodges, K. V., Khan, A. A., and Allen, C. M., 2004, Thermochronology of the modern Indus River bedload: New insight into the controls on the marine stratigraphic record: *Tectonics*, v. 23, no. 5, p. TC5013, doi: 10.1029/2003TC00155.
- Clift, P. D., Carter, A., and Jonell, T. N., 2014, U–Pb dating of detrital zircon grains in the Paleocene Stumpata Formation, Tethyan Himalaya, Zanskar, India: *Journal of Asian Earth Sciences*, v. 82, p. 80–89, doi: 10.1016/j.jseaes.2013.12.014.
- Clift, P. D., Carter, A., Krol, M., and Kirby, E., 2002a, Constraints on India-Eurasia collision in the Arabian Sea region taken from the Indus Group, Ladakh Himalaya, India, *in* Clift, P. D., Kroon, D., Gaedicke, C., and Craig, J., eds., *The tectonic and climatic evolution of the Arabian Sea region*, Volume 195: London, Geological Society, p. 97–116, doi: 10.1144/GSL.SP.2002.195.01.07.

- Clift, P. D., Hodges, K. V., Heslop, D., Hannigan, R., Van Long, H., and Calves, G., 2008, Correlation of Himalayan exhumation rates and Asian monsoon intensity: *Nature Geoscience*, v. 1, no. 12, p. 875–880, doi: 10.1038/ngeo351.
- Clift, P. D., Lee, J. I., Hildebrand, P., Shimizu, N., Layne, G. D., Blusztajn, J., Blum, J. D., Garzanti, E., and Khan, A. A., 2002b, Nd and Pb isotope variability in the Indus River system; implications for sediment provenance and crustal heterogeneity in the western Himalaya: *Earth and Planetary Science Letters*, v. 200, no. 1-2, p. 91–106, doi: 10.1016/S0012-821X(02)00620-9.
- Clift, P. D., Shimizu, N., Layne, G. D., Blusztajn, J. S., Gaedicke, C., Schlüter, H. U., Clark, M. K., and Amjad, S., 2001, Development of the Indus Fan and its significance for the erosional history of the Western Himalaya and Karakoram: *Geological Society of America Bulletin*, v. 113, no. 8, p. 1039–1051, doi: 10.1130/0016-7606(2001)113<1039:DOTIFA>2.0.CO;2.
- Condie, K. C., 1993, Chemical composition and evolution of the upper continental crust: contrasting results from surface samples and shales: *Chemical geology*, v. 104, no. 1–4, p. 1–37, doi: 10.1016/0009-2541(93)90140-E.
- Craddock, W. H., Burbank, D. W., Bookhagen, B., and Gabet, E. J., 2007, Bedrock channel geometry along an orographic rainfall gradient in the upper Marsyandi River valley in central Nepal: *Journal of Geophysical Research: Earth Surface* v. 112, no. F3, p. F03007, doi: 10.1029/2006JF000589.
- Damm, B., 2006, Late Quaternary glacier advances in the upper catchment area of the Indus River (Ladakh and western Tibet): *Quaternary International*, v. 154–155, p. 87–99, doi: 10.1016/j.quaint.2006.02.013.
- DeCelles, P. G., Gehrels, G. E., Najman, Y., Martin, A. J., Carter, A., and Garzanti, E., 2004, Detrital geochronology and geochemistry of Cretaceous-Early Miocene strata of Nepal: implications for timing and diachroneity of initial Himalayan orogenesis: *Earth and Planetary Science Letters*, v. 227, no. 3–4, p. 313–330, doi: 10.1016/j.epsl.2004.08.019.
- DeCelles, P. G., Gehrels, G. E., Quade, J., LaReau, B., and Spurlin, M., 2000, Tectonic implications of U-Pb zircon ages of the Himalayan orogenic belt in Nepal: *Science*, v. 288, no. 5465, p. 497–499, doi: 10.1126/science.288.5465.497.
- Demske, D., Tarasov, P. E., Wünnemann, B., and Riedel, F., 2009, Late glacial and Holocene vegetation, Indian monsoon and westerly circulation in the Trans-Himalaya recorded in the lacustrine pollen sequence from Tso Kar, Ladakh, NW India: *Palaeogeography, Palaeoclimatology, Palaeoecology*, v. 279, no. 3-4, p. 172–185, doi: 10.1016/j.palaeo.2009.05.008.
- Derry, L. A., and France-Lanord, C., 1996, Neogene Himalayan weathering history and river $^{87}\text{Sr}/^{86}\text{Sr}$; impact on the marine Sr record: *Earth and Planetary Science Letters*, v. 142, no. 1–2, p. 59–74, doi: 10.1016/0012-821X(96)00091-X.
- Dèzes, P. J., Vannay, J. C., Steck, A., Bussy, F., and Cosca, M., 1999, Synorogenic extension: quantitative constraints on the age and displacement of the Zanskar shear zone (Northwest Himalaya): *Geological Society of America Bulletin*, v. 111, no. 3, p. 364–374, doi: 10.1130/0016-7606(1999)111<0364:SEQCOT>2.3.CO;2.
- DiBiase, R. A., Whipple, K. X., Heimsath, A. M., and Ouimet, W. B., 2010, Landscape form and millennial erosion rates in the San Gabriel Mountains, CA: *Earth and Planetary Science Letters*, v. 289, no. 1–2, p. 134–144, doi: 10.1016/j.epsl.2009.10.036.

- Dietsch, C., Dortch, J. M., Reynhout, S. A., Owen, L. A., and Caffee, M. W., 2015, Very slow erosion rates and landscape preservation across the southwestern slope of the Ladakh Range, India: *Earth Surface Processes and Landforms*, v. 40, no. 3, p. 389–402, doi: 10.1002/esp.3640.
- Dortch, J. M., Dietsch, C., Owen, L. A., Caffee, M. W., and Ruppert, K., 2011a, Episodic fluvial incision of rivers and rock uplift in the Himalaya and Transhimalaya: *Journal of the Geological Society*, v. 168, no. 3, p. 783–804, doi: 10.1144/0016-76492009-158.
- Dortch, J. M., Owen, L. A., and Caffee, M. W., 2013, Timing and climatic drivers for glaciation across semi-arid western Himalayan–Tibetan orogen: *Quaternary Science Reviews*, v. 78, p. 188–208, doi: 10.1016/j.quascirev.2013.07.025.
- Dortch, J. M., Owen, L. A., Haneberg, W. C., Caffee, M. W., Dietsch, C., and Kamp, D. U., 2009, Nature and timing of large-landslides in the Himalaya and Transhimalaya of northern India: *Quaternary Science Reviews*, v. 28, no. 11–12, p. 1037–1054, doi: 10.1016/j.quascirev.2008.05.002.
- Dortch, J. M., Owen, L. A., Schoenbohm, L. M., and Caffee, M. W., 2011b, Asymmetrical erosion and morphological development of the central Ladakh Range, northern India: *Geomorphology*, v. 135, no. 1-2, p. 167–180, doi: 10.1016/j.geomorph.2011.08.014.
- Fedo, C. M., Nesbitt, H. W., and Young, G. M., 1995, Unraveling the effects of potassium metasomatism in sedimentary rocks and paleosols, with implications for paleoweathering conditions and provenance: *Geology*, v. 23, no. 10, p. 921–924, doi: 10.1130/0091-7613(1995)023<0921:UTEOPM>2.3.CO;2.
- Flint, J. J., 1974, Stream gradient as a function of order, magnitude, and discharge: *Water Resources Research*, v. 10, no. 5, p. 969–973, doi: 10.1029/WR010i005p00969.
- Frank, W., Thöni, M., and Purtscheller, F., Geology and petrography of Kulu-South Lahul area, *in Proceedings Colloq. Internat. CNRS Himalaya1977*, Volume 268, p. 147–160,
- Frihy, O., Lotfy, M., and Komar, P., 1995, Spatial variations in heavy minerals and patterns of sediment sorting along the Nile Delta, Egypt: *Sedimentary Geology*, v. 97, no. 1, p. 33–41, doi: 10.1016/0037-0738(94)00135-H.
- Fuchs, G., 1987, The Geology of Southern Zanskar (Ladakh) - Evidence for the Autochthony of the Tethys Zone of the Himalaya: *Jahrbuch der Geologischen Bundesanstalt*, v. 130, no. 4, p. 465–491,
- Gabet, E. J., Burbank, D. W., Pratt-Sitaula, B., Putkonen, J., and Bookhagen, B., 2008, Modern erosion rates in the High Himalayas of Nepal: *Earth and Planetary Science Letters*, v. 267, no. 3, p. 482–494, doi: 10.1016/j.epsl.2007.11.059.
- Gaetani, M., Casnedi, P., Fois, E., Garzanti, E., Jadoul, F., Nicora, A., and Tintori, A., 1986, Stratigraphy of the Tethys Himalaya in Zanskar, Ladakh: *Rivista Italiana di Paleontologia e Stratigrafia*, v. 91, no. 4, p. 443–478,
- Gaetani, M., Nicora, A., Silva, I. P., Fois, E., Garzanti, E., and Tintori, A., 1983, Upper Cretaceous and Paleocene in Zanskar Range (NW Himalaya), *Istituti di geologia e paleontologia dell'Università degli studi di Milano, Riv. It. Paleont. Strat.*,
- Garzanti, E., and Andò, S., 2007a, Heavy mineral concentration in modern sands: implications for provenance interpretation, *in* Mange, M. A., and Wright, D. T., eds., *Heavy Minerals in Use*, Volume 58, Elsevier, p. 517–545, doi: 10.1016/S0070-4571(07)58020-9.
- , 2007b, Plate tectonics and heavy mineral suites of modern sands, *in* Mange, M. A., and Wright, D. T., eds., *Heavy Minerals in Use*, Volume 58, Elsevier, p. 741–763, doi: 10.1016/S0070-4571(07)58029-5.

- Garzanti, E., Andò, S., France-Lanord, C., Censi, P., Vignola, P., Galy, V., and Lupker, M., 2011, Mineralogical and chemical variability of fluvial sediments 2. Suspended-load silt (Ganga–Brahmaputra, Bangladesh): *Earth and Planetary Science Letters*, v. 302, no. 1–2, p. 107–120, doi: 10.1016/j.epsl.2010.11.043.
- Garzanti, E., Andò, S., and Vezzoli, G., 2009, Grain-size dependence of sediment composition and environmental bias in provenance studies: *Earth and Planetary Science Letters*, v. 277, no. 3–4, p. 422–432, doi: 10.1016/j.epsl.2008.11.007.
- Garzanti, E., Casnedi, R., and Jadoul, F., 1986, Sedimentary evidence of a Cambro-Ordovician orogenic event in the northwestern Himalaya: *Sedimentary Geology*, v. 48, no. 3–4, p. 237–265, doi: 10.1016/0037-0738(86)90032-1.
- Garzanti, E., and Vezzoli, G., 2003, A classification of metamorphic grains in sands based on their composition and grade: *Journal of Sedimentary Research*, v. 73, no. 5, p. 830–837, DOI: 10.1306/012203730830.
- Garzanti, E., Vezzoli, G., Andò, S., Lavé, J. r. m., Attal, M. I., France-Lanord, C., and DeCelles, P., 2007, Quantifying sand provenance and erosion (Marsyandi River, Nepal Himalaya): *Earth and Planetary Science Letters*, v. 258, no. 3–4, p. 500–515, doi: 10.1016/j.epsl.2007.04.010.
- Gazzi, P., Zuffa, G. G., Gandolfi, G., and Paganelli, L., 1973, Provenienza e dispersione litoranea delle sabbie delle spiagge adriatiche fra le foci dell'Isonzo e del Foglia: inquadramento regionale: *Memorie della Società Geologica Italiana*, v. 12, p. 1–37,
- Gehrels, G. E., 2014, Detrital zircon U-Pb geochronology applied to tectonics: *Annual Review of Earth and Planetary Sciences*, v. 42, p. 127–149, doi: 10.1146/annurev-earth-050212-124012.
- Gehrels, G. E., Kapp, P., DeCelles, P., Pullen, A., Blakely, R., Weislgel, A., Ding, L., Guynn, J., Marin, A., McQuarrie, N., and Yin, A., 2011, Detrital zircon geochronology of pre-Tertiary strata in the Tibetan-Himalayan orogen: *Tectonics*, v. 30, no. 5, p. TC5016, doi 10.1029/2011TC002868.
- Girard, M., and Bussy, F., 1999, Late Pan-African magmatism in the Himalaya: new geochronological and geochemical data from the Ordovician Tso Morari metagranites (Ladakh, NW India): *Schweizerische mineralogische und petrographische Mitteilungen*, v. 79, no. 3, p. 399–418,
- Godard, V., Burbank, D. W., Bourlès, D. L., Bookhagen, B., Braucher, R., and Fisher, G. B., 2012, Impact of glacial erosion on ^{10}Be concentrations in fluvial sediments of the Marsyandi catchment, central Nepal: *Journal of Geophysical Research: Earth Surface*, v. 117, no. F3, p. F03013, doi: 10.1029/2011JF002230.
- Godin, L., 2001, The Chako Dome: an enigmatic structure in the hanging wall of the South Tibetan detachment, Nar Valley central Nepal: *Journal of Asian Earth Sciences*, v. 19, no. 3A, p. 22–23,
- Goldstein, S. L., O'Nions, R. K., and Hamilton, P. J., 1984, A Sm-Nd isotopic study of atmospheric dusts and particulates from major river systems: *Earth and Planetary Science Letters*, v. 70, no. 2, p. 221–236, doi: 10.1016/0012-821X(84)90007-4.
- Goodbred, S. L., 2003, Response of the Ganges dispersal system to climate change: a source-to-sink view since the last interstadial: *Sedimentary Geology*, v. 162, no. 1–2, p. 83–104, doi: 10.1016/S0037-0738(03)00217-3.
- Green, O. R., Searle, M. P., Corfield, R. I., and Corfield, R. M., 2008, Cretaceous-Tertiary carbonate platform evolution and the age of the India-Asia collision along the Ladakh

- Himalaya (northwest India): The Journal of Geology, v. 116, no. 4, p. 331–353, doi: 10.1086/588831.
- Griffin, W. L., Powell, W. J., Pearson, N. J., and O'Reilly, S. Y., 2008, GLITTER: data reduction software for laser ablation ICP-MS: Laser Ablation-ICP-MS in the earth sciences. Mineralogical association of Canada short course series, v. 40, p. 204–207,
- Hack, J. T., 1957, Studies of longitudinal stream profiles in Virginia and Maryland, 2330-7102,
- Hales, T., and Roering, J. J., 2007, Climatic controls on frost cracking and implications for the evolution of bedrock landscapes: Journal of Geophysical Research: Earth Surface, v. 112, no. F2,
- He, M., Zheng, H., and Clift, P. D., 2013, Zircon U-Pb geochronology and Hf isotope data from the Yangtze River sands: Implications for major magmatic events and crustal evolution in Central China: Chemical Geology, v. 360–261, p. 186–203, doi: 10.1016/j.chemgeo.2013.10.020.
- Hedrick, K. A., Seong, Y. B., Owen, L. A., Caffee, M. W., and Dietsch, C., 2011, Towards defining the transition in style and timing of Quaternary glaciation between the monsoon-influenced Greater Himalaya and the semi-arid Transhimalaya of Northern India: Quaternary International, v. 236, no. 1–2, p. 21–33, doi: 10.1016/j.quaint.2010.07.023.
- Henderson, A. L., Najman, Y., Parrish, R., BouDagher-Fadel, M., Barford, D., Garzanti, E., and Andò, S., 2010, Geology of the Cenozoic Indus Basin sedimentary rocks: Paleoenvironmental interpretation of sedimentation from the western Himalaya during the early phases of India-Eurasia collision Tectonics, v. 29, no. 6, p. TC6015, doi: 10.1029/2009TC002651.
- Herren, E., 1987, Zanskar Shear Zone: northeast-south- west extension within the Higher Himalaya: Geology, v. 15, no. 5, p. 409–413, doi: 10.1130/0091-7613(1987)15<409:ZSZN>2.0.CO;2.
- Herzschuh, U., 2006, Palaeo-moisture evolution in monsoonal Central Asia during the last 50,000 years: Quaternary Science Reviews, v. 25, no. 1-2, p. 163-178, doi: 10.1016/j.quascirev.2005.02.006.
- Hobley, D. E., Sinclair, H. D., and Mudd, S. M., 2012, Reconstruction of a major storm event from its geomorphic signature: The Ladakh floods, 6 August 2010: Geology, v. 40, no. 6, p. 483–486, doi: 10.1130/G32935.1.
- Hodges, K. V., Wobus, C., Ruhl, K., Schildgen, T., and Whipple, K., 2004, Quaternary deformation, river steepening, and heavy precipitation at the front of the Higher Himalayan ranges: Earth and Planetary Science Letters, v. 220, no. 3–4, p. 379–389, doi: 10.1016/S0012-821X(04)00063-9.
- Honegger, K., Dietrich, V., Frank, W., Gansser, A., Thoni, M., and Trommsdorf, V. F., 1982, Magmatism and metamorphism in the Ladakh Himalayas (The Indus-Tsangpo suture zone): Earth and Planetary Science Letters, v. 60, no. 2, p. 253–292, doi: 10.1016/0012-821X(82)90007-3.
- Honegger, K. H., 1983, Strukturen und metamorphose im ZanskarkristallinPhD]: Eidgenössische Technische Hochschule (E.T.H.), 117 p,
- Horton, F., Lee, J., Hacker, B., Bowman-Kamaha'o, M., and Cosca, M., 2015, Himalayan gneiss dome formation in the middle crust and exhumation by normal faulting: New geochronology of Gianbul dome, northwestern India: Geological Society of America Bulletin, v. 127, no. 1–2, p. 162–180, doi: 10.1130/B31005.1.

- Horton, F., and Leech, M. L., 2013, Age and origin of granites in the Karakoram shear zone and Greater Himalaya Sequence, NW India: *Lithosphere*, v. 5, no. 3, p. 300–320, doi: 10.1130/L213.1.
- Hu, X.-M., Garzanti, E., An, W., and Hu, X.-F., 2015, Provenance and drainage system of the Early Cretaceous volcanic detritus in the Himalaya as constrained by detrital zircon geochronology: *Journal of Palaeogeography*, v. 4, no. 1, p. 85–98, doi: 10.3724/SP.J.1261.2015.00069.
- Hu, X.-M., Sinclair, H. D., Wang, J., Jiang, H., and Wu, F., 2012, Late Cretaceous-Palaeogene stratigraphic and basin evolution in the Zhepure Mountain of southern Tibet: implications for the timing of India-Asia initial collision: *Basin Research*, v. 24, no. 5, p. 520–543, doi: 10.1111/j.1365-2117.2012.00543.x.
- Ingersoll, R. V., Bullard, T. F., Ford, R. L., Grimm, J. P., Pickle, J. D., and Sares, S. W., 1984, The effect of grain size on detrital modes: A test of the Gazzi-Dickinson point-counting method: *Journal of Sedimentary Petrology*, v. 54, no. 1, p. 103–116, doi: 10.1306/212F83B9-2B24-11D7-8648000102C1865D.
- Jacobsen, S. B., and Wasserburg, G. J., 1980, Sm-Nd isotopic evolution of chondrites: *Earth and Planetary Science Letters*, v. 50, no. 1, p. 139–155, doi: 10.1016/0012-821X(80)90125-9.
- Jade, S., Rao, H. J. R., Vijayan, M. S. M., Gaur, V. K., Bhatt, B. C., Kumar, K., Jaganathan, S., Ananda, M. B., and Kumar, P. D., 2010, GPS-derived deformation rates in northwestern Himalaya and Ladakh: *International Journal of Earth Sciences*, v. 100, no. 6, p. 1293–1301, doi: 10.1007/s00531-010-0532-3.
- Jarvis, A., Reuter, H. I., Nelson, A., and Guevara, E., 2008, Hole-filled SRTM for the globe Version 4, in Research, C. G. o. I. A., ed., CGIAR-CSI SRTM 90m Database <http://srtm.cgiar.org>,
- Kirby, E., and Ouimet, W., 2011, Tectonic geomorphology along the eastern margin of Tibet: Insights into the pattern and processes of active deformation adjacent to the Sichuan Basin, in Gloaguen, R., and Ratschbacher, L., eds., *Growth and Collapse of the Tibetan Plateau*, Volume 353: London, Geological Society, p. 165–188, doi: 10.1144/SP353.9.
- Kirby, E., and Whipple, K., 2001, Quantifying differential rock-uplift rates via stream profile analysis: *Geology*, v. 29, no. 5, p. 415–418, doi: 10.1130/0091-7613(2001)029<0415:QDRURV>2.0.CO;2.
- Kwatra, S. K., Singh, S., Singh, V. P., Sharma, R. K., Rai, B., and Kishor, N., 1999, Geochemical and geochronological characteristics of the Early Paleozoic granitoids from Sutlej-Baspa Valleys, Himachal Himalayas: *Gondwana Research Group Memoirs*, v. 6, p. 145–158,
- Lavé, J., and Avouac, J. P., 2001, Fluvial incision and tectonic uplift across the Himalaya of central Nepal: *Journal of Geophysical Research*, v. 106, no. B11, p. 26561–26592, doi: 10.1029/2001JB000359.
- Leipe, C., Demske, D., Tarasov, P. E., Wünnemann, B., and Riedel, F., 2014, Potential of pollen and non-pollen palynomorph records from Tso Moriri (Trans-Himalaya, NW India) for reconstructing Holocene limnology and human–environmental interactions: *Quaternary International*, v. 348, p. 113–129, doi: 10.1016/j.quaint.2014.02.026.
- Leloup, P. H., Mahéo, G., Arnaud, N., Kali, E., Boutonnet, E., Liu, D., Xiaohan, L., and Haibing, L., 2010, The South Tibet detachment shear zone in the Dinggye area Time constraints on extrusion models of the Himalayas: *Earth and Planetary Science Letters*, v. 292, no. 1–2, p. 1–16, doi:10.1016/j.epsl.2009.12.035.

- McQuarrie, N., Robinson, D., Long, S., Tobgay, T., Grujic, D., Gehrels, G., and Ducea, M., 2008, Preliminary stratigraphic and structural architecture of Bhutan: Implications for the along strike architecture of the Himalayan system: *Earth and Planetary Science Letters*, v. 272, no. 1–2, p. 105–117, doi: 10.1016/j.epsl.2008.04.030.
- Mehta, P. K., 1977, Rb-Sr geochronology of the Kulu-Mandi belt: its implications for the Himalayan tectogenesis: *Geologische Rundschau*, v. 66, no. 1, p. 156–175, doi: 10.1007/BF01989570.
- Miller, C., Thöni, M., Frank, W., Grasemann, B., Klötzli, U., Guntli, P., and Draganits, E., 2001, The early Palaeozoic magmatic event in the Northwest Himalaya, India: source, tectonic setting and age of emplacement: *Geological Magazine*, v. 138, no. 03, p. 237–251, doi: 10.1017/S0016756801005283.
- Milliman, J. D., and Meade, R. H., 1983, World-wide delivery of sediment to the oceans: *Journal of Geology*, v. 91, no. 1, p. 1–21,
- Mitchell, W. A., Taylor, P. J., and Osmaston, H., 1999, Quaternary geology in Zanskar, NW Indian Himalaya: evidence for restricted glaciation and preglacial topography: *Journal of Asian Earth Sciences*, v. 17, no. 3, p. 307–318, doi: 10.1016/S0743-9547(98)00069-5.
- Munack, H., Blöthe, J. H., Fülop, R. H., Codilean, A. T., Fink, D., and Korup, O., 2016, Recycling of Pleistocene valley fills dominates 135 ka of sediment flux, upper Indus River: *Quaternary Science Reviews*, v. 149, p. 122–134, <http://dx.doi.org/10.1016/j.quascirev.2016.07.030>.
- Munack, H., Korup, O., Resentini, A., Limonta, M., Garzanti, E., Blöthe, J. H., Scherler, D., Wittmann, H., and Kubik, P. W., 2014, Postglacial denudation of western Tibetan Plateau margin outpaced by long-term exhumation: *Geological Society of America Bulletin*, v. 126, no. 11–12, p. 1580–1594, doi: 10.1130/B30979.1.
- Myrow, P. M., Hughes, N. C., Goodge, J. W., Fanning, C. M., Williams, I. S., Peng, S., Bhargava, O. N., Parcha, S. K., and Pogue, K. R., 2010, Extraordinary transport and mixing of sediment across Himalayan central Gondwana during the Cambrian-Ordovician: *Geological Society of America Bulletin*, v. 122, no. 9–10, p. 1660–1670, doi: 10.1130/B30123.1.
- Myrow, P. M., Hughes, N. C., Paulsen, T., Williams, I., Parcha, S. K., Thompson, K. R., Bowring, S. A., Peng, S.-C., and Ahluwalia, A. D., 2003, Integrated tectonostratigraphic analysis of the Himalaya and implications for its tectonic reconstruction: *Earth and Planetary Science Letters*, v. 212, no. 3–4, p. 433–441, doi: 10.1016/S0012-821X(03)00280-2.
- Nesbitt, H. W., Markovics, G., and Price, R. C., 1980, Chemical processes affecting alkalis and alkaline earths during continental weathering: *Geochimica et Cosmochimica Acta*, v. 44, no. 11, p. 1659–1666, doi: 10.1016/0016-7037(80)90218-5.
- Noble, S. R., and Searle, M. P., 1995, Age of Crustal Melting and Leukogranite Formation from U-Pb Zircon and Monazite Dating in the Western Himalaya, Zanskar, India: *Geology*, v. 23, no. 12, p. 1135–1138, doi: 10.1130/0091-7613(1995)023<1135:AOCMAL>2.3.CO;2.
- Noble, S. R., Searle, M. P., and Walker, C. B., 2001, Age and tectonic significance of Permian granites in western Zanskar, High Himalaya: *Journal of Geology*, v. 109, no. 1, p. 127–135,
- Ouimet, W. B., Whipple, K. X., and Granger, D. E., 2009, Beyond threshold hillslopes: Channel adjustment to base-level fall in tectonically active mountain ranges: *Geology*, v. 37, no. 7, p. 579–582, doi: 10.1130/G30013A.1.

- Owen, L. A., 2011, Quaternary Glaciation of Northern India, *Developments in Quaternary Science*, Volume 15, Elsevier, p. 14, doi: 10.1016/b978-0-444-53447-7.00067-2.
- Owen, L. A., and Benn, D. I., 2005, Equilibrium-line altitudes of the last glacial maximum for the Himalaya and Tibet; an assessment and evaluation of results: *Quaternary International*, v. 138–139, p. 55–78, doi: 10.1016/j.quaint.2005.02.006.
- Owen, L. A., Finkel, R. C., Barnard, P. L., Ma, H., Asahi, K., Caffee, M. W., and Derbyshire, E., 2005, Climatic and topographic controls on the style and timing of late Quaternary glaciation throughout Tibet and the Himalaya defined by ^{10}Be cosmogenic radionuclide surface exposure dating: *Quaternary Science Reviews*, v. 24, no. 12–13, p. 1391–1411, doi: 10.1016/j.quascirev.2004.10.014.
- Owen, L. A., Finkel, R. C., and Caffee, M. W., 2002, A note on the extent of glaciation throughout the Himalaya during the global Last Glacial Maximum: *Quaternary Science Reviews*, v. 21, no. 1–3, p. 147–157, doi: 10.1016/S0277-3791(01)00104-4.
- Pearce, N. J. G., Perkins, W. T., Westgate, J. A., Gorton, M. P., Jackson, S. E., Neal, C. R., and Chenery, S. P., 1997, A Compilation of New and Published Major and Trace Element Data for NIST SRM 610 and NIST SRM 612 Glass Reference Materials: *Geostandards Newsletter*, v. 21, no. 1, p. 115–144, doi: 10.1111/j.1751-908X.1997.tb00538.x.
- Pedersen, R. B., Searle, M. P., and Corfield, R. I., 2001, U–Pb zircon ages from the Spontang Ophiolite, Ladakh Himalaya: *Journal of the Geological Society*, v. 158, no. 3, p. 513–520, doi: 10.1144/jgs.158.3.513.
- Pognante, U., Castelli, D., Benna, P., Genovese, G., Oberli, F., Meier, M., and Tonarini, S., 1990, The crystalline units of the High Himalayas in the Lahul-Zanskar region (northwest India): metamorphic history and geochronology of the collided and imbricated Indian plate: *Geological Magazine*, v. 127, no. 02, p. 101–116, doi: 10.1017/S0016756800013807.
- Pognante, U., and Lombardo, B., 1989, Metamorphic evolution of the High Himalayan Crystallines in SE Zanskar, India: *Journal of Metamorphic Geology*, v. 7, p. 9–17,
- Raczek, I., Jochum, K. P., and Hofmann, A. W., 2003, Neodymium and Strontium Isotope Data for USGS Reference Materials BCR-1, BCR-2, BHVO-1, BHVO-2, AGV-1, AGV-2, GSP-1, GSP-2 and Eight MPI-DING Reference Glasses: *Geostandards Newsletter*, v. 27, no. 2, p. 173–179, doi: 10.1111/j.1751-908X.2003.tb00644.x.
- Robinson, D. M., DeCelles, P. G., and Copeland, P., 2006, Tectonic evolution of the Himalayan thrust belt in western Nepal; implications for channel flow models: *Geological Society of America Bulletin*, v. 118, no. 7–8, p. 865–885,
- Robinson, D. M., DeCelles, P. G., Patchett, P. J., and Garzione, C. N., 2001, The kinematic evolution of the Nepalese Himalaya interpreted from Nd isotopes: *Earth and Planetary Science Letters*, v. 192, no. 4, p. 507–521, doi: 10.1016/S0012-821X(01)00451-4.
- Robinson, R. A. J., Brezina, C. A., Parrish, R. R., Horstwood, M. S. A., Oo, N. W., Bird, M. I., Thein, M., Walters, A. S., Oliver, G. J., and Zaw, K., 2014, Large rivers and orogens: The evolution of the Yarlung Tsangpo–Irrawaddy system and the eastern Himalayan syntaxis: *Gondwana Research*, v. 26, no. 1, p. 112–121, doi: 10.1016/j.gr.2013.07.002.
- Robyr, M., Hacker, B. R., and Mattinson, J. M., 2006, Doming in compressional orogenic settings: new geochronological constraints from the NW Himalaya: *Tectonics*, v. 25, no. 2, p. TC2007, doi: 10.1029/2004TC001774.

- Roe, G. H., Montgomery, D. R., and Hallet, B., 2002, Effects of orographic precipitation variations on the concavity of steady-state river profiles: *Geology*, v. 30, no. 2, p. 143–146, doi: 10.1130/0091-7613(2002)030<0143:EOOPVO>2.0.CO;2.
- Scherler, D., 2014, Climatic limits to headwall retreat in the Khumbu Himalaya, eastern Nepal: *Geology*, v. 42, no. 11, p. 1019–1022,
- Schlup, M., Carter, A., Cosca, M., and Steck, A., 2003, Exhumation history of eastern Ladakh revealed by ^{40}Ar - ^{39}Ar and fission track ages: The Indus River-Tso Morari transect, NW Himalaya: *Journal of the Geological Society*, v. 160, p. 385–399, doi: 10.1144/0016-764902-084.
- Schlup, M., Steck, A., Carter, A., Cosca, M., Epard, J.-L., and Hunziker, J., 2011, Exhumation history of the NW Indian Himalaya revealed by fission track and ^{40}Ar / ^{39}Ar ages: *Journal of Asian Earth Sciences*, v. 40, no. 1, p. 334–350, doi: 10.1016/j.jseas.2010.06.008.
- Schwanghart, W., and Scherler, D., 2014, Short Communication: TopoToolbox 2 – MATLAB-based software for topographic analysis and modeling in Earth surface sciences: *Earth Surf. Dynam.*, v. 2, no. 1, p. 1–7, 10.5194/esurf-2-1-2014.
- Searle, M., Waters, D. J., Rex, D. C., and Wilson, R. N., 1992, Pressure, temperature, and time constraints on Himalayan metamorphism from eastern Kashmir and western Zanskar: *Journal of the Geological Society*, London, v. 149, p. 753–773,
- Searle, M. P., 1983, On the Tectonics of the Western Himalaya: *Episodes*, no. 4, p. 21–26,
- Searle, M. P., Pickering, K. T., and Cooper, D. J. W., 1990, Restoration and Evolution of the Intermontane Indus Molasse Basin, Ladakh Himalaya, India: *Tectonophysics*, v. 174, no. 3–4, p. 301–314, doi: 10.1016/0040-1951(90)90327-5.
- Shellnutt, J., Bhat, G., Brookfield, M., and Jahn, B. M., 2011, No link between the Panjal Traps (Kashmir) and the Late Permian mass extinctions: *Geophysical Research Letters*, v. 38, no. 19, p. L19308, doi: 10.1029/2011GL049032.
- Shellnutt, J. G., Bhat, G. M., Wang, K.-L., Brookfield, M. E., Jahn, B.-M., and Dostal, J., 2014, Petrogenesis of the flood basalts from the Early Permian Panjal Traps, Kashmir, India: Geochemical evidence for shallow melting of the mantle: *Lithos*, v. 204, p. 159–171, doi: 10.1016/j.lithos.2014.01.008.
- Shi, Y., Yu, G., Liu, X., Li, B., and Yao, T., 2001, Reconstruction of the 30–40ka bp enhanced Indian monsoon climate based on geological records from the Tibetan Plateau: *Palaeogeography, Palaeoclimatology, Palaeoecology*, v. 169, no. 1, p. 69–83, 10.1016/S0031-0182(01)00216-4.
- Shrestha, F., Bajracharya, S., Maharjan, S., and Guo, W., 2014, GLIMS Glacier Database Version 1: Boulder, Colorado USA, NSIDC: National Snow and Ice Data Center, <http://dx.doi.org/10.7265/N5V98602>.
- Singh, M., Sharma, M., and Tobschall, H. J., 2005, Weathering of the Ganga alluvial plain, northern India: implications from fluvial geochemistry of the Gomati River: *Applied Geochemistry*, v. 20, no. 1, p. 1–21, doi: 10.1016/j.apgeochem.2004.07.005.
- Singh, M. P., Manda, M. M., and Sinha, P. K., 1976, The Ralakung volcanics of the Zanskar valley (Ladakh), its geological setting, petrography, petrogeochemistry and a comparative study with the Panjal volcanics of the NW Himalaya: *Geological Survey of India Miscellaneous Publications*, v. 41, p. 218–228,
- Sklar, L., and Dietrich, W. E., 1998, River longitudinal profiles and bedrock incision models: Stream power and the influence of sediment supply, in Tinkler, K. J., and Wohl, E. E., eds., *Rivers over rock: fluvial processes in bedrock channels*, Volume Geophysical

- Monograph: Washington, D.C., American Geophysical Union, p. 237–260, doi: 10.1029/GM107p0237.
- Sláma, J., Košler, J., Condon, D. J., Crowley, J. L., Gerdes, A., Hanchar, J. M., Horstwood, M. S. A., Morris, G. A., Nasdala, L., Norberg, N., Schaltegger, U., Schoene, B., Tubrett, M. N., and Whitehouse, M. J., 2008, Plezovice zircon A new natural reference material for U–Pb and Hf isotopic microanalysis: *Chemical Geology*, v. 249, no. 1–2, p. 1–35, doi: 10.1016/j.chemgeo.2007.11.005.
- Spring, L., Bussy, F., Vannay, J.-C., Huon, S., and Cosca, M., 1993, Early Permian granitic dykes of alkaline affinity in the Indian High Himalaya of Upper Lahul and SE Zanskar: geochemical characterization and geotectonic implications: Geological Society, London, Special Publications, v. 74, no. 1, p. 251–264, doi: 10.1144/GSL.SP.1993.074.01.18.
- Srivastava, P., Tripathi, J. K., Islam, R., and Jaiswal, M. K., 2008, Fashion and phases of Late Pleistocene aggradation and incision in Alaknanda River, western Himalaya India: *Quaternary Research*, v. 70, no. 1, p. 68–80, doi: 10.1016/j.yqres.2008.03.009.
- Steck, A., Spring, L., Vannay, J. C., Masson, H., Stutz, E., Bucher, H., ... & Tièche, J. C. , 1993, Geological transect across the northwestern Himalaya in eastern Ladakh and Lahul (a model for the continental collision of India and Asia): *Eclogae Geologicae Helvetiae* v. 86, no. 1, p. 219–263,
- Stolle, A., Langer, M., Blöthe, J. H., and Korup, O., 2015, On predicting debris flows in arid mountain belts: *Global and Planetary Change*, v. 126, p. 1–13, <http://dx.doi.org/10.1016/j.gloplacha.2014.12.005>.
- Stutz, E., and Thöni, M., 1987, The lower Paleozoic Nyimaling granite in the Indian Himalaya (Ladakh): new Rb/Sr data versus zircon typology: *Geologische Rundschau*, v. 76, no. 2, p. 307–315, doi: 10.1007/BF01821076.
- Tanaka, T., Togashi, S., Kamioka, H., Amakawa, H., Kagami, H., Hamamoto, T., Yuhara, M., Orihashi, Y., Yoneda, S., Shimizu, H., Kunimaru, T., Takahashi, K., Yanagi, T., Nakano, T., Fujimaki, H., Shinjo, R., Asahara, Y., Tanimizu, M., and Dragusanu, C., 2000, JNd-1: a neodymium isotopic reference in consistency with LaJolla neodymium: *Chemical Geology*, v. 168, no. 3–4, p. 279–281, doi: 10.1016/S0009-2541(00)00198-4.
- Taylor, P. J., and Mitchell, W. A., 2000, The Quaternary glacial history of the Zanskar Range, north-west Indian Himalaya: *Quaternary International*, v. 65–66, p. 81–99, doi: 10.1016/S1040-6182(99)00038-5.
- Thiede, R. C., Bookhagen, B., Arrowsmith, J. R., Sobel, E. R., and Strecker, M. R., 2004, Climatic control on rapid exhumation along the Southern Himalayan Front: *Earth and Planetary Science Letters*, v. 222, no. 3–4, p. 791–806, doi: 10.1016/j.epsl.2004.03.015.
- Thirlwall, M. F., 1991, Long-term reproducibility of multicollector Sr and Nd isotope ratio analysis: *Chemical Geology: Isotope Geoscience section*, v. 94, no. 2, p. 85–104, doi: 10.1016/0168-9622(91)90002-E.
- Tucker, G. E., and Whipple, K. X., 2002, Topographic outcomes predicted by stream erosion models: Sensitivity analysis and intermodel comparison: *Journal of Geophysical Research: Solid Earth*, v. 107, no. B9, p. ETG 1-1–ETG 1-16, doi: 10.1029/2001JB000162.
- Vermeesch, P., 2004, How many grains are needed for a provenance study?: *Earth and Planetary Science Letters*, v. 224, no. 3–4, p. 351–441, doi: 10.1016/j.epsl.2004.05.037.
- Vermeesch, P., 2012, On the visualisation of detrital age distributions: *Chemical Geology*, v. 312–313, p. 190–194, doi: 10.1016/j.chemgeo.2012.04.021.

- Vermeesch, P., 2013, Multi-sample comparison of detrital age distributions: *Chemical Geology*, v. 341, p. 140–146, doi: 10.1016/j.chemgeo.2013.01.010.
- Vermeesch, P., Resentini, A., and Garzanti, E., 2016, An R package for statistical provenance analysis: *Sedimentary Geology*, v. 336, p. 14–25, doi: 10.1016/j.sedgeo.2016.01.009.
- Walker, C. B., Searle, M. P., and Waters, D. J., 2001, An integrated tectonothermal model for the evolution of the High Himalaya in western Zanskar with constraints from thermobarometry and metamorphic modeling: *Tectonics*, v. 20, no. 6, p. 810–833, doi: 10.1029/2000TC001249.
- Walker, J., Martin, M. W., Bowring, S. A., Searle, M., Waters, D. J., and Hodges, K., 1999, Metamorphism, melting, and extension: Age constraints from the High Himalayan Slab of southeast Zanskar and northwest Lahaul: *Journal of Geology*, v. 107, no. 4, p. 473–495,
- Wallis, D., Carter, A., Phillips, R. J., Parsons, A. J., and Searle, M. P., 2016, Spatial variation in exhumation rates across Ladakh and the Karakoram: New apatite fission track data from the Eastern Karakoram, NW India: *Tectonics*, v. 35, no. 3, p. 704–721, doi: 10.1002/2015TC003943.
- Whipple, K., Wobus, C., Crosby, B., Kirby, E., and Sheehan, D., 2007, New tools for quantitative geomorphology: extraction and interpretation of stream profiles from digital topographic data, Geological Society of America Short Course, Volume 506: Boulder, CO, GSA,
- Whipple, K. X., and Tucker, G. E., 2002, Implications of sediment-flux-dependent river incision models for landscape evolution: *Journal of Geophysical Research: Solid Earth*, v. 107, no. B2, p. ETG 3-1-ETG 3-20, 10.1029/2000JB000044.
- White, L. T., Ahmad, T., Ireland, T. R., Lister, G. S., and Forster, M. A., 2011, Deconvolving episodic age spectra from zircons of the Ladakh Batholith, northwest Indian Himalaya: *Chemical Geology*, v. 289, no. 3–4, p. 179–196, doi: 10.1016/j.chemgeo.2011.07.024.
- Wiedenbeck, M., Hanchar, J. M., Peck, W. H., Sylvester, P., Valley, J., Whitehouse, M., Kronz, A., Morishita, Y., Nasdala, L., Fiebig, J., Franchi, I., Girard, J. P., Greenwood, R. C., Hinton, R., Kita, N., Mason, P. R. D., Norman, M., Ogasawara, M., Piccoli, P. M., Rhede, D., Satoh, H., Schulz-Dobrick, B., Skår, O., Spicuzza, M. J., Terada, K., Tindle, A., Togashi, S., Vennemann, T., Xie, Q., and Zheng, Y. F., 2004, Further Characterisation of the 91500 Zircon Crystal: *Geostandards and Geoanalytical Research*, v. 28, no. 1, p. 9–39, doi: 10.1111/j.1751-908X.2004.tb01041.x.
- Winter, J. D., 2010, Principles of igneous and metamorphic petrology, New York, Prentice Hall
- Wobus, C., Whipple, K. X., Kirby, E., Snyder, N., Johnson, J., Spyropolou, K., Crosby, B., and Sheehan, D., 2006, Tectonics from topography: Procedures, promise, and pitfalls, in Willett, S. D., Hovius, N., Brandon, M. T., and Fisher, D. M., eds., *Tectonics, Climate, and Landscape Evolution*, Volume 398: Boulder, CO, Geological Society of America, p. 55–74, 10.1130/2006.2398(04).
- Wu, F. Y., Clift, P. D., and Yang, J. H., 2007, Zircon Hf isotopic constraints on the sources of the Indus Molasse, Ladakh Himalaya, India: *Tectonics*, v. 26, no. 2, p. TC2014, doi: 10.1029/2006TC002051.
- Wulf, H., Bookhagen, B., and Scherler, D., 2010, Seasonal precipitation gradients and their impact on fluvial sediment flux in the Northwest Himalaya: *Geomorphology*, v. 118, no. 1–2, p. 13–21, doi: 10.1016/j.geomorph.2009.12.003.

- Wulf, H., Bookhagen, B., and Scherler, D., 2012, Climatic and geologic controls on suspended sediment flux in the Sutlej River Valley, western Himalaya: Hydrology and Earth System Sciences Discussions, v. 9, p. 541–594, doi: 10.5194/hessd-9-541-2012.
- Wünnemann, B., Demske, D., Tarasov, P., Kotlia, B. S., Reinhardt, C., Bloemendal, J., Diekmann, B., Hartmann, K., Krois, J., and Riedel, F., 2010, Hydrological evolution during the last 15kyr in the Tso Kar lake basin (Ladakh, India), derived from geomorphological, sedimentological and palynological records: Quaternary Science Reviews, v. 29, no. 9-10, p. 1138-1155, 10.1016/j.quascirev.2010.02.017.
- Yang, S., Zhang, F., and Wang, Z., 2012, Grain size distribution and age population of detrital zircons from the Changjiang (Yangtze) River system, China: Chemical Geology, v. 296-297, p. 26–38, doi: 10.1016/j.chemgeo.2011.12.016.

FIGURE CAPTIONS

Figure 1. Digital elevation model (DEM) maps of South Asia, the Himalaya, and Zanskar River basin. (A) Shuttle Radar Topography Mission 90 m (SRTM90) map of South Asia depicting the Indus River (gray lines) and all Himalayan river drainage outlines above 500 m (black lines). Gray overlay shows location of Figure 4; (B) SRTM DEM and hillshade of all Himalayan drainage basins with location of the Zanskar River basin (Fig. 1C) outlined in black; (C) Topographic map of the Zanskar River basin with sample numbers and locations. Glacial extent from Global Land Ice Measurements from Space (GLIMS) Version 1 data (Shrestha et al., 2014). Drainage basin polygons provided freely online by Bodo Bookhagen. Sample locations noted with white dots and village locations with black squares. Numbers in circles are after Table 1. Dashed gray line indicates extent of internally drained Tso Kar basin. Village names abbreviated as: C = Chilling; HN = Hanumil; PG = Pang; PM = Padum; PS = Pishu; and SR = Sarchu.

Figure 2. Swath profiles for topography and rainfall across the Himalayan front and into the Himalayan rain shadow. Values for profiles were extracted from a 50 km by 280 km transect shown in Fig. 1A. Solid lines indicate mean values with shaded regions signifying $\pm 2\sigma$.

Figure 3. Simplified geologic map of the Zanskar River basin after Fuchs (1987) with additions from Zanskar Shear Zone from Dèzes et al. (1999), southern Zanskar (Lahul) from Steck et al. (1993) and Tso Kar area (Epard and Steck, 2008). N-T = Nyimaling-Tso Morari gneiss dome.

Figure 4. Parameter maps for evaluating morphology and erosion in the Zanskar River basin. (A) TRMM mean annual rainfall distribution map illustrating the precipitation gradient from west to east. Rainfall map was created using the 1998–2009 TRMM time series for mean annual rainfall; (B) Mean slope for the Zanskar River basin calculating using a 1-km radius circular moving window; (C) Local 5-km relief expressed as the difference between maximum and minimum elevation in a given area of a 5-km radius circular moving window; (D) Normalized channel steepness index (k_{sn}) calculated using TopoToolbox 2.0 (Schwanghart and Scherler, 2014). Subcatchments within the Zanskar River basin are outlined in gray in Figs. 2A-C.

Figure 5. Longitudinal profiles for tributaries of the Zanskar River. (A) Raw channel profiles were smoothed using a 2 km radius moving average window to remove elevation spikes. Black dashed lines mark trunk river tributaries; light gray dotted lines mark minor tributaries to Tsarap River catchment. Arrows indicate published locations of recessional moraines (Burbank and Fort, 1985; Damm, 2006; Mitchell et al., 1999; Owen and Benn, 2005); (B) Mean normalized channel steepness index (k_{sn}) values plotted for every 2 km segment along river longitudinal

profiles for all main streams. Values were extracted using MATLAB code adapted from TopoToolbox 2.0 (Schwanghart and Scherler, 2014). Abbreviations for streams are: K = Khurna; M = Markha; O = Oma Chu; S = Stod;; T = Tsarap; TC = Tsarap Chu; TZ = Toze Lungpa; and Y = Yunam.

Figure 6. Bulk petrographic compositions of Zanskar sediments. (A) Bulk compositions classified by Q (quartz), F (feldspathic), and L (lithic) framework grains following the Gazzi-Dickinson method of point counting (Ingersoll et al., 1984) and classified after Garzanti and Vezzoli (2003). Gray lines indicate data corrections for Source Rock Density (SRD; Vermeesch et al., (in press). Open diamonds are petrographic data from the lower Zanskar Gorge, where Z = Zanskar-Indus confluence and M = Markha River (Blöthe et al., 2014); (B) Bulk composition of Zanskar sediments plotted onto the (garnet + kyanite + sillimanite) – pyroxene – (zircon + tourmaline + rutile + amphibole + epidote) ternary diagram. Fields for Greater Himalaya “Formation I” kyanite- and fibrolite-bearing gneiss, Tethyan and Lesser Himalaya drawn after Garzanti et al. (2007). Samples are numbered after Table 1.

Figure 7. Bulk major element geochemistry of Zanskar River sediments plotted on the ternary $\text{Al}_2\text{O}_3\text{-CaO+Na}_2\text{O-K}_2\text{O}$ diagram (Fedo et al., 1995) with Chemical Index of Alteration (CIA) values (Nesbitt et al., 1980). Mineral abbreviations are as follows: bt = biotite; chl = chlorite; gb = gibbsite; il = illite; kao = kaolinite; ksp = potassium feldspar; m = muscovite; pl = plagioclase; sm = smectite. Samples for average Archean upper crust (gray square), average granodiorite (open square), average granite (open diamond), and average A-type granite (gray diamond) are shown (Anderson and Bender, 1989; Condie, 1993; Winter, 2010). Line indicates typical

weathering evolution path for bedrock unaffected by K-metasomatism (Fedo et al., 1995).

Samples are numbered after Table 1.

Figure 8. Crossplot of ϵ_{Nd} and $^{87}\text{Sr}/^{86}\text{Sr}$ compositions for Zanskar River sediments compared to other bedrock data from the Panjal Traps (Shellnutt et al., 2012; Shellnutt et al., 2014), the Greater and Lesser Himalaya (Ahmad et al., 2000; Deniel et al., 1987; Inger and Harris, 1993; Parrish and Hodges, 1996), Transhimalaya (Rolland et al., 2002), and additional Tethyan Himalaya (diamonds) and Greater Himalaya (squares) (Richards et al., 2005) from the Sutlej River. Samples are numbered after Table 1.

Figure 9. Diagram showing the progressive downstream variation in bulk sediment (A) $^{87}\text{Sr}/^{86}\text{Sr}$ and (B) ϵ_{Nd} compositions for the Zanskar River. Error bars are smaller than symbol size for propagated Sr and ϵ_{Nd} errors. Samples are numbered after Table 1.

Figure 10. KDE diagrams of U-Pb zircon ages from Zanskar River sediments.

Figure 11. Schematic diagram illustrating detrital framework grain and detrital zircon populations of Zanskar sands. Q = quartz; F = feldspars; Lc = lithic carbonate; Lsm = other sedimentary and low-rank metasedimentary; Lm = medium- to high-rank metamorphic; and Lv = volcanic and metavolcanic. Rank of metamorphic grains and MI index (0–500; Garzanti and Vezzoli (2003). Concentrations of Zr $>>$ 300 ppm may indicate hydraulic sorting and enrichment of sample in dense phases. Black line denotes trunk Zanskar River, with gray lines for tributaries. Samples are numbered after Table 1.

Figure 12. Multidimensional scaling (MDS) plots showing the Kolmogorov-Smirnov distances between Zanskar River sediments and selected bedrock. (A) Classical MDS plot of bulk major element geochemistry data; (B) Nonmetric MDS plot of SRD-corrected bulk petrographic data; (C) Nonmetric MDS of Zanskar River detrital zircon U-Pb ages; and (D) Nonmetric MDS of selected Himalaya bedrock and Zanskar River detrital zircon U-Pb ages. Regional Himalayan U-Pb zircon data are same as Figure S2. Samples are numbered after Table 1. Data were plotted using R code ‘provenance’ written by Vermeesch et al. (2016). Solid lines indicate closest neighbor and dashed lines near neighbors in similarity calculations. Bedrock abbreviations in Fig. 12D mostly follow depositional ages: pЄ-Є = Proterozoic to Cambrian; D-O = Devonian to Ordovician; M-P = Mississippian to Permian; T-J = Triassic to Jurassic; LK = lower Cretaceous; uK-Pg = upper Cretaceous to Paleogene; and ZGH = Zanskar Greater Himalayan bedrock (Horton and Leech, 2013).

Figure S1. KDE diagrams for selected bedrock U-Pb data for the Zanskar River Basin. Selected samples are from the Indus and Tar Groups (Henderson et al., 2010; Wu et al., 2007), Zanskar region Greater Himalaya (Horton and Leech, 2013), Panjal Traps (Shellnutt et al., 2011), and Cambro-Ordovician granites in Zanskar and the NW Himalaya (Cawood et al., 2007; Girard and Bussy, 1999; Kwatra et al., 1999; Miller et al., 2001; Pognante et al., 1990). Selected bedrock ages for southern Tethyan Himalaya, Greater Himalaya, and correlative strata from the eastern and central Himalaya were plotted (in gray) according to depositional age and compiled into composite KDE diagrams (Clift et al., 2014; DeCelles et al., 2000; Gehrels et al., 2011; Hu et al., 2015; Hu et al., 2012; McQuarrie et al., 2008; Myrow et al., 2010; Myrow et al., 2003).

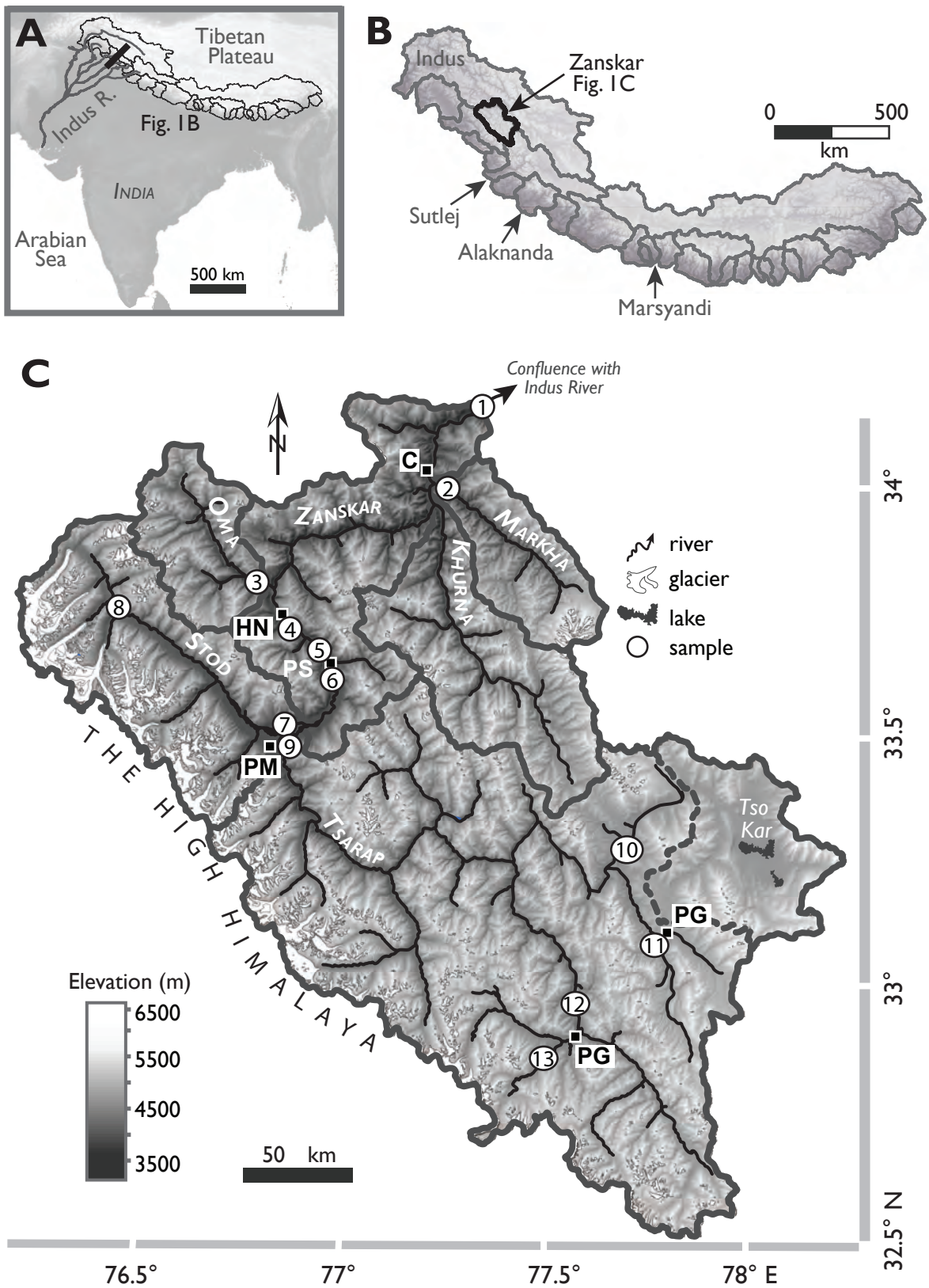


Figure 1

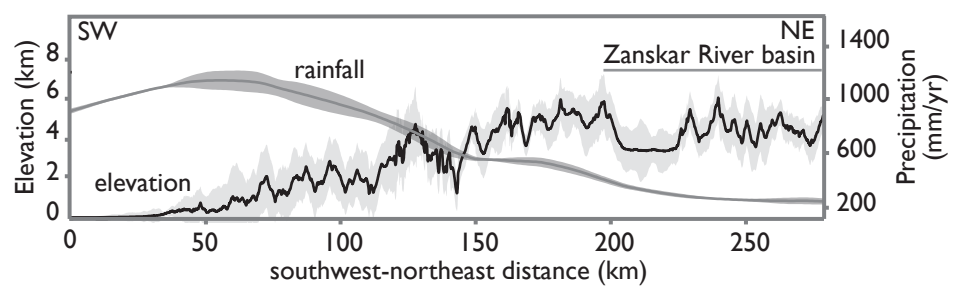


Figure 2

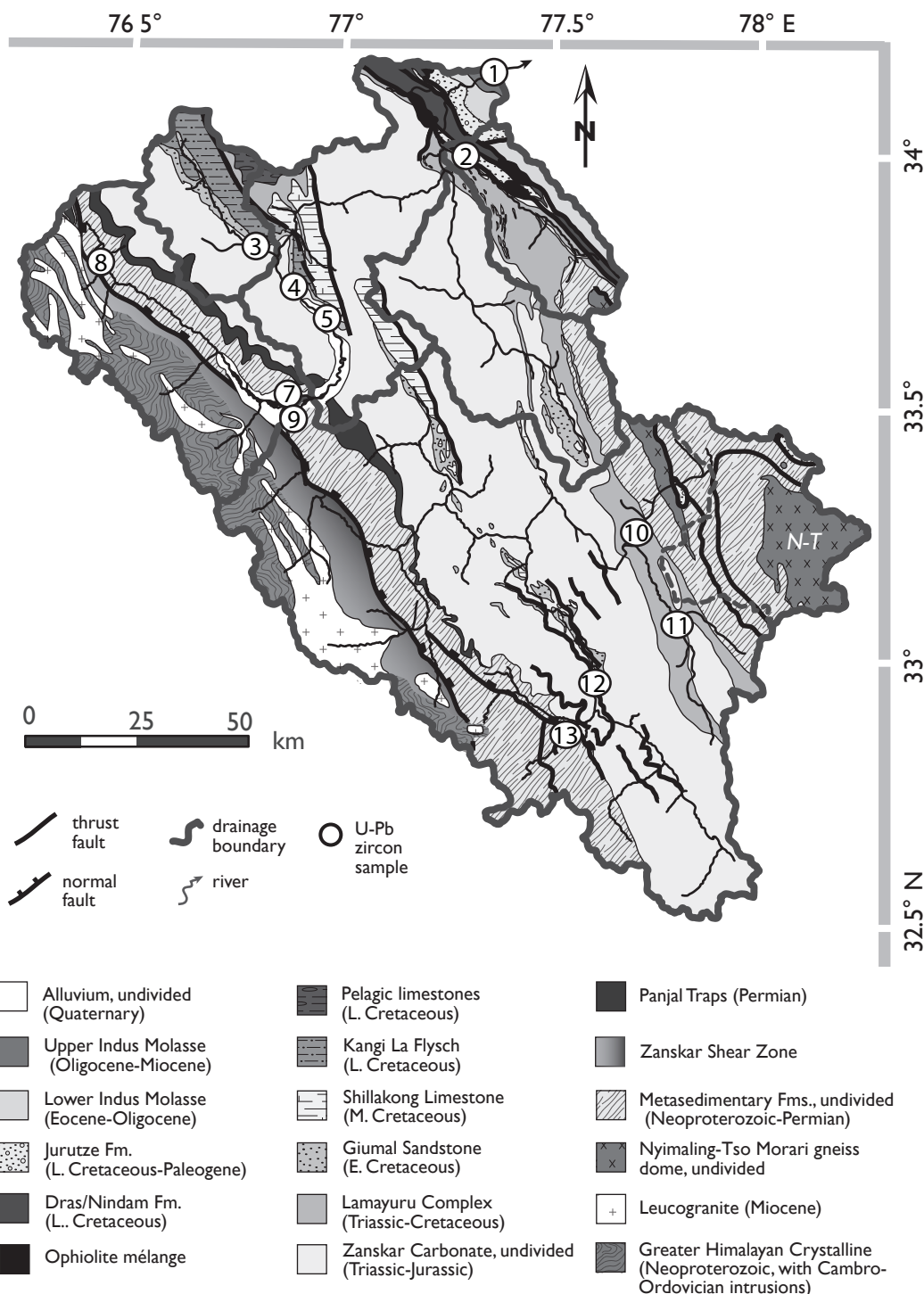
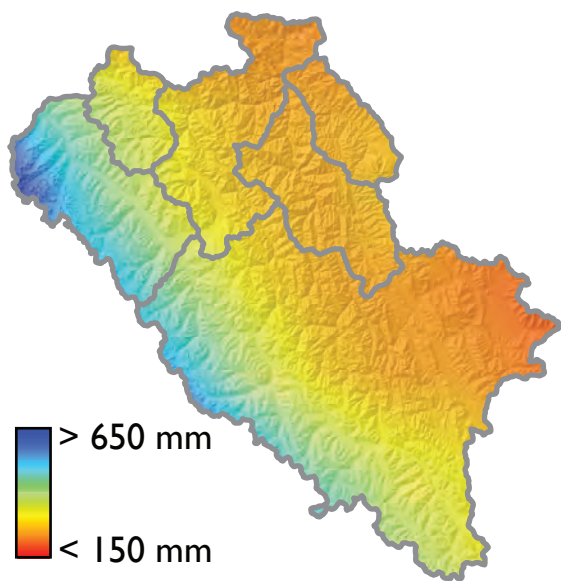
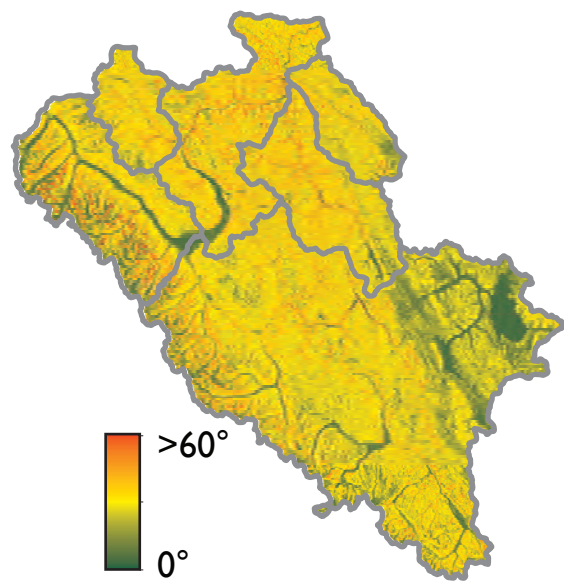


Figure 3

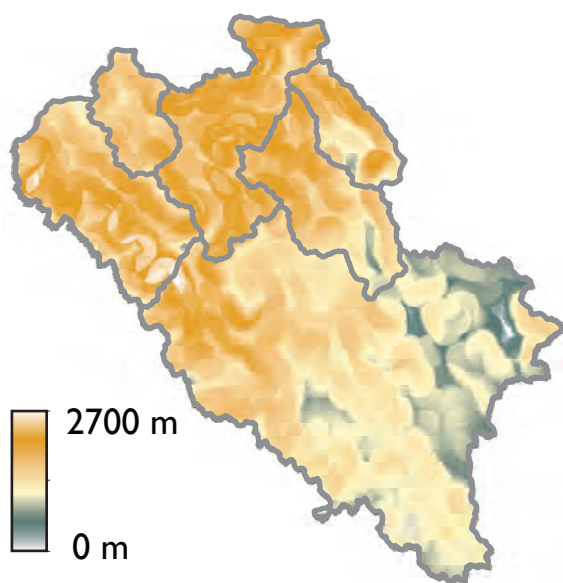
A. Mean annual rainfall



B. Slope



C. Local 5-km relief



D. Normalized channel steepness (k_{sn})

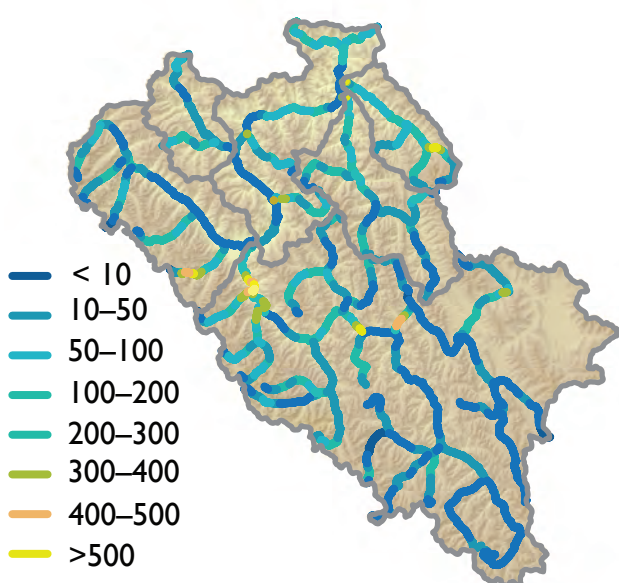


Figure 4

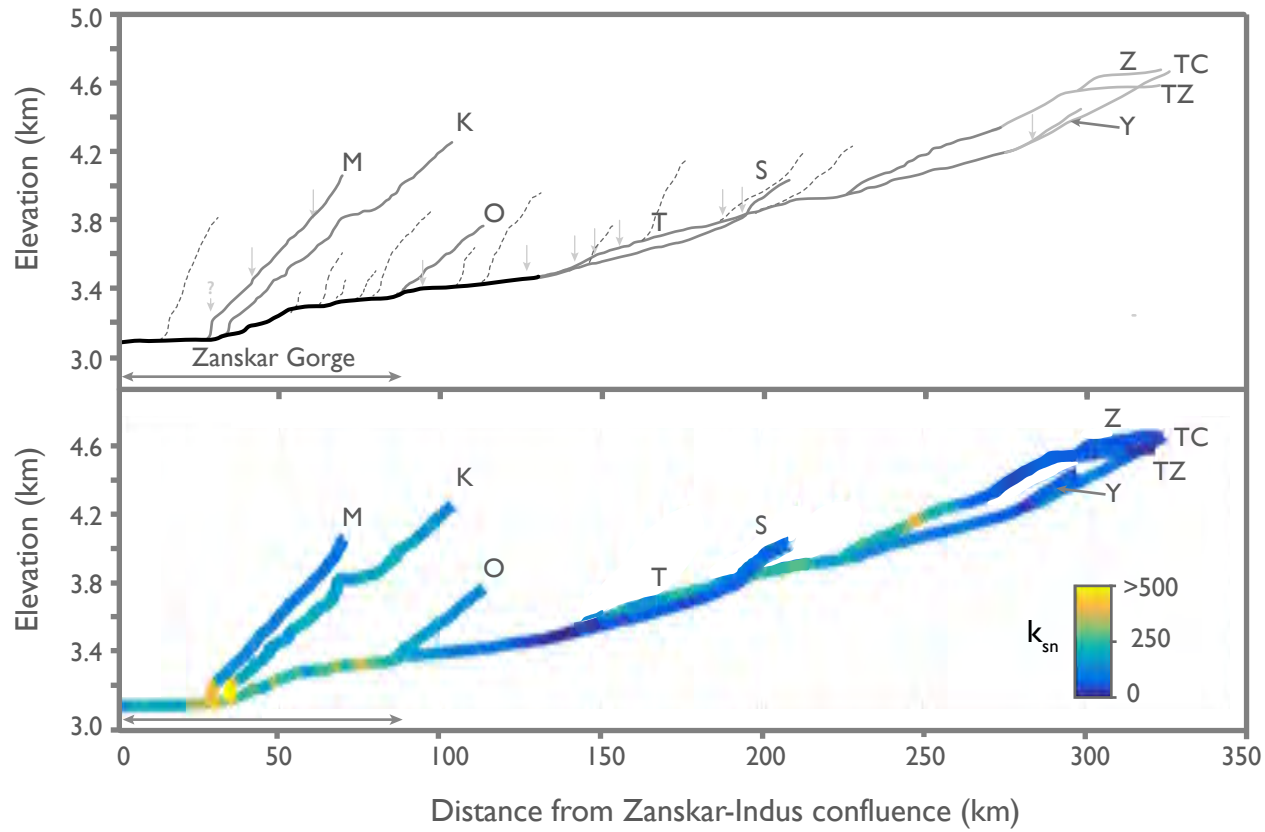


Figure 5

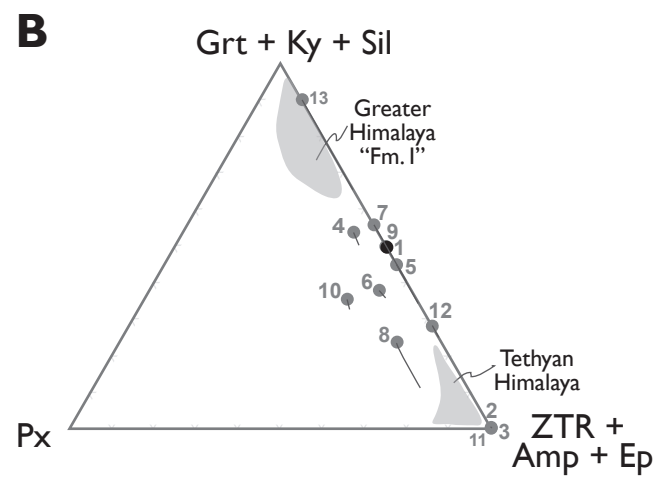
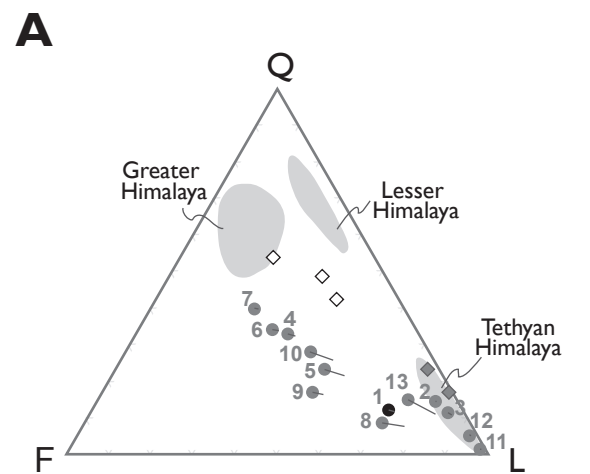


Figure 6

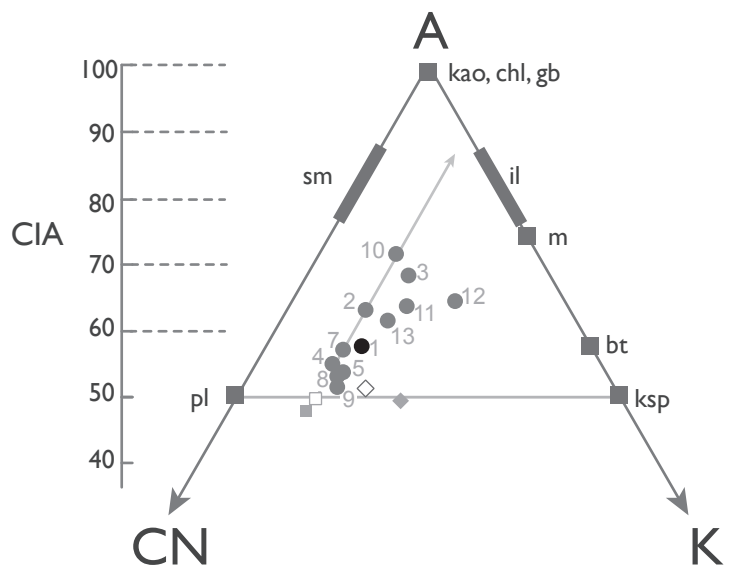


Figure 7

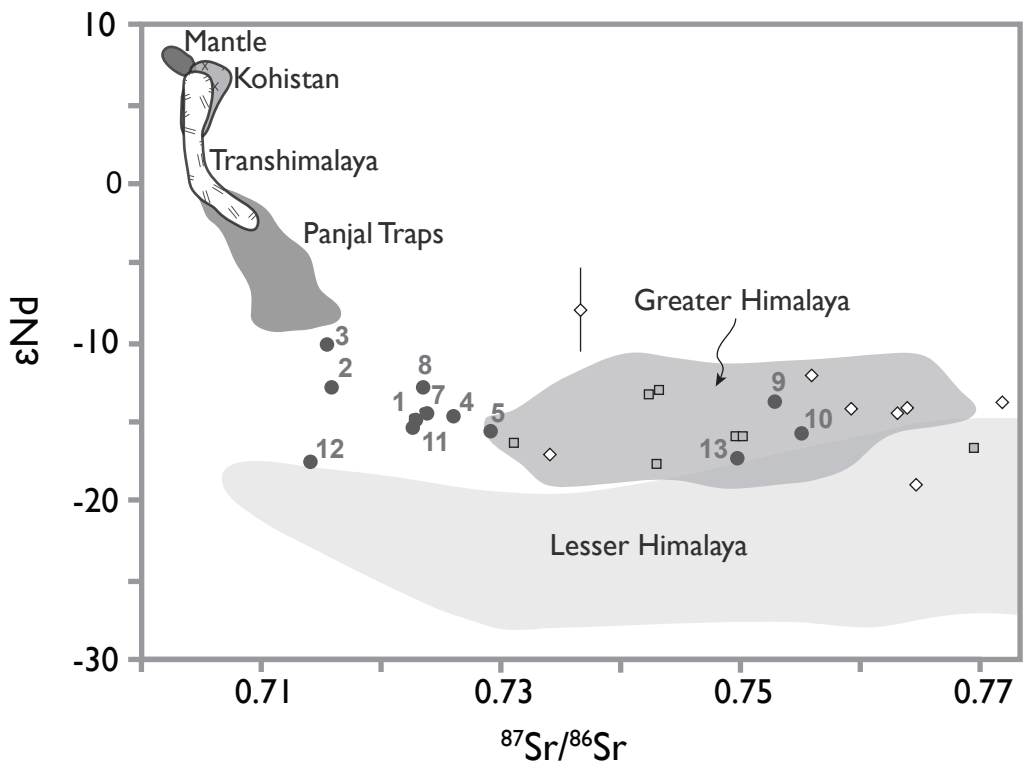


Figure 8
Jonell et al.

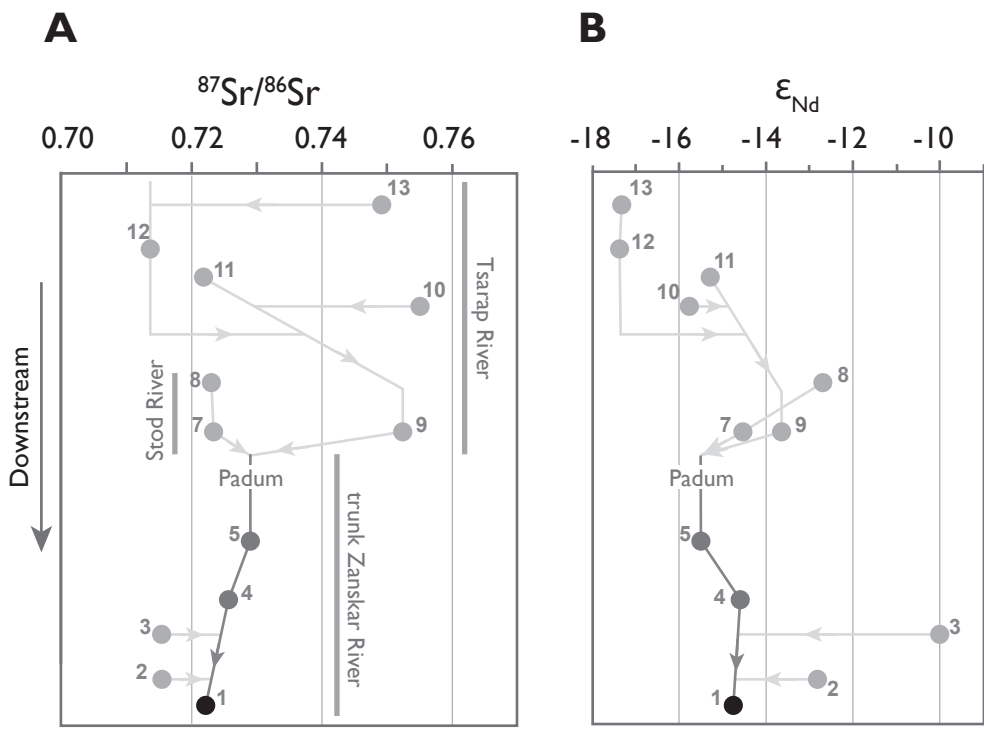


Figure 9

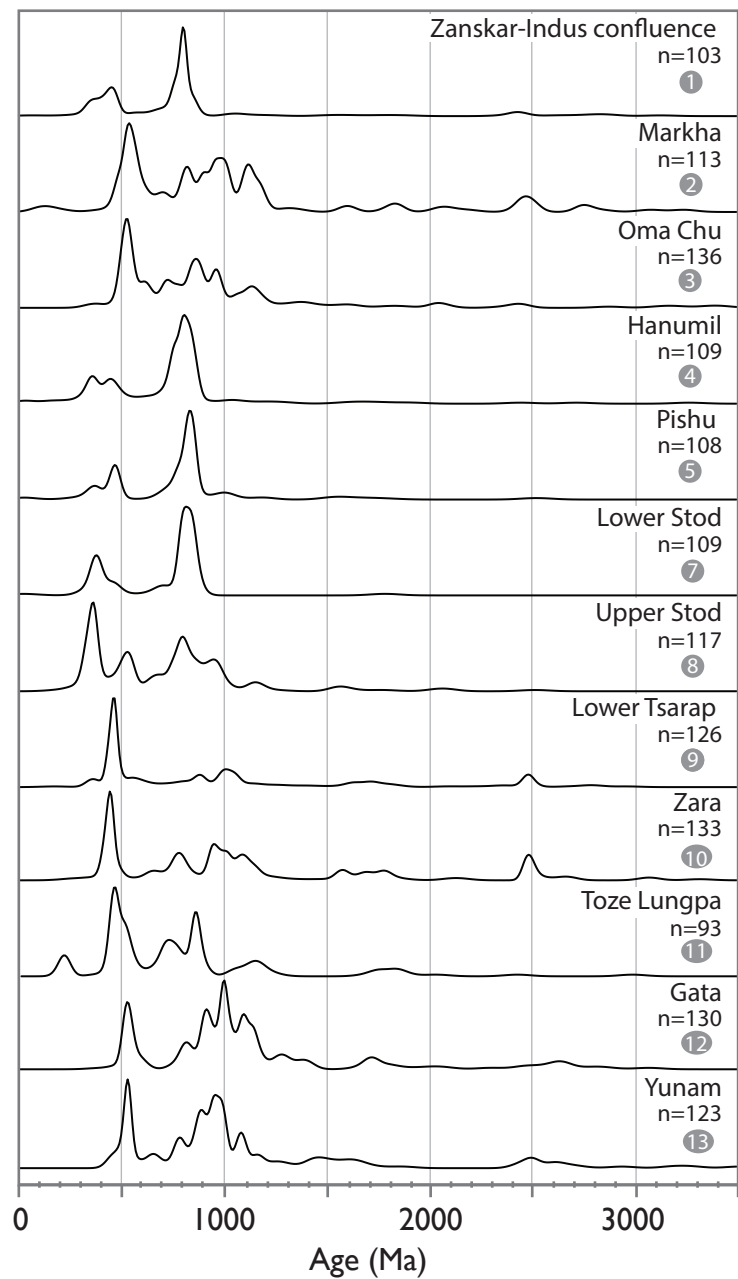


Figure 10

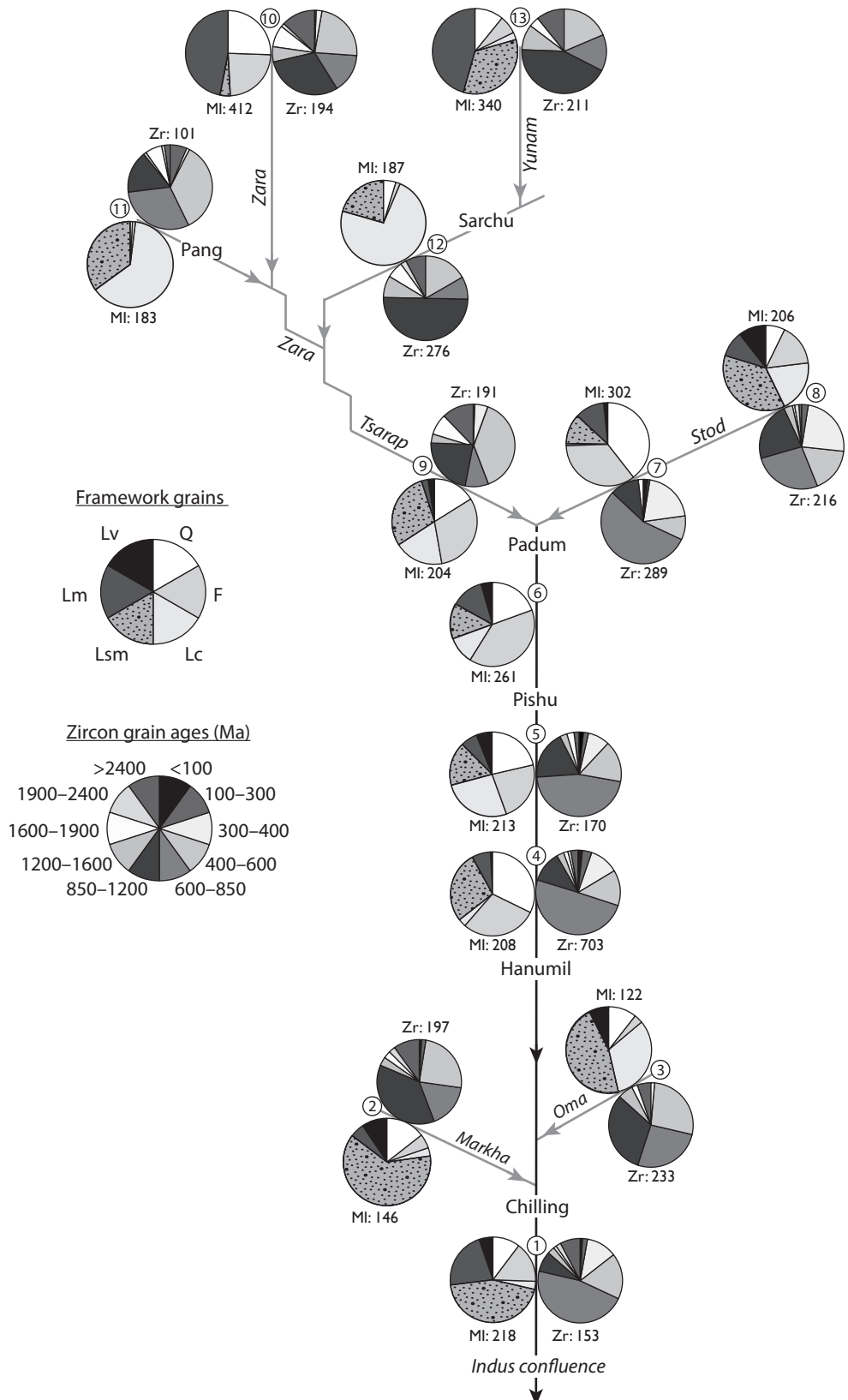
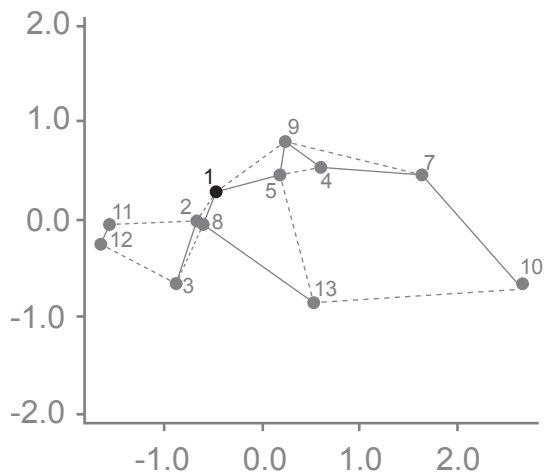
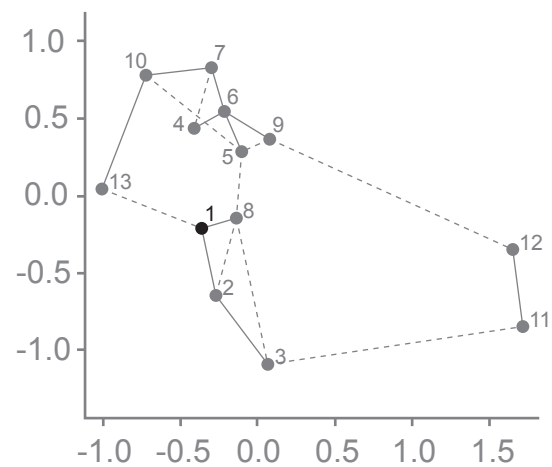


Figure 11

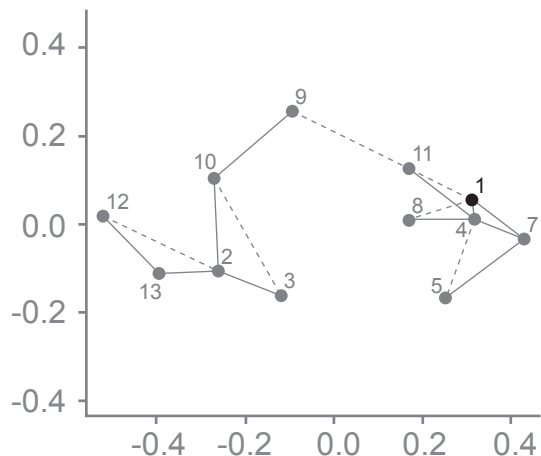
A. Major element



B. Bulk petrography



C. Zanskar U-Pb zircon



D. Bedrock & Zanskar U-Pb zircon

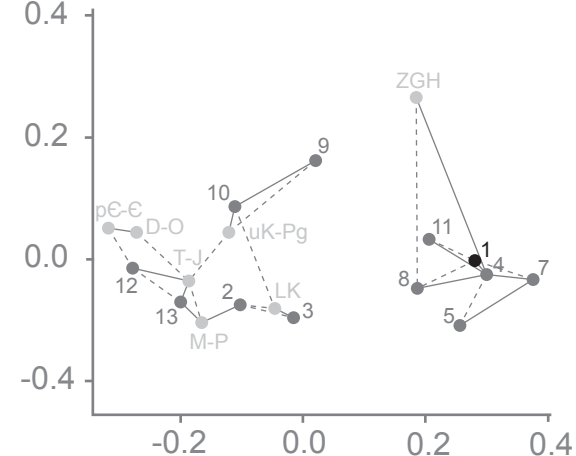


Figure 12

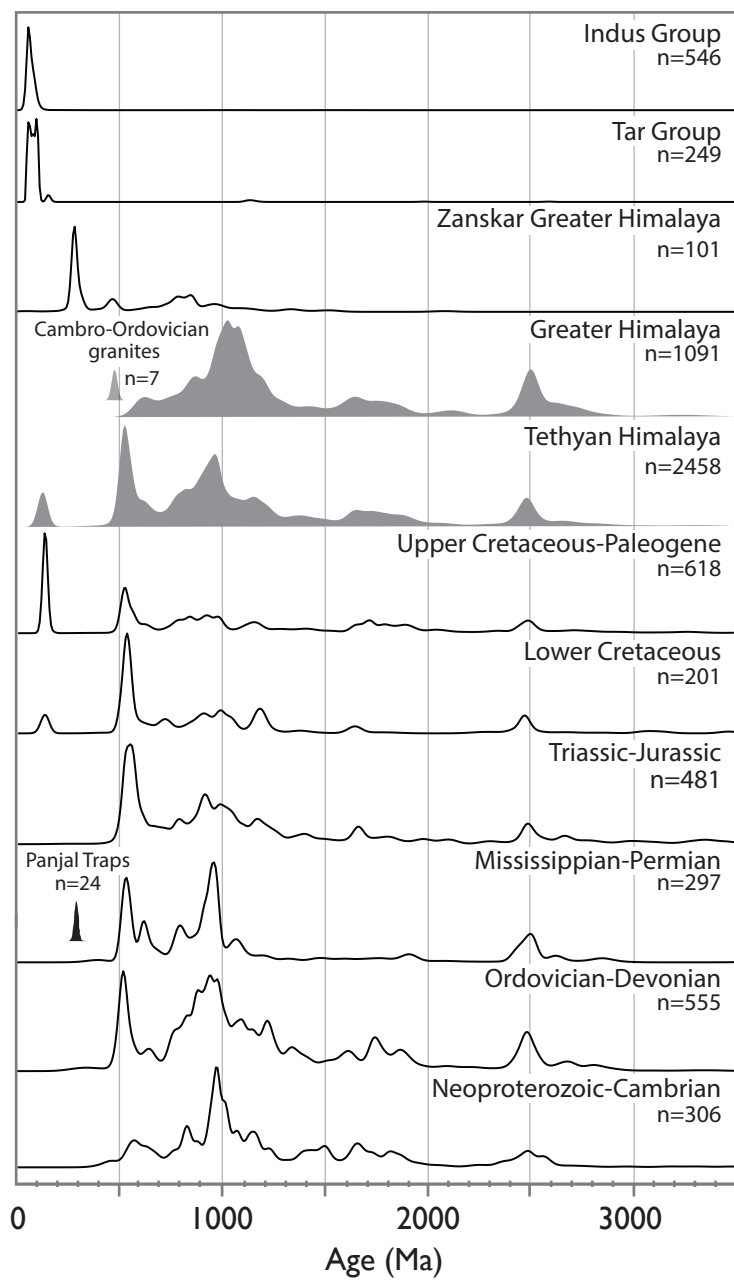


Figure S1

TABLE 1. SAMPLE LOCATIONS FOR ZANSKAR RIVER SEDIMENTS.

ID	Sample	Location	Lat (°N)	Long (°E)	Elevation (m)
1	8081203	Zanskar-Indus	34.162	77.326	3129
2	14072807	Markha	33.992	77.241	3311
3	12072207	Oma Chu	33.792	76.829	3420
4	13071402	Hanumil	33.716	76.877	3407
5	12072401	Pishu	33.682	76.941	3411
6	13071201	Pishu	33.635	76.983	3433
7	12072504	Lower Stod	33.518	76.911	3520
8	13071703	Upper Stod	33.817	76.432	4027
9	12072507	Lower Tsarap	33.461	76.883	3540
10	14080401	Zara	33.342	77.713	4454
11	13072301	Toze Lungpa	33.124	77.774	4496
12	13072302	Gata	33.008	77.594	4185
13	14080609	Yunam	32.885	77.533	4328

TABLE 2. BULK PETROGRAPHY OF ZANSKAR RIVER SEDIMENTS.

ID	Sample	Location	Framework grains						Mica		Dense minerals								
			Q	F	Lc	Lsm	Lm	Lv	Mu	B	ZTR	Ep	Gt	Ky	Sil	A	Px	Ap	&
1	8081203	Zanskar-Indus	22	31	11	77	41	5	3	5.5	1	1	1	0	3	3	0	0	0
2	14072807	Markha	28	10	6	119	10	18	0	3	0	0	0	0	0	0	0	1	0
3	12072201	Oma Chu	19	6	58	82	0	13	3	0	4	0	0	0	0	0	0	0	0
4	13071402	Hanumil	53	48	5	45	12	1	1	6	1	0	2	0	6	6	1	1	1
5	12072401	Pishu	36	39	44	28	11	10	2	16	1	2	1	0	3	4	0	0	0
6	13071201	Pishu	58	56	15	19	18	6	1	5	3	2	2	0	3	3	1	1	0
7	12072504	Lower Stod	73	64	2	21	21	3	2	4	2	1	0	1	3	1	0	0	0
8	13071703	Upper Stod	12	26	32	60	16	17	0	6	1	8	0	0	2	5	2	0	1
9	12072507	Lower Tsarap	27	51	31	48	4	4	7	11	4	0	2	0	3	2	0	2	2
10	14080401	Zara	39	36	0	6	71	0	14	16	1	2	1	0	1	0	1	2	0
11	13072301	Toze Lungpa	2	2	117	65	0	0	0	1	1	0	0	0	0	0	0	0	0
12	13072302	Gata	9	3	137	38	0	0	1	3	3	0	0	1	0	0	0	0	0
13	14080609	Yunam	19	12	5	59	79	0	4	0	1	0	0	1	0	0	0	0	1

TABLE 3. MAJOR AND TRACE ELEMENT GEOCHEMISTRY FOR ZANSKAR RIVER SEDIMENTS.

ID	Sample	Location	SiO ₂	TiO ₂	Al ₂ O ₃	Fe ₂ O ₃	MnO	MgO	CaO	Na ₂ O	K ₂ O	P ₂ O ₅
1	8081203	Zanskar-Indus	46.87	0.41	8.57	3.13	0.05	2.03	19.79	1.30	1.69	0.12
2	14072807	Markha	46.16	0.43	7.43	4.33	0.07	2.38	20.46	0.94	1.11	0.14
3	12072207	Oma Chu	43.04	0.70	7.52	4.77	0.04	2.81	20.57	0.60	1.48	0.14
4	13071402	Hanumil	61.78	0.63	9.60	3.43	0.17	1.56	11.44	1.82	1.62	0.39
5	12072401	Pishu	58.89	0.39	9.49	2.72	0.05	1.61	12.49	1.79	2.03	0.14
6	13071201	Pishu										
7	12072504	Lower Stod	71.57	0.43	12.14	2.77	0.09	1.12	3.85	2.41	2.60	0.21
8	13071703	Upper Stod	46.37	0.56	8.19	3.99	0.06	3.40	19.48	1.38	1.26	0.12
9	12072507	Lower Tsarap	59.69	0.31	8.76	2.28	0.08	1.31	13.34	1.84	1.78	0.13
10	14080401	Zara	76.97	0.64	10.64	3.91	0.07	1.31	0.83	1.78	2.25	0.14
11	13072301	Toze Lungpa	26.23	0.30	6.54	3.65	0.04	2.10	32.97	0.52	0.81	0.08
12	13072302	Gata	31.42	0.37	4.42	2.26	0.03	2.80	32.05	0.44	0.94	0.09
13	14080609	Yunam	74.47	0.45	6.64	3.13	0.08	1.88	5.33	0.44	1.95	0.12

TABLE 3. MAJOR AND TRACE ELEMENT GEOCHEMISTRY FOR ZANSKAR RIVER SEDIMENTS.

ID	Sample	As	Ba	Ce	Co	Cr	Cu	Ga	Mo	Ni	Nb	Pb	Rb	Sr	Th	Y	V	U	Zn	Zr
1	8081203	8	313	75	8	59	16	11	0	30	11	20	70	612	11	20	51	5	39	153
2	14072807	12	173	55	15	263	22	10	1	83	10	16	50	794	11	25	62	3	52	197
3	12072207	15	222	79	10	103	17	11	1	42	17	12	50	442	10	19	90	3	61	233
4	13071402	14	419	278	8	33	9	11	0	7	21	23	57	349	38	69	48	10	31	703
5	12072401	5	442	73	7	37	8	10	0	17	12	25	82	343	14	21	46	9	32	170
6	13071201																			
7	12072504	5	691	154	8	32	8	13	0	12	15	31	92	358	19	36	42	6	32	289
8	13071703	5	262	59	10	70	17	9	2	31	11	12	48	365	13	22	85	1	31	216
9	12072507	6	293	51	6	23	10	10	0	11	7	23	71	280	11	29	34	7	25	191
10	14080401	10	300	46	12	43	12	13	0	21	14	17	113	72	14	26	57	7	41	194
11	13072301	3	115	39	10	43	13	10	1	23	9	10	43	838	11	18	57	-2	40	101
12	13072302	9	130	46	7	27	7	5	1	11	10	8	37	611	11	18	44	0	19	276
13	14080609	12	315	57	8	31	10	8	1	16	11	10	78	80	10	18	45	2	19	211

TABLE 4. Nd AND Sr ISOTOPE GEOCHEMISTRY OF ZANSKAR RIVER SEDIMENTS.

ID	Sample	Location	Size fraction	normalized $^{143}\text{Nd}/^{144}\text{Nd}$ [§]	internal error $^{143}\text{Nd}/^{144}\text{Nd}$ (2σ)	ε_{Nd}	external error (2σ SD)	external error ($\varepsilon_{\text{Nd}}, 2\sigma$ SD)	propagated error (2σ) ^{&}	normalized $^{87}\text{Sr}/^{86}\text{Sr}$ [€]	internal error (2σ SD)	external error (2σ SD)	propagated error (2σ) ^{&}
1	8081203	Zanskar-Indus	<300um	0.511877	0.000010	-14.8	0.000008	0.16	0.25	0.722856	0.00001	0.000025	0.000027
2	14072807	Markha	bulk	0.511983	0.000004	-12.8	0.000010	0.21	0.21	0.715952	0.00003	0.000021	0.000036
3	12072207	Oma Chu	<300um	0.512125	0.000009	-10.0	0.000007	0.14	0.23	0.715388	0.00002	0.000025	0.000030
4	13071402	Hanumil	bulk	0.511891	0.000006	-14.6	0.000010	0.21	0.23	0.725956	0.00001	0.000021	0.000025
5	12072401	Pishu	<300um	0.511842	0.000005	-15.5	0.000011	0.22	0.24	0.729091	0.00001	0.000030	0.000033
7	12072504	Lower Stod	<300um	0.511897	0.000004	-14.5	0.000008	0.16	0.17	0.723722	0.00001	0.000025	0.000027
8	13071703	Upper Stod	bulk	0.511985	0.000008	-12.7	0.000010	0.21	0.25	0.723463	0.00001	0.000021	0.000022
9	12072507	Lower Tsarap	<300um	0.511939	0.000009	-13.6	0.000008	0.16	0.23	0.752802	0.00002	0.000025	0.000029
10	14080401	Zara	bulk	0.511835	0.000003	-15.7	0.000010	0.21	0.21	0.755070	0.00002	0.000021	0.000028
11	13072301	Toze Lungpa	bulk	0.511852	0.000006	-15.3	0.000010	0.21	0.23	0.722722	0.00001	0.000021	0.000023
12	13072302	Gata	bulk	0.511745	0.000012	-17.4	0.000010	0.21	0.30	0.713990	0.00001	0.000021	0.000026
13	14080609	Yunam	bulk	0.511753	0.000006	-17.3	0.000010	0.21	0.23	0.749729	0.00003	0.000021	0.000039

[§] measured $^{143}\text{Nd}/^{144}\text{Nd}$ ratios were normalized to the JNd-1 value of 0.512115 (Tanaka et al., 2000).

[€] measured $^{87}\text{Sr}/^{86}\text{Sr}$ ratios were normalized to the NBS987 value of 0.710248 (Thirlwall, 1991).

[&] reported error, determined as $\sqrt{(\text{internal error})^2 + (\text{external error})^2}$

Table 2. U-Pb zircon ages of Zanskar River sands

TABLE S1. U-Pb ZIRCON AGES OF ZANSKAR RIVER SEDIMENTS.

Sample 08081203 Zanskar-Indus Confluence

Grain No.	Pb (ppm)	U (ppm)	Atomic Th/U	Ratios						Ages (Ma)						% concord. (206/238 / 207/235)	% concord. (206/238 / 207/235)	Best Age (Ma)	± 2σ
				$^{206}\text{Pb}/^{238}\text{U}$	± 1 σ	$^{207}\text{Pb}/^{235}\text{U}$	± s.e.	$^{207}\text{Pb}/^{206}\text{Pb}$	± s.e.	$^{206}\text{Pb}/^{238}\text{U}$	± 2σ	$^{207}\text{Pb}/^{235}\text{U}$	± 2σ	$^{207}\text{Pb}/^{206}\text{Pb}$	± 2σ				
G53	3.4	346.7	0.58	0.0090	0.0001	0.0661	0.0026	0.0532	0.0021	57.8	1.2	65.0	5.0	337.8	25.6	11.1	82.9	57.76	1.15
G10	47.2	1149.1	0.39	0.0388	0.0002	0.2910	0.0047	0.0529	0.0008	245.5	2.9	259.3	7.1	326.2	11.7	5.3	24.7	245.51	2.85
G112	20.5	390.3	0.58	0.0478	0.0003	0.3735	0.0093	0.0565	0.0013	301.0	4.2	322.3	12.8	472.5	20.2	6.6	36.3	301.00	4.18
G52	53.5	938.6	0.44	0.0536	0.0003	0.4201	0.0070	0.0554	0.0008	336.6	3.9	356.1	9.5	427.6	13.9	5.5	21.3	336.65	3.92
G11	13.0	211.4	0.72	0.0539	0.0004	0.3858	0.0089	0.0526	0.0011	338.4	4.5	331.3	12.3	309.4	14.3	-2.1	-9.4	338.42	4.53
G20	59.8	890.1	1.06	0.0544	0.0003	0.4185	0.0067	0.0551	0.0008	341.3	3.9	355.0	9.2	417.1	13.3	3.9	18.2	341.30	3.91
G70	43.8	628.0	1.08	0.0557	0.0004	0.4120	0.0081	0.0530	0.0009	349.2	4.3	350.3	10.9	326.7	13.3	0.3	-6.9	349.18	4.27
G110	96.7	1391.2	1.00	0.0568	0.0003	0.4549	0.0081	0.0551	0.0009	356.0	4.1	380.7	10.5	417.5	14.5	6.5	14.7	356.01	4.15
G16	18.4	266.1	0.88	0.0569	0.0004	0.4606	0.0110	0.0575	0.0012	356.6	4.9	384.7	13.9	509.6	20.2	7.3	30.0	356.62	4.88
G55	38.1	559.0	0.83	0.0585	0.0004	0.4383	0.0081	0.0547	0.0009	366.3	4.4	369.0	10.9	399.2	14.4	0.7	8.2	366.31	4.39
G50	10.5	140.6	1.04	0.0607	0.0005	0.4552	0.0121	0.0557	0.0013	379.6	5.5	380.9	15.8	439.6	20.1	0.3	13.7	379.58	5.47
G33	164.0	2772.1	0.05	0.0638	0.0004	0.5106	0.0074	0.0562	0.0007	398.6	4.5	418.9	9.6	461.9	13.1	4.8	13.7	398.63	4.48
G65	38.7	537.6	0.65	0.0639	0.0004	0.4732	0.0085	0.0543	0.0009	399.4	4.7	393.4	11.3	382.3	13.7	-1.5	-4.5	399.36	4.73
G106	65.2	1095.7	0.04	0.0639	0.0004	0.5525	0.0103	0.0596	0.0010	399.4	4.7	446.6	12.4	590.5	18.4	10.6	32.4	399.42	4.73
G21	71.7	927.5	1.10	0.0642	0.0004	0.5176	0.0087	0.0575	0.0009	400.9	4.7	423.5	11.1	509.2	15.5	5.3	21.3	400.94	4.72
G79	427.4	6837.1	0.03	0.0676	0.0004	0.5521	0.0083	0.0566	0.0008	421.9	4.7	446.4	10.4	477.5	13.8	5.5	11.7	421.86	4.71
G45	133.9	2081.0	0.09	0.0683	0.0004	0.5518	0.0082	0.0556	0.0007	426.1	4.7	446.2	10.1	438.0	12.9	4.5	2.7	426.09	4.71
G88	41.3	567.4	0.51	0.0686	0.0004	0.5912	0.0112	0.0616	0.0010	427.7	5.2	471.6	13.4	659.2	19.7	9.3	35.1	427.66	5.19
G80	66.6	947.5	0.34	0.0687	0.0004	0.5822	0.0102	0.0595	0.0009	428.5	5.1	465.9	12.3	584.7	17.4	8.0	26.7	428.50	5.07
G4	54.6	555.0	1.55	0.0709	0.0004	0.5714	0.0107	0.0577	0.0009	441.5	5.3	458.9	12.8	516.9	16.7	3.8	14.6	441.46	5.30
G62	425.2	6478.4	0.00	0.0717	0.0004	0.5720	0.0082	0.0556	0.0007	446.3	4.9	459.3	10.2	437.6	12.7	2.8	-2.0	446.27	4.93
G104	93.5	1386.3	0.04	0.0726	0.0004	0.6089	0.0107	0.0574	0.0009	451.5	5.3	482.9	12.5	508.5	16.0	6.5	11.2	451.50	5.29
G99	46.6	517.1	1.00	0.0728	0.0005	0.6454	0.0129	0.0635	0.0011	453.0	5.5	505.7	14.7	724.0	21.6	10.4	37.4	453.00	5.53
G17	8.7	106.8	0.58	0.0745	0.0006	0.5837	0.0164	0.0575	0.0014	462.9	6.7	466.8	18.8	510.8	22.6	0.8	9.4	462.91	6.72
G89	90.0	1243.4	0.19	0.0745	0.0004	0.6056	0.0103	0.0565	0.0009	463.2	5.3	480.8	12.2	472.9	15.0	3.7	2.0	463.21	5.28
G32	85.1	1157.5	0.21	0.0746	0.0004	0.6774	0.0100	0.0640	0.0008	464.0	5.2	525.2	11.6	741.0	17.3	11.6	37.4	464.05	5.16
G40	134.5	1684.5	0.50	0.0753	0.0004	0.6096	0.0093	0.0573	0.0008	467.8	5.3	483.3	11.2	501.6	14.3	3.2	6.7	467.83	5.28
G94	67.7	942.1	0.10	0.0755	0.0005	0.6503	0.0120	0.0581	0.0009	469.0	5.5	508.7	13.2	532.8	16.9	7.8	12.0	468.97	5.51
G72	25.3	288.4	0.81	0.0755	0.0005	0.5763	0.0117	0.0557	0.0010	469.4	5.8	462.1	14.1	441.6	16.2	-1.6	-6.3	469.39	5.75
G25	47.3	640.0	0.14	0.0766	0.0005	0.6152	0.0097	0.0578	0.0008	475.7	5.4	486.9	11.6	522.2	14.8	2.3	8.9	475.68	5.39
G48	73.8	769.9	0.51	0.0893	0.0005	0.7244	0.0120	0.0572	0.0008	551.5	6.3	553.2	13.2	499.3	14.9	0.3	-10.5	551.46	6.27
G46	32.5	313.3	0.66	0.0928	0.0006	0.7128	0.0136	0.0568	0.0009	572.1	6.8	546.4	15.0	483.0	16.1	-4.7	-18.5	572.13	6.84
G59	15.6	169.6	0.19	0.0931	0.0007	0.8357	0.0209	0.0649	0.0013	573.6	7.8	616.8	20.0	770.8	25.6	7.0	25.6	573.61	7.78
G27	64.4	605.7	0.18	0.1075	0.0007	0.9343	0.0160	0.0642	0.0009	658.3	7.6	669.9	15.5	746.6	18.8	1.7	11.8	658.33	7.57
G85	247.9	1623.5	1.75	0.1087	0.0006	1.0853	0.0175	0.0683	0.0010	664.9	7.4	746.2	15.8	878.9	20.2	10.9	24.3	664.90	7.44
G74	45.4	349.4	0.83	0.1101	0.0007	0.9453	0.0173	0.0628	0.0010	673.4	7.9	675.6	16.6	702.1	19.3	0.3	4.1	673.44	7.90
G90	100.2	831.3	0.44	0.1141	0.0007	1.0376	0.0184	0.0660	0.0010	696.3	8.0	722.7	17.0	806.1	20.5	3.7	13.6	696.34	7.99
G9	59.9	500.7	0.35	0.1161	0.0007	1.0485	0.0165	0.0663	0.0009	707.9	8.0	728.1	15.3	816.5	18.5	2.8	13.3	707.90	7.97
G19	47.2	378.7	0.40	0.1184	0.0007	1.0724	0.0200	0.0670	0.0010	721.3	8.5	739.9	17.6	837.2	21.0	2.5	13.8	721.35	8.53
G14	133.4	725.4	2.14	0.1208	0.0007	1.2215	0.0207	0.0725	0.0010	735.2	8.4	810.5	17.0	1001.1	21.4	9.3	26.6	735.22	8.40
G82	154.6	749.9	2.44	0.1225	0.0007	1.1509	0.0199	0.0683	0.0010	744.9	8.5	777.7	17.5	876.2	21.0	4.2	15.0	744.94	8.50
G35	165.6	1178.9	0.72	0.1235	0.0007	1.1576	0.0166	0.0665	0.0008	750.7	8.1	780.8	15.0	821.5	17.7	3.9	8.6	750.68	8.15
G58	148.3	838.9	1.75	0.1237	0.0007	1.1506	0.0178	0.0660	0.0009	752.1	8.3	777.5	15.8	805.4	18.5	3.3	6.6	752.05	8.26
G24	45.2	337.3	0.51	0.1238	0.0008	1.1127	0.0190	0.0654	0.0009	752.5	8.6	759.5	16.6	786.6	19.1	0.9	4.3	752.51	8.60
G78	184.0	1037.8	1.71	0.1238	0.0007	1.1891	0.0188	0.0673	0.0009	752.6	8.3	795.5	16.4	848.0	19.5	5.4	11.2	752.63	8.26
G43	59.1	337.3	1.66	0.1251	0.0008	1.1258	0.0225	0.0670	0.0011	759.9	9.2	765.8	19.0	837.5	22.0	0.8	9.3	759.91	9.17
G12	58.3	352.9	1.35	0.1251	0.0008	1.1259	0.0190	0.0658	0.0009	760.1	8.6	765.8	16.6	800.3	19.1	0.7	5.0	760.08	8.59
G108	60.3	373.8	1.19	0.1257	0.0008	1.1488	0.0233	0.0674	0.0012	763.2	9.2	776.7	19.9	849.9	23.1	1.7	10.2	763.17	9.16
G23	133.2	896.8	0.75	0.1271	0.0007	1.1809	0.0180	0.0651	0.0009	771.2	8.5	791.7	15.5	776.9	17.7	2.6	0.7	771.24	8.46
G75	199.0	1480.6	0.44	0.1273	0.0007	1.2283	0.0188	0.0668	0.0009	772.2	8.5	813.6	16.2	831.9	19.0	5.1	7.2	772.22	8.46
G2	205.3	1598.6	0.29	0.1273	0.0007	1.1716	0.0157	0.0648	0.0008	772.3	8.2	787.4	14.2	7					

Table 2. U-Pb zircon ages of Zanskar River sands

Sample 14072807 Markha

Campion 1982, Marmara

Table 2. U-Pb zircon ages of Zanskar River sands

Grain No.	Γ_U (ppm)	U (ppm)	Th/U	$^{206}\text{Pb}/^{238}\text{U}$	$\pm 1\sigma$	$^{207}\text{Pb}/^{235}\text{U}$	$\pm \text{s.e.}$	$^{207}\text{Pb}/^{206}\text{Pb}$	$\pm \text{s.e.}$	$^{206}\text{Pb}/^{238}\text{U}$	$\pm 2\sigma$	$^{207}\text{Pb}/^{235}\text{U}$	$\pm 2\sigma$	$^{207}\text{Pb}/^{206}\text{Pb}$	$\pm 2\sigma$	$(^{206}/^{238})_{^{207}/^{235}}$	$(^{206}/^{238})_{^{207}/^{206}}$	Dates Myc (Ma)	$\pm 2\sigma$
G20	0.3	18.6	0.92	0.0152	0.0002	0.1011	0.0044	0.0483	0.0021	97.2	2.8	97.8	8.7	112.5	9.4	0.6	13.6	97.2	2.8
G33	0.6	25.6	1.04	0.0205	0.0003	0.1369	0.0045	0.0486	0.0016	130.5	3.4	130.3	8.7	127.6	7.9	-0.2	-2.3	130.5	3.4
G59	0.5	14.5	1.06	0.0305	0.0005	0.2162	0.0092	0.0514	0.0022	193.7	5.8	198.8	16.4	260.6	19.7	2.5	25.7	193.7	5.8
G118	10.1	167.8	0.07	0.0644	0.0008	0.5017	0.0096	0.0565	0.0010	402.6	10.2	412.8	14.7	471.3	13.1	2.5	14.6	402.6	10.2
G98	8.9	130.0	0.06	0.0732	0.0009	0.5750	0.0098	0.0570	0.0009	455.5	11.2	461.2	14.8	491.1	12.0	1.2	7.3	455.5	11.2
G90	0.5	15.5	1.73	0.0768	0.0011	0.6278	0.0171	0.0593	0.0016	476.9	12.6	494.7	23.6	579.2	23.7	3.6	17.7	476.9	12.6
G39	1.6	21.0	0.21	0.0771	0.0010	0.5984	0.0123	0.0563	0.0011	478.9	11.5	476.2	18.0	465.0	15.0	-0.6	-3.0	478.9	11.5
G21	2.6	35.0	0.14	0.0774	0.0009	0.6045	0.0107	0.0567	0.0010	480.6	11.1	480.1	16.0	478.7	13.1	-0.1	-0.4	480.6	11.1
G2	4.2	55.6	0.12	0.0791	0.0009	0.6142	0.0102	0.0564	0.0009	490.6	11.1	486.2	15.3	466.2	11.9	-0.9	-5.2	490.6	11.1
G16	1.6	16.2	1.01	0.0798	0.0010	0.6150	0.0145	0.0559	0.0013	494.9	11.9	486.7	20.5	449.6	17.0	-1.7	-10.1	494.9	11.9
G111	1.1	12.8	0.27	0.0823	0.0011	0.6622	0.0178	0.0584	0.0015	510.0	13.5	515.9	23.9	543.7	22.1	1.2	6.2	510.0	13.5
G76	0.4	3.2	2.25	0.0827	0.0014	0.6466	0.0327	0.0568	0.0029	512.1	16.6	506.4	43.0	482.2	39.4	-1.1	-6.2	512.1	16.6
G82	0.8	6.3	1.97	0.0835	0.0012	0.6729	0.0231	0.0585	0.0020	516.8	14.0	522.4	30.2	548.9	29.0	1.1	5.8	516.8	14.0
G34	1.7	14.4	1.67	0.0846	0.0011	0.6784	0.0148	0.0582	0.0013	523.8	12.6	525.8	20.4	536.2	17.9	0.4	2.3	523.8	12.6
G36	1.7	20.3	0.17	0.0852	0.0011	0.6641	0.0164	0.0566	0.0014	527.1	12.9	517.1	22.3	474.8	18.5	-1.9	-11.0	527.1	12.9
G14	1.6	18.8	0.24	0.0856	0.0011	0.6645	0.0154	0.0563	0.0013	529.3	12.7	517.3	21.2	465.8	17.1	-2.3	-13.6	529.3	12.7
G72	1.4	14.3	0.79	0.0857	0.0011	0.6777	0.0154	0.0574	0.0013	529.9	13.2	525.4	20.9	507.7	17.5	-0.9	-4.4	529.9	13.2
G121	1.8	18.1	0.91	0.0858	0.0012	0.7277	0.0186	0.0615	0.0015	530.6	14.0	555.2	24.1	658.2	23.8	4.4	19.4	530.6	14.0
G46	1.4	13.3	0.88	0.0863	0.0011	0.6854	0.0156	0.0576	0.0013	533.9	13.1	530.0	21.2	515.3	18.0	-0.7	-3.6	533.9	13.1
G30	1.3	14.1	0.52	0.0881	0.0011	0.7087	0.0155	0.0584	0.0013	544.0	13.0	544.0	21.0	545.5	18.2	0.0	0.3	544.0	13.0
G61	3.2	30.5	0.88	0.0885	0.0011	0.6969	0.0133	0.0572	0.0010	546.4	13.0	536.9	18.4	498.5	14.3	-1.8	-9.6	546.4	13.0
G62	2.3	19.9	1.34	0.0889	0.0012	0.7145	0.0164	0.0584	0.0013	548.7	13.6	547.4	21.9	543.7	18.9	-0.2	-0.9	548.7	13.6
G116	0.7	7.0	0.87	0.0893	0.0013	0.7153	0.0211	0.0581	0.0017	551.2	14.9	547.9	27.2	535.0	24.0	-0.6	-3.0	551.2	14.9
G12	2.8	30.0	0.33	0.0897	0.0011	0.7498	0.0152	0.0607	0.0012	553.5	13.0	568.1	20.3	628.3	18.5	2.6	11.9	553.5	13.0
G122	2.0	21.1	0.45	0.0918	0.0013	0.7734	0.0194	0.0611	0.0015	566.1	14.8	581.7	24.5	643.8	22.9	2.7	12.1	566.1	14.8
G29	1.4	11.2	1.44	0.0921	0.0012	0.7274	0.0192	0.0573	0.0015	567.9	14.2	555.0	25.1	504.3	20.9	-2.3	-12.6	567.9	14.2
G68	1.9	15.9	1.19	0.0923	0.0012	0.7510	0.0162	0.0591	0.0012	569.1	13.9	568.8	21.3	569.3	18.2	-0.1	0.0	569.1	13.9
G85	2.8	31.3	0.27	0.0925	0.0012	0.7729	0.0181	0.0606	0.0014	570.4	14.4	581.4	23.2	626.1	21.1	1.9	8.9	570.4	14.4
G49	3.2	33.2	0.27	0.0949	0.0012	0.8005	0.0138	0.0612	0.0010	584.4	13.7	597.1	18.4	647.3	15.6	2.1	9.7	584.4	13.7
G11	1.5	12.7	1.07	0.0958	0.0013	0.7695	0.0228	0.0583	0.0017	589.7	15.1	579.4	28.9	540.3	25.0	-1.8	-9.2	589.7	15.1
G51	3.9	35.8	0.60	0.0972	0.0012	0.8386	0.0155	0.0626	0.0011	598.2	14.2	618.4	20.0	694.3	17.7	3.3	13.8	598.2	14.2
G32	5.4	48.1	0.67	0.1003	0.0012	0.8615	0.0142	0.0623	0.0010	616.2	14.2	631.0	18.6	685.8	15.7	2.3	10.2	616.2	14.2
G13	5.6	48.1	0.84	0.1004	0.0012	0.8411	0.0130	0.0608	0.0009	616.8	13.9	619.7	17.5	631.5	13.8	0.5	2.3	616.8	13.9
G79	3.5	31.0	0.60	0.1025	0.0013	0.9461	0.0203	0.0670	0.0014	628.9	15.6	676.1	24.0	838.1	23.5	7.0	25.0	628.9	15.6
G24	7.9	57.6	1.12	0.1089	0.0013	0.9166	0.0138	0.0611	0.0009	666.1	15.0	660.6	17.9	643.1	13.4	-0.8	-3.6	666.1	15.0
G15	3.9	36.5	0.18	0.1101	0.0013	0.9276	0.0163	0.0611	0.0010	673.3	15.3	666.4	20.2	644.2	16.1	-1.0	-4.5	673.3	15.3
G27	3.1	27.5	0.23	0.1125	0.0014	0.9704	0.0164	0.0626	0.0010	687.3	15.6	688.6	20.1	694.3	16.2	0.2	1.0	687.3	15.6
G75	5.1	44.7	0.21	0.1177	0.0015	1.0879	0.0203	0.0671	0.0012	717.2	17.1	747.5	22.9	840.9	20.1	4.1	14.7	717.2	17.1
G35	5.7	43.3	0.63	0.1181	0.0014	1.0784	0.0175	0.0663	0.0010	719.7	16.4	742.9	20.5	814.6	17.1	3.1	11.6	719.7	16.4
G25	1.0	5.9	1.54	0.1182	0.0016	1.0680	0.0300	0.0656	0.0019	720.4	18.3	737.8	32.8	792.0	31.0	2.4	9.0	720.4	18.3
G55	2.9	21.7	0.36	0.1277	0.0016	1.1753	0.0222	0.0668	0.0012	774.6	18.3	789.1	24.0	832.2	20.4	1.8	6.9	774.6	18.3
G54	1.5	9.4	0.97	0.1296	0.0017	1.2908	0.0297	0.0723	0.0016	785.8	19.5	841.7	30.0	993.6	28.8	6.6	20.9	785.8	19.5
G94	5.4	42.1	0.33	0.1318	0.0017	1.3268	0.0227	0.0731	0.0011	798.1	18.9	857.5	23.1	1015.6	19.9	6.9	21.4	798.1	18.9
G17	10.1	77.0	0.25	0.1325	0.0016	1.4121	0.0202	0.0773	0.0010	802.2	17.8	894.1	21.0	1129.7	18.0	10.3	29.0	802.2	17.8
G3	2.4	17.5	0.41	0.1327	0.0016	1.1829	0.0236	0.0647	0.0013	803.1	18.4	792.7	25.3	764.3	20.9	-1.3	-5.1	803.1	18.4
G97	1.9	13.2	0.39	0.1347	0.0018	1.2748	0.0306	0.0687	0.0016	814.6	20.6	834.5	30.6	889.1	27.6	2.4	8.4	814.6	20.6
G100	1.8	13.4	0.20	0.1368	0.0018	1.2775	0.0298	0.0678	0.0015	826.8	20.8	835.8	29.8	860.9	26.0	1.1	4.0	826.8	20.8
G87	4.5	32.1	0.33	0.1369	0.0017	1.3303	0.0249	0.0706	0.0012	826.8	19.7	859.0	25.0	944.4	21.4	3.7	12.4	826.8	19.7
G28	3.1	20.2	0.57	0.1377	0.0017	1.3243	0.0245	0.0698	0.0013	831.5	19.2	856.4	25.1	922.8	21.7	2.9	9.9	831.5	19.2
G80	3.9	28.1	0.30	0.1378	0.0017	1.3218	0.0230	0.0696	0.0011	832.0	19.6	855.3	23.6	917.8	19.4	2.7	9.3	832.0	19.6
G108	5.2	35.9	0.33	0.1424	0.0018	1.3329	0.0253	0.0679	0.0012	858.3	20.8	860.1	25.3	865.8	20.4	0.2	0.9	858.3	20.8
G38	0.3	1.5	0.91	0.1442	0.0023	1.3345	0.0568	0.0672	0.0029	868.3	25.9	860.8	53.4	843.0	49.5	-0.9	-3.0	868.3	25.9
G104	2.9	14.9	1.20	0.1532	0.0020	1.4438	0.0286	0.0684	0.0013	918.8	22.2	907.3	27.1	880.4	21.7	-1.3	-4.4	880.4	21.7
G92	3																		

Table 2. U-Pb zircon ages of Zanskar River sands

G71	7.4	43.0	0.25	0.1710	0.0021	1.6653	0.0272	0.0707	0.0011	1017.8	23.2	995.4	24.6	947.9	18.5	-2.3	-7.4	947.9	18.5
G48	5.2	26.9	0.96	0.1600	0.0020	1.5629	0.0254	0.0709	0.0011	956.7	21.7	955.6	24.0	954.8	18.7	-0.1	-0.2	954.8	18.7
G124	3.0	18.8	0.22	0.1608	0.0021	1.5728	0.0309	0.0709	0.0013	961.4	23.4	959.5	27.6	955.7	22.2	-0.2	-0.6	955.7	22.2
G63	1.7	8.5	0.63	0.1733	0.0022	1.6999	0.0354	0.0712	0.0014	1030.3	24.5	1008.5	30.5	962.9	25.0	-2.2	-7.0	962.9	25.0
G7	2.3	12.3	0.77	0.1621	0.0020	1.6010	0.0331	0.0717	0.0015	968.5	22.4	970.6	29.9	976.3	25.6	0.2	0.8	976.3	25.6
G45	3.5	20.9	0.16	0.1716	0.0021	1.6989	0.0299	0.0719	0.0012	1020.9	23.2	1008.1	26.5	981.7	21.0	-1.3	-4.0	981.7	21.0
G18	3.5	21.9	0.19	0.1645	0.0020	1.6293	0.0260	0.0719	0.0011	981.8	21.7	981.6	24.3	982.3	19.1	0.0	0.0	982.3	19.1
G58	2.0	10.1	0.81	0.1705	0.0022	1.6934	0.0366	0.0721	0.0015	1014.6	24.2	1006.1	31.6	989.0	26.6	-0.9	-2.6	989.0	26.6
G66	7.9	37.7	0.78	0.1798	0.0022	1.7941	0.0298	0.0724	0.0011	1065.8	24.3	1043.3	25.7	998.0	19.5	-2.2	-6.8	998.0	19.5
G119	5.1	32.3	0.14	0.1631	0.0021	1.6343	0.0314	0.0727	0.0013	974.2	23.6	983.5	27.5	1005.0	22.3	0.9	3.1	1005.0	22.3
G123	7.9	43.2	0.54	0.1684	0.0022	1.6912	0.0326	0.0729	0.0013	1003.2	24.3	1005.2	27.9	1010.1	22.5	0.2	0.7	1010.1	22.5
G107	3.8	21.1	0.35	0.1761	0.0023	1.7723	0.0357	0.0730	0.0014	1045.6	25.2	1035.4	29.7	1014.8	24.1	-1.0	-3.0	1014.8	24.1
G88	5.7	35.2	0.46	0.1532	0.0020	1.5434	0.0295	0.0731	0.0013	919.0	21.9	947.8	27.1	1017.0	23.0	3.0	9.6	1017.0	23.0
G117	4.1	23.4	0.31	0.1707	0.0022	1.7300	0.0331	0.0735	0.0013	1015.9	24.6	1019.8	28.0	1028.9	22.5	0.4	1.3	1028.9	22.5
G86	3.0	18.6	0.38	0.1539	0.0020	1.5629	0.0283	0.0737	0.0012	922.6	21.8	955.6	26.1	1033.8	21.8	3.5	10.8	1033.8	21.8
G50	10.7	59.5	0.89	0.1544	0.0019	1.6023	0.0253	0.0753	0.0011	925.6	21.0	971.1	23.8	1077.1	19.4	4.7	14.1	1077.1	19.4
G10	4.8	23.3	0.43	0.1959	0.0023	2.0382	0.0323	0.0755	0.0011	1153.4	25.1	1128.4	26.2	1081.6	20.1	-2.2	-6.6	1081.6	20.1
G53	1.7	8.5	0.49	0.1816	0.0024	1.8975	0.0414	0.0759	0.0016	1075.5	25.8	1080.2	33.3	1091.1	28.6	0.4	1.4	1091.1	28.6
G19	4.9	25.4	0.84	0.1703	0.0021	1.7886	0.0295	0.0762	0.0012	1013.9	22.6	1041.3	25.8	1100.3	21.2	2.6	7.9	1100.3	21.2
G47	4.8	23.5	0.63	0.1826	0.0022	1.9174	0.0305	0.0762	0.0011	1081.3	24.2	1087.1	25.6	1100.3	19.9	0.5	1.7	1100.3	19.9
G65	3.4	17.3	0.06	0.2068	0.0026	2.1854	0.0406	0.0767	0.0014	1211.6	27.9	1176.4	30.2	1113.7	23.8	-3.0	-8.8	1113.7	23.8
G41	5.9	31.6	0.08	0.1933	0.0023	2.0480	0.0309	0.0769	0.0011	1139.2	25.1	1131.6	25.1	1118.6	18.9	-0.7	-1.8	1118.6	18.9
G84	3.7	19.9	0.25	0.1843	0.0023	1.9539	0.0340	0.0769	0.0012	1090.5	25.3	1099.8	27.5	1119.6	21.9	0.8	2.6	1119.6	21.9
G114	5.4	30.1	0.20	0.1828	0.0024	1.9452	0.0353	0.0772	0.0013	1082.0	25.7	1096.8	27.9	1126.9	22.2	1.3	4.0	1126.9	22.2
G64	12.1	69.0	0.02	0.1858	0.0023	1.9810	0.0319	0.0774	0.0011	1098.6	24.9	1109.1	25.9	1131.3	20.1	0.9	2.9	1131.3	20.1
G93	6.0	31.2	0.44	0.1824	0.0023	1.9632	0.0353	0.0781	0.0013	1080.1	25.3	1103.0	28.2	1149.7	22.9	2.1	6.0	1149.7	22.9
G105	3.3	18.4	0.26	0.1762	0.0023	1.9080	0.0385	0.0786	0.0015	1046.0	25.3	1083.9	30.6	1161.8	26.1	3.5	10.0	1161.8	26.1
G106	3.4	13.3	1.04	0.2070	0.0027	2.2484	0.0428	0.0788	0.0014	1212.7	28.6	1196.3	30.6	1167.6	24.3	-1.4	-3.9	1167.6	24.3
G40	7.7	41.0	0.59	0.1691	0.0020	1.8420	0.0275	0.0791	0.0011	1007.2	22.4	1060.6	24.1	1173.4	19.2	5.0	14.2	1173.4	19.2
G102	3.4	19.1	0.05	0.1873	0.0024	2.0558	0.0374	0.0797	0.0013	1106.6	26.2	1134.2	28.8	1188.6	23.4	2.4	6.9	1188.6	23.4
G120	1.9	7.2	1.17	0.2020	0.0028	2.2190	0.0521	0.0797	0.0018	1186.2	29.7	1187.1	36.7	1189.3	31.3	0.1	0.3	1189.3	31.3
G110	2.7	10.4	0.91	0.2122	0.0029	2.4450	0.0537	0.0836	0.0017	1240.7	30.4	1255.9	35.7	1283.0	30.3	1.2	3.3	1283.0	30.3
G78	10.1	46.1	0.38	0.2116	0.0027	2.5142	0.0455	0.0863	0.0015	1237.1	28.5	1276.2	30.7	1344.0	25.2	3.1	8.0	1344.0	25.2
G70	4.4	11.3	1.30	0.2910	0.0037	3.9406	0.0673	0.0983	0.0016	1646.5	36.5	1622.1	32.8	1591.9	25.5	-1.5	-3.4	1591.9	25.5
G9	6.5	20.4	0.60	0.2831	0.0034	3.8486	0.0582	0.0987	0.0014	1606.8	33.9	1603.0	30.0	1598.9	23.0	-0.2	-0.5	1598.9	23.0
G112	6.6	17.8	0.63	0.3240	0.0042	4.8989	0.0863	0.1097	0.0017	1809.0	40.7	1802.1	34.4	1794.8	26.6	-0.4	-0.8	1794.8	26.6
G56	3.4	7.8	1.18	0.3313	0.0042	5.1079	0.0935	0.1119	0.0020	1844.6	41.1	1837.4	36.7	1830.7	29.6	-0.4	-0.8	1830.7	29.6
G42	2.7	5.8	1.39	0.3372	0.0042	5.2225	0.0887	0.1124	0.0018	1873.0	40.5	1856.3	34.7	1838.9	27.4	-0.9	-1.9	1838.9	27.4
G99	9.5	22.8	0.70	0.3563	0.0045	6.1859	0.1026	0.1260	0.0019	1964.7	43.0	2002.5	34.0	2042.8	26.0	1.9	3.8	2042.8	26.0
G69	7.5	19.6	0.29	0.3670	0.0045	6.4876	0.0993	0.1283	0.0018	2015.3	42.6	2044.2	32.6	2074.9	24.5	1.4	2.9	2074.9	24.5
G5	5.9	12.6	0.47	0.4140	0.0049	7.7432	0.1130	0.1357	0.0019	2233.3	45.0	2201.6	32.7	2173.0	24.6	-1.4	-2.8	2173.0	24.6
G8	10.5	20.5	0.65	0.4411	0.0052	9.5009	0.1343	0.1563	0.0021	2355.5	46.8	2387.6	32.6	2416.0	24.3	1.3	2.5	2416.0	24.3
G43	33.1	75.3	0.19	0.4262	0.0051	9.3005	0.1287	0.1584	0.0020	2288.5	46.0	2368.1	31.6	2438.5	23.0	3.4	6.2	2438.5	23.0
G95	13.1	30.6	0.19	0.4161	0.0052	9.1520	0.1464	0.1596	0.0023	2242.8	47.6	2353.3	34.7	2451.6	26.3	4.7	8.5	2451.6	26.3
G6	17.6	30.4	0.91	0.4621	0.0054	10.2886	0.1376	0.1615	0.0020	2449.0	47.6	2461.1	31.4	2471.8	22.8	0.5	0.9	2471.8	22.8
G57	8.5	18.0	0.13	0.4570	0.0056	10.3528	0.1536	0.1644	0.0022	2426.2	49.5	2466.8	33.7	2501.8	25.0	1.6	3.0	2501.8	25.0
G113	13.9	30.6	0.24	0.4362	0.0056	9.8986	0.1700	0.1647	0.0025	2333.4	50.4	2425.4	36.8	2504.2	28.3	3.8	6.8	2504.2	28.3
G91	10.5	19.4	0.61	0.4725	0.0060	12.3556	0.1996	0.1898	0.0028	2494.6	52.4	2631.8	36.1	2740.2	27.4	5.2	9.0	2740.2	27.4
G67	3.8	6.4	0.41	0.5195	0.0066	13.5831	0.2169	0.1898	0.0028	2696.9	55.7	2721.1	36.7	2740.3	27.8	0.9	1.6	2740.3	27.8
G60	2.5	4.1	0.42	0.5361	0.0068	14.7103	0.2368	0.1992	0.0030	2767.3	57.2	2796.7	37.3	2819.2	28.4	1.1	1.8	2819.2	28.4
G77	18.8	26.7	0.52	0.5962	0.0074	19.0633	0.2852	0.2321	0.0031	3014.6	59.4	3045.0	35.0	3066.4	25.7	1.0	1.7	3066.4	25.7
G83	9.8	17.1	0.19	0.5609	0.0070	19.9047	0.3044	0.2576	0.0035	2870.1	57.6	3086.7	35.7	3232.0	26.5	7.0	11.2	3232.0	26.5
G31	3.7	55.9	0.36	0.0658	0.0008	0.5834	0.0095	0.0644	0.0010	410.6	9.6	466.6	14.6	754.1	16.4	12.0	45.6	410.6	9.6
G44	7.7	112.6	0.06	0.0741	0.0009	0.6788	0.0109	0.0665	0.0010	460.8	10.8	526.1	15.9	821.8	16.9	12.4	43.9	460.8	10.8
G115	1.4	18.6	0.11	0.0799	0.0011	0.7418	0.0188	0.0674	0.0017	495.5	13.1	563.4	24.3	849.2	28.2	12.1	41.7	495.5	13.1
G																			

Table 2. U-Pb zircon ages of Zanskar River sands

Sample 12072207 Oma Chu

Grain No.	Pb (ppm)	U (ppm)	Atomic Th/U	Ratios						Ages (Ma)						% concord. (206/238)	% concord. (206/238)	Best Age (Ma)	$\pm 2\sigma$
				$^{206}\text{Pb}/^{238}\text{U}$	$\pm 1\sigma$	$^{207}\text{Pb}/^{235}\text{U}$	$\pm \text{s.e.}$	$^{207}\text{Pb}/^{206}\text{Pb}$	$\pm \text{s.e.}$	$^{206}\text{Pb}/^{238}\text{U}$	$\pm 2\sigma$	$^{207}\text{Pb}/^{235}\text{U}$	$\pm 2\sigma$	$^{207}\text{Pb}/^{206}\text{Pb}$	$\pm 2\sigma$				
G79	24.5	346.4	1.12	0.0566	0.0004	0.4289	0.0091	0.0554	0.0010	355.2	4.6	362.4	12.2	428.8	206.1	2.0	17.2	355.16	4.64
G58	33.4	528.7	0.53	0.0588	0.0004	0.4333	0.0073	0.0549	0.0008	368.1	4.4	365.5	10.2	409.4	203.2	-0.7	10.1	368.08	4.38
G23	14.9	149.2	1.86	0.0671	0.0005	0.5148	0.0143	0.0561	0.0013	418.7	6.0	421.7	17.4	455.5	19.4	0.7	8.1	418.66	6.04
G46	14.3	119.5	2.31	0.0747	0.0006	0.6672	0.0178	0.0667	0.0015	464.3	6.8	519.0	19.5	827.8	218.3	10.5	43.9	464.35	6.84
G38	39.3	497.6	0.40	0.0767	0.0005	0.5991	0.0093	0.0577	0.0008	476.5	5.4	476.6	11.5	519.5	204.1	0.0	8.3	476.51	5.39
G53	100.9	1126.3	0.77	0.0783	0.0005	0.6375	0.0093	0.0577	0.0008	486.0	5.5	500.8	11.1	519.1	203.6	2.9	6.4	486.03	5.50
G103	36.1	354.5	1.23	0.0789	0.0006	0.6336	0.0167	0.0596	0.0013	489.6	7.1	498.3	18.7	588.4	212.8	1.8	16.8	489.61	7.05
G82	60.7	678.6	0.70	0.0794	0.0005	0.6238	0.0110	0.0580	0.0009	492.7	5.9	492.2	13.0	530.5	205.7	-0.1	7.1	492.72	5.85
G63	11.0	113.4	1.03	0.0796	0.0006	0.6197	0.0169	0.0591	0.0014	493.9	7.2	489.6	19.2	571.9	213.0	-0.9	13.6	493.85	7.17
G67	45.0	490.9	0.72	0.0810	0.0005	0.6386	0.0103	0.0583	0.0008	501.9	5.8	501.4	12.3	541.4	204.8	-0.1	7.3	501.91	5.84
G1	35.7	247.8	2.80	0.0811	0.0005	0.6407	0.0141	0.0576	0.0011	502.7	6.4	502.7	15.8	513.8	15.1	0.0	2.2	502.69	6.44
G75	36.8	403.1	0.69	0.0813	0.0005	0.6506	0.0109	0.0592	0.0009	504.1	6.0	508.8	12.8	573.4	205.7	0.9	12.1	504.06	5.96
G37	50.4	555.7	0.68	0.0814	0.0005	0.6502	0.0097	0.0591	0.0008	504.5	5.7	508.6	11.8	569.3	204.7	0.8	11.4	504.53	5.72
G47	9.1	64.1	2.75	0.0817	0.0008	0.6739	0.0261	0.0604	0.0019	506.4	9.2	523.1	27.1	616.5	222.2	3.2	17.9	506.44	9.18
G11	13.4	103.3	2.16	0.0821	0.0007	0.6522	0.0197	0.0594	0.0015	508.7	7.7	509.8	21.6	582.9	24.2	0.2	12.7	508.70	7.74
G132	25.7	214.7	1.71	0.0836	0.0006	0.6393	0.0141	0.0564	0.0011	517.5	6.8	501.9	15.9	467.8	207.0	-3.1	-10.6	517.46	6.78
G93	37.4	437.6	0.35	0.0836	0.0005	0.6656	0.0116	0.0592	0.0009	517.8	6.2	518.1	13.4	573.7	206.2	0.1	9.8	517.75	6.19
G15	6.2	43.2	2.50	0.0845	0.0009	0.6676	0.0332	0.0563	0.0023	522.6	10.9	519.3	34.0	465.4	32.3	-0.6	-12.3	522.63	10.94
G108	15.4	129.6	1.67	0.0846	0.0006	0.6959	0.0174	0.0616	0.0013	523.5	7.3	536.4	18.7	661.6	213.2	2.4	20.9	523.46	7.25
G141	28.2	219.5	1.97	0.0846	0.0006	0.6737	0.0152	0.0573	0.0011	523.5	6.9	523.0	16.5	501.9	208.1	-0.1	-4.3	523.46	6.89
G106	25.5	195.8	2.05	0.0846	0.0006	0.6558	0.0147	0.0555	0.0011	523.7	6.8	512.0	16.2	434.0	206.5	-2.3	-20.7	523.70	6.78
G100	14.4	95.9	2.83	0.0849	0.0007	0.6353	0.0179	0.0566	0.0013	525.0	7.7	499.4	20.1	477.5	211.0	-5.1	-9.9	525.01	7.72
G104	78.2	833.9	0.61	0.0851	0.0005	0.6658	0.0114	0.0586	0.0009	526.3	6.3	518.2	13.3	551.9	205.6	-1.6	4.6	526.31	6.30
G109	20.2	256.6	0.02	0.0854	0.0006	0.6955	0.0152	0.0586	0.0011	528.4	6.9	536.1	16.3	550.8	208.7	1.4	4.1	528.39	6.89
G14	91.9	923.7	0.78	0.0861	0.0005	0.6837	0.0106	0.0574	0.0008	532.3	5.9	529.0	12.3	506.9	12.8	-0.6	-5.0	532.25	5.94
G137	10.5	75.6	2.23	0.0863	0.0008	0.7443	0.0293	0.0616	0.0020	533.6	9.9	564.9	28.6	658.5	223.9	5.5	19.0	533.62	9.85
G8	89.9	962.2	0.50	0.0874	0.0005	0.7070	0.0111	0.0577	0.0008	540.0	6.0	543.0	12.5	519.9	13.1	0.6	-3.9	539.96	6.05
G136	20.4	154.6	1.93	0.0876	0.0007	0.7231	0.0202	0.0598	0.0014	541.3	7.9	552.5	20.6	596.3	213.7	2.0	9.2	541.33	7.94
G13	65.6	783.3	0.11	0.0879	0.0005	0.7117	0.0124	0.0593	0.0009	543.2	6.3	545.8	13.7	576.3	15.0	0.5	5.7	543.22	6.28
G120	12.9	112.1	1.29	0.0882	0.0007	0.7114	0.0208	0.0599	0.0014	544.8	8.3	545.6	21.7	600.3	214.8	0.1	9.2	544.82	8.29
G31	54.9	538.2	0.74	0.0893	0.0005	0.7454	0.0127	0.0591	0.0009	551.5	6.4	565.5	13.6	572.3	14.7	2.5	3.6	551.46	6.39
G144	21.8	171.5	1.69	0.0895	0.0006	0.7350	0.0168	0.0616	0.0012	552.6	7.5	559.5	17.8	659.2	211.4	1.2	16.2	552.58	7.46
G86	10.4	72.9	2.21	0.0897	0.0008	0.7931	0.0280	0.0638	0.0018	553.6	9.3	592.9	26.6	735.7	222.7	6.6	24.7	553.64	9.35
G17	124.9	1286.3	0.56	0.0898	0.0005	0.7718	0.0122	0.0632	0.0009	554.5	6.3	580.8	13.4	715.3	15.9	4.5	22.5	554.47	6.27
G123	373.5	4364.7	0.03	0.0910	0.0010	0.7397	0.0369	0.0610	0.0025	561.4	12.2	562.2	37.0	638.2	231.4	0.1	12.0	561.45	12.17
G119	78.7	725.2	0.83	0.0930	0.0006	0.7626	0.0130	0.0597	0.0009	573.1	6.8	575.5	14.0	590.9	206.1	0.4	3.0	573.14	6.84
G35	50.4	459.2	0.85	0.0940	0.0006	0.7525	0.0113	0.0595	0.0008	578.9	6.5	569.7	12.8	584.3	204.8	-1.6	0.9	578.86	6.48
G57	16.2	164.1	0.36	0.0963	0.0006	0.7857	0.0164	0.0609	0.0011	592.7	7.4	588.8	16.9	636.1	209.4	-0.7	6.8	592.69	7.41
G139	17.9	161.4	0.75	0.0972	0.0007	0.8561	0.0220	0.0629	0.0013	598.0	8.5	628.0	20.5	703.2	214.1	4.8	14.9	598.04	8.46
G74	62.5	480.8	1.32	0.0992	0.0006	0.8064	0.0125	0.0604	0.0008	609.4	6.9	600.4	13.5	617.2	205.4	-1.5	1.3	609.43	6.92
G73	54.3	564.5	0.17	0.0994	0.0006	0.8254	0.0126	0.0605	0.0008	611.0	6.9	611.0	13.5	621.9	205.4	0.0	1.8	610.95	6.92
G85	552.7	5918.4	0.01	0.0007	0.9263	0.0211	0.0675	0.0012	614.9	8.1	665.7	19.2	853.5	214.2	7.6	28.0	614.94	8.09	
G55	56.1	530.7	0.41	0.0102	0.0006	0.8540	0.0133	0.0633	0.0009	621.4	7.0	626.9	14.0	719.7	206.8	0.9	13.7	621.38	7.02
G2	16.0	111.4	1.58	0.1027	0.0008	0.8627	0.0231	0.0613	0.0013	629.9	8.8	631.6	21.5	648.7	22.5	0.3	2.9	629.92	8.77
G126	143.7	1386.9	0.20	0.1047	0.0006	0.9094	0.0147	0.0619	0.0009	641.8	7.5	656.7	14.5	669.6	206.6	2.3	4.1	641.84	7.47
G115	8.6	66.2	0.99	0.1062	0.0010	0.9105	0.0356	0.0647	0.0020	650.6	11.8	657.3	31.7	765.9	225.9	1.0	15.1	650.58	11.77
G125	84.1	763.7	0.35	0.1075	0.0007	0.8802	0.0144	0.0607	0.0009	658.0	7.7	641.1	14.8	629.3	206.3	-2.6	-4.6	658.04	7.68
G133	23.0	198.5	0.50	0.1126	0.0008	1.0265	0.0269	0.0657	0.0014	687.6	9.6	717.2	22.5	797.8	215.9	4.1	13.8	687.60	9.62
G54	104.8	964.2	0.08	0.1156	0.0007	1.0332	0.0145	0.0639	0.0008	705.2	7.7	720.5	14.0	739.0	206.0	2.1	4.6	705.19	7.74
G113	57.7	482.8	0.35	0.1168	0.0007	1.0200	0.0177	0.0649	0.0010	712.0	8.4	713.9	16.5	769.5	208.8	0.3	7.5	712.00	8.43
G26	254.4	1772.5	1.08	0.1168	0.0007	1.1117	0.0153	0.0690	0.0008										

Table 2. U-Pb zircon ages of Zanskar River sands

G131	49.2	343.7	0.68	0.1268	0.0008	1.0919	0.0223	0.0636	0.0011	769.4	9.6	749.4	19.0	728.7	210.2	-2.7	-5.6	769.36	9.61
G16	38.1	281.6	0.48	0.1270	0.0008	1.1310	0.0221	0.0657	0.0010	770.4	9.2	768.2	18.5	797.8	19.3	-0.3	3.4	770.44	9.15
G111	59.9	397.7	0.83	0.1287	0.0008	1.1002	0.0192	0.0640	0.0009	780.3	9.1	753.4	17.1	740.6	208.3	-3.6	-5.4	780.33	9.14
G59	56.5	385.6	0.66	0.1315	0.0008	1.1871	0.0188	0.0679	0.0009	796.2	8.9	794.6	16.4	865.2	208.6	-0.2	8.0	796.19	8.89
G9	36.0	217.4	1.08	0.1326	0.0009	1.1613	0.0243	0.0652	0.0011	802.7	9.8	782.6	19.8	779.2	20.0	-2.6	-3.0	802.68	9.79
G114	38.9	232.3	1.07	0.1347	0.0009	1.2324	0.0242	0.0685	0.0011	814.8	9.9	815.4	19.5	883.7	211.8	0.1	7.8	814.79	9.88
G24	5991.6	47049.5	0.01	0.1368	0.0010	1.2487	0.0319	0.0675	0.0013	826.4	11.0	822.8	23.7	854.2	24.4	-0.4	3.2	826.43	11.00
G95	57.0	361.2	0.71	0.1379	0.0009	1.2656	0.0216	0.0672	0.0010	832.8	9.6	830.4	17.6	844.3	209.2	-0.3	1.4	832.78	9.63
G52	40.9	274.8	0.53	0.1383	0.0008	1.2741	0.0211	0.0682	0.0009	834.9	9.4	834.2	17.1	874.0	209.0	-0.1	4.5	834.87	9.40
G87	54.3	382.9	0.40	0.1383	0.0008	1.2518	0.0207	0.0673	0.0009	835.2	9.5	824.2	17.2	848.3	208.9	-1.3	1.5	835.21	9.51
G77	591.9	1501.7	5.33	0.1397	0.0008	1.4526	0.0198	0.0734	0.0009	842.9	9.2	911.0	15.8	1026.1	208.5	7.5	17.9	842.85	9.16
G29	205.3	941.3	2.09	0.1398	0.0008	1.2737	0.0187	0.0660	0.0008	843.5	9.0	834.0	15.9	806.7	16.0	-1.1	-4.6	843.47	9.05
G51	30.5	187.0	0.84	0.1398	0.0009	1.2919	0.0257	0.0695	0.0011	843.5	10.2	842.1	19.7	914.8	211.9	-0.2	7.8	843.53	10.18
G18	116.2	733.3	0.64	0.1413	0.0008	1.4227	0.0239	0.0733	0.0010	852.2	9.5	898.5	17.9	1021.7	19.6	5.2	16.6	852.18	9.49
G41	14.2	89.1	0.65	0.1422	0.0011	1.5174	0.0470	0.0757	0.0017	857.0	12.8	937.4	28.3	1086.6	222.3	8.6	21.1	856.98	12.76
G61	32.1	183.0	1.04	0.1434	0.0009	1.4025	0.0251	0.0725	0.0010	864.0	10.0	890.0	18.7	1000.6	211.2	2.9	13.7	863.97	10.04
G98	35.6	205.3	0.95	0.1441	0.0009	1.3277	0.0257	0.0694	0.0011	867.9	10.5	857.9	19.7	910.1	211.5	-1.2	4.6	867.86	10.48
G49	42.2	265.4	0.61	0.1446	0.0009	1.3638	0.0225	0.0701	0.0010	870.6	9.8	873.5	17.6	931.9	209.5	0.3	6.6	870.62	9.80
G122	42.7	249.2	0.66	0.1520	0.0010	1.4391	0.0288	0.0681	0.0011	911.9	11.1	905.4	20.5	871.3	211.5	-0.7	-4.7	871.29	211.55
G138	35.0	228.2	0.41	0.1459	0.0010	1.3495	0.0264	0.0686	0.0011	877.7	10.7	867.3	20.1	885.8	211.6	-1.2	0.9	877.71	10.69
G66	118.9	811.0	0.33	0.1460	0.0009	1.4649	0.0228	0.0721	0.0009	878.4	9.8	916.0	17.2	989.3	209.5	4.1	11.2	878.45	9.79
G60	3.4	18.9	0.91	0.1485	0.0018	1.5125	0.0852	0.0698	0.0027	892.4	19.8	935.4	48.2	923.7	239.7	4.6	3.4	892.38	19.76
G44	36.4	197.2	1.11	0.1488	0.0009	1.4400	0.0245	0.0724	0.0010	894.1	10.1	905.7	18.3	997.5	210.5	1.3	10.4	894.06	10.10
G149	77.4	463.2	0.55	0.1523	0.0010	1.4356	0.0273	0.0689	0.0011	913.8	11.0	903.9	20.2	894.8	211.5	-1.1	-2.1	894.85	211.47
G22	27.5	155.3	0.89	0.1491	0.0010	1.3519	0.0298	0.0674	0.0012	895.8	11.0	868.4	21.6	848.9	21.5	-3.2	-5.5	895.80	11.00
G107	62.3	391.0	0.47	0.1495	0.0009	1.3661	0.0247	0.0681	0.0010	897.9	10.5	874.5	18.9	870.7	210.2	-2.7	-3.1	897.94	10.54
G116	65.4	353.1	0.72	0.1622	0.0010	1.5273	0.0285	0.0700	0.0011	969.0	11.4	941.4	20.2	928.6	211.2	-2.9	-4.4	928.65	211.25
G143	36.2	214.0	0.57	0.1538	0.0010	1.4721	0.0300	0.0701	0.0011	922.0	11.4	919.0	21.2	930.4	212.6	-0.3	0.9	930.41	212.64
G110	108.3	652.3	0.55	0.1525	0.0009	1.4452	0.0244	0.0704	0.0010	915.0	10.5	907.9	18.6	939.8	210.2	-0.8	2.6	939.75	210.24
G62	40.5	202.6	1.33	0.1530	0.0010	1.4627	0.0267	0.0706	0.0010	917.6	10.6	915.1	19.1	945.3	210.8	-0.3	2.9	945.27	210.77
G92	53.5	334.2	0.28	0.1583	0.0010	1.5273	0.0269	0.0706	0.0010	947.3	10.9	941.4	19.0	947.0	210.4	-0.6	0.0	947.01	210.43
G105	25.2	119.5	1.20	0.1639	0.0011	1.6011	0.0352	0.0709	0.0012	978.5	12.2	970.6	22.4	953.7	213.6	-0.8	-2.6	953.67	213.59
G6	79.6	517.9	0.14	0.1588	0.0010	1.5615	0.0273	0.0712	0.0010	950.3	10.7	955.0	18.9	961.7	19.3	0.5	1.2	961.73	19.28
G112	109.5	707.6	0.13	0.1604	0.0010	1.5657	0.0249	0.0712	0.0010	959.1	10.8	956.7	18.4	962.6	209.8	-0.3	0.4	962.59	209.77
G102	50.2	234.3	1.34	0.1628	0.0011	1.5929	0.0321	0.0712	0.0011	972.5	11.8	967.4	21.1	963.4	212.4	-0.5	-0.9	963.45	212.39
G90	13.8	66.8	1.07	0.1663	0.0012	1.6320	0.0424	0.0714	0.0014	991.8	13.3	982.6	25.5	969.8	216.6	-0.9	-2.4	968.89	216.60
G5	80.1	413.2	0.83	0.1646	0.0010	1.6285	0.0264	0.0715	0.0010	982.1	10.7	981.3	18.3	972.6	18.4	-0.1	-1.0	972.60	18.43
G68	38.5	188.4	1.35	0.1556	0.0010	1.5154	0.0277	0.0716	0.0010	932.4	10.8	936.6	19.4	975.2	211.2	0.5	4.4	975.16	211.20
G43	85.4	478.7	0.84	0.1529	0.0009	1.4992	0.0228	0.0722	0.0009	917.4	10.1	930.1	17.2	990.5	209.1	1.4	7.4	990.46	209.12
G99	35.5	176.9	1.38	0.1502	0.0010	1.4393	0.0292	0.0724	0.0012	902.2	11.0	905.4	20.9	996.9	213.2	0.4	9.5	996.93	213.17
G81	87.4	505.7	0.39	0.1651	0.0010	1.6415	0.0252	0.0737	0.0010	985.3	10.8	986.3	18.1	1031.9	209.7	0.1	4.5	1031.89	209.71
G48	153.1	911.6	0.35	0.1634	0.0009	1.6806	0.0239	0.0742	0.0009	975.4	10.4	1001.2	17.1	1046.9	208.8	2.6	6.8	1046.91	208.84
G129	46.6	212.0	0.90	0.1838	0.0012	1.8794	0.0370	0.0748	0.0012	1087.9	13.0	1073.8	22.2	1062.9	213.3	-1.3	-2.4	1062.86	213.26
G84	41.8	226.9	0.56	0.1690	0.0011	1.7314	0.0335	0.0749	0.0011	1006.3	11.9	1020.3	21.0	1064.7	212.7	1.4	5.5	1064.75	212.73
G7	96.9	490.9	0.57	0.1792	0.0011	1.8776	0.0341	0.0753	0.0011	1062.4	11.9	1073.2	20.4	1076.8	20.7	1.0	1.3	1076.79	20.67
G118	79.4	376.8	0.78	0.1819	0.0011	1.8537	0.0317	0.0759	0.0011	1077.2	12.3	1064.7	20.4	1091.1	211.7	-1.2	1.3	1091.11	211.68
G28	30.2	114.8	2.20	0.1663	0.0011	1.7816	0.0433	0.0769	0.0014	991.5	12.6	1038.7	24.4	1118.9	25.6	4.5	11.4	1118.86	25.61
G142	40.4	202.6	0.49	0.1851	0.0012	1.9863	0.0419	0.0771	0.0012	1094.8	13.4	1110.9	23.4	1123.8	214.9	1.4	2.6	1123.78	214.86
G71	23.5	112.8	0.77	0.1811	0.0012	1.8743	0.0388	0.0772	0.0012	1072.7	12.9	1072.0	22.4	1127.4	214.0	-0.1	4.9	1127.39	213.97
G3	90.1	409.2	0.74	0.1911	0.0011	2.0406	0.0327	0.0773	0.0010	1127.5	12.1	1129.2	19.5	1127.9	19.6	0.1	0.0	1127.91	19.61
G80	97.5	455.1	0.55	0.1966	0.0012	2.1063	0.0329	0.0776	0.0010	1157.1	12.6	1150.9	19.4	1137.2	210.4	-0.5	-1.8	1137.16	210.44
G134	76.9	310.6	0.92	0.2050	0.0013	2.1878	0.0393	0.0785	0.0011	1201.9	13.8	1177.2	22.0	1158.3	212.9	-2.1	-3.8	1158.29	212.90
G89	15.8	67.5	1.37	0.1764	0.0014	1.8054	0.0537	0.0787	0.0016	1047.3	15.0	1047.4	29.5	1163.6	221.7	0.0	10.0	1163.59	221.70
G21	66.7	278.9	0.79	0.2046	0.0013	2.3102	0.0441	0.0793	0.0011	1200.0	13.5	1215.4	21.8	1179.4	21.7	1.3	-1.8	1179.38	21.69
G33	132.8	569.9	0.82	0.1971	0.0012														

Table 2. U-Pb zircon ages of Zanskar River sands

G97	69.4	217.4	0.60	0.2844	0.0018	3.7855	0.0661	0.0983	0.0013	1613.4	17.6	1589.7	23.5	1592.5	214.2	-1.5	-1.3	1592.50	214.25
G27	60.8	190.4	0.49	0.2910	0.0018	4.0995	0.0775	0.0998	0.0013	1646.6	17.7	1654.2	23.8	1620.2	23.4	0.5	-1.6	1620.17	23.39
G25	48.9	136.4	0.58	0.3185	0.0020	4.8213	0.1053	0.1091	0.0015	1782.5	19.9	1788.6	26.0	1784.6	25.5	0.3	0.1	1784.61	25.53
G83	40.7	91.2	1.70	0.3129	0.0021	4.7969	0.1142	0.1139	0.0017	1755.0	20.8	1784.4	27.4	1863.2	218.2	1.6	5.8	1863.18	218.16
G91	212.0	528.7	0.72	0.3457	0.0021	5.7736	0.0919	0.1250	0.0016	1913.9	19.8	1942.5	24.0	2028.1	214.8	1.5	5.6	2028.09	214.77
G127	66.2	133.0	0.81	0.4070	0.0026	6.8302	0.1404	0.1255	0.0018	2201.3	24.1	2089.6	27.6	2036.0	217.8	-5.3	-8.1	2036.00	217.78
G39	105.6	279.5	0.74	0.3271	0.0019	5.6588	0.0910	0.1278	0.0015	1824.1	18.7	1925.1	23.1	2068.3	214.1	5.2	11.8	2068.34	214.13
G145	19.4	37.1	1.01	0.4138	0.0031	8.2341	0.2438	0.1518	0.0025	2232.1	28.5	2257.1	32.9	2366.1	223.1	1.1	5.7	2366.08	223.07
G101	268.4	503.0	0.83	0.4392	0.0026	9.4591	0.1503	0.1577	0.0020	2346.8	23.6	2383.6	25.4	2431.5	215.9	1.5	3.5	2431.47	215.93
G94	123.1	241.7	0.62	0.4402	0.0027	9.4395	0.1566	0.1583	0.0020	2351.3	23.7	2381.7	25.3	2437.4	215.9	1.3	3.5	2437.37	215.86
G32	19.6	25.0	1.38	0.5463	0.0044	15.5857	0.5883	0.2050	0.0031	2809.8	36.6	2851.7	32.9	2866.3	31.0	1.5	2.0	2866.27	30.98
G20	218.2	231.6	1.40	0.6321	0.0037	21.2096	0.3580	0.2402	0.0029	3157.7	29.1	3148.2	25.6	3121.0	24.8	-0.3	-1.2	3120.96	24.79
G88	57.4	85.1	0.97	0.5571	0.0039	17.8938	0.4723	0.2512	0.0033	2854.5	32.0	2984.0	28.8	3192.5	218.7	4.3	10.6	3192.47	218.67
G146	192.2	277.5	0.75	0.6004	0.0038	22.7174	0.4264	0.2785	0.0038	3031.5	30.6	3214.9	29.5	3354.4	219.9	5.7	9.6	3354.43	219.90
G45	182.3	274.8	0.65	0.5970	0.0035	22.5344	0.3557	0.2893	0.0033	3017.8	28.0	3207.1	24.8	3413.7	215.2	5.9	11.6	3413.69	215.22
G65	81.8	274.0	0.07	0.0268	0.0004	10.8194	0.9108	0.3161	0.0097	170.7	5.1	2507.7	37.5	3551.0	253.4	93.2	95.2		
G19	1.4	50.0	0.93	0.0230	0.0004	0.5512	0.0257	0.1746	0.0073	146.3	4.7	445.8	32.2	2602.6	79.7	67.2	94.4		
G148	173.5	1847.4	0.16	0.0956	0.0008	1.0911	0.0346	0.0873	0.0021	588.5	9.8	749.0	28.3	1367.8	229.8	21.4	57.0		
G124	24.5	203.9	1.54	0.0862	0.0006	0.8900	0.0200	0.0757	0.0014	533.1	7.2	646.4	19.0	1086.4	217.7	17.5	50.9		
G70	29.6	287.0	1.34	0.0803	0.0005	0.7912	0.0134	0.0728	0.0011	498.0	6.0	591.9	14.4	1007.3	211.6	15.9	50.6		
G121	100.6	1163.4	0.38	0.0870	0.0005	0.8557	0.0145	0.0713	0.0010	537.9	6.4	627.8	14.8	965.2	211.2	14.3	44.3	537.95	6.40
G96	37.0	236.3	0.86	0.1312	0.0009	1.5353	0.0311	0.0871	0.0014	794.8	9.9	944.6	21.2	1362.7	216.6	15.9	41.7		
G78	186.7	1126.3	0.65	0.1470	0.0009	1.9122	0.0261	0.0915	0.0011	884.1	9.6	1085.4	17.6	1456.8	211.6	18.5	39.3		
G56	9.6	58.7	0.54	0.1485	0.0011	1.6402	0.0459	0.0866	0.0017	892.5	12.8	985.8	27.8	1351.4	222.8	9.5	34.0	892.55	12.80
G42	11.7	91.8	1.79	0.0900	0.0006	0.7909	0.0192	0.0671	0.0013	555.8	7.6	591.7	19.6	839.9	215.8	6.1	33.8	555.77	7.57
G40	19.3	141.1	2.56	0.0812	0.0006	0.6929	0.0197	0.0635	0.0015	503.3	7.5	534.5	20.9	724.7	217.3	5.8	30.5	503.34	7.51
G64	71.9	163.4	0.98	0.3642	0.0022	8.2728	0.1586	0.1556	0.0019	2001.8	21.1	2261.3	24.9	2408.8	215.8	11.5	16.9		
G135	69.9	185.0	1.43	0.2856	0.0019	5.4987	0.1159	0.1416	0.0021	1619.4	19.0	1900.4	27.6	2246.3	219.4	14.8	27.9		

Sample 13071402 Hanumil

Grain No.	Pb (ppm)	U (ppm)	Atomic Th/U	Ratios				Ages (Ma)				% concord. (206/238)		% concord. (206/238)		Best Age (Ma)	± 2σ		
				$^{206}\text{Pb}/^{238}\text{U}$	± 1 σ	$^{207}\text{Pb}/^{235}\text{U}$	± s.e.	$^{207}\text{Pb}/^{206}\text{Pb}$	± s.e.	$^{206}\text{Pb}/^{238}\text{U}$	± 2σ	$^{207}\text{Pb}/^{235}\text{U}$	± 2σ	$^{207}\text{Pb}/^{206}\text{Pb}$	± 2σ				
G1	5.6	1679.4	0.01	0.0040	0.0001	0.0252	0.0012	0.0466	0.0022	25.4	0.8	25.3	2.5	27.2	69.7	-0.6	6.7	25.4	0.8
G79	1.6	416.8	0.01	0.0041	0.0001	0.0275	0.0023	0.0501	0.0042	26.5	1.2	27.5	4.9	197.3	97.6	3.7	86.6	26.5	1.2
G93	42.8	1406.4	0.72	0.0238	0.0003	0.1839	0.0055	0.0569	0.0016	151.8	4.0	171.4	9.7	488.0	88.3	11.4	68.9	151.8	4.0
G16	3.8	150.8	0.09	0.0262	0.0005	0.1912	0.0141	0.0559	0.0039	167.0	6.4	177.7	24.7	447.6	117.7	6.0	62.7	167.0	6.4
G101	73.9	1609.2	0.55	0.0408	0.0005	0.3020	0.0080	0.0542	0.0013	257.9	6.6	268.0	12.8	378.1	82.1	3.8	31.8	257.9	6.6
G23	35.4	752.9	0.55	0.0424	0.0005	0.3174	0.0083	0.0538	0.0013	267.6	6.7	279.9	13.0	363.5	81.6	4.4	26.4	267.6	6.7
G90	20.2	228.0	2.53	0.0500	0.0007	0.3622	0.0125	0.0545	0.0017	314.7	8.5	313.8	18.6	393.4	87.0	-0.3	20.0	314.7	8.5
G48	10.5	176.5	0.81	0.0502	0.0007	0.3558	0.0125	0.0542	0.0017	315.8	8.5	309.1	19.0	378.1	87.0	-2.2	16.5	315.8	8.5
G97	70.4	1191.9	0.65	0.0528	0.0007	0.3908	0.0101	0.0533	0.0012	331.8	8.3	335.0	14.8	339.9	80.3	1.0	2.4	331.8	8.3
G35	9.7	157.8	0.65	0.0554	0.0008	0.4054	0.0145	0.0539	0.0017	347.7	9.3	345.6	20.4	366.9	86.6	-0.6	5.2	347.7	9.3
G74	86.2	1096.6	1.63	0.0557	0.0007	0.4159	0.0087	0.0544	0.0010	349.5	8.5	353.1	13.1	388.1	78.8	1.0	9.9	349.5	8.5
G55	8.9	137.9	0.74	0.0561	0.0008	0.4125	0.0156	0.0547	0.0018	351.8	9.5	350.7	21.8	399.6	89.2	-0.3	12.0	351.8	9.5
G12	47.9	682.7	1.03	0.0567	0.0007	0.4219	0.0090	0.0541	0.0010	355.6	8.5	357.4	13.6	376.9	79.1	0.5	5.6	355.6	8.5
G103	29.4	498.0	0.34	0.0580	0.0008	0.4272	0.0109	0.0538	0.0012	363.1	9.1	361.2	15.6	361.4	80.7	-0.5	-0.5	363.1	9.1
G22	89.2	1146.3	1.33	0.0583	0.0007	0.4447	0.0083	0.0544	0.0009	365.2	8.6	373.6	12.6	386.0	77.7	2.2	5.4	365.2	8.6
G96	2.1	26.3	1.40	0.0592	0.0015	0.4357	0.0528	0.0485	0.0052	370.8	18.4	367.2	63.1	121.8	91.7	-1.0	-204.5	370.8	18.4
G47	65.9	1125.8	0.17	0.0606	0.0008	0.4525	0.0094	0.0542	0.0010	379.0	9.1	379.0	13.9	378.1	78.6	0.0	-0.2	379.0	9.1
G65	53.2	740.6	0.69	0.0636	0.0008	0.5218	0.0121	0.0598	0.0012	397.6	9.7	426.4	16.5	596.3	85.3	6.7	33.3	397.6	9.7
G10	150.9	2441.0	0.05	0.0662	0.0008	0.5440	0.0095	0.0600	0.0009	413.3	9.7	441.0	13.9	603.2	81.0	6.3	31.5	413.3	9.7
G15	80.1	1083.7	0.50	0.0683	0.0008	0.5327	0.0099	0.0571	0.0009	426.1	10.0	433.6	14.3	494.2	79.8	1.7	13.8	426.1	10.0
G77	111.6	1709.2	0.09	0.0691	0.0009	0.5406	0.0108	0.0566	0.0010	430.9	10.4	438.8	15.1	476.4	80.2	1.8	9.5	430.9	10.4

Table 2. U-Pb zircon ages of Zanskar River sands

G67	32.0	325.6	0.66	0.0876	0.0011	0.6881	0.0181	0.0589	0.0013	541.0	13.3	531.6	21.5	563.8	86.3	-1.8	4.0	541.0	13.3
G11	57.3	652.9	0.16	0.0879	0.0011	0.7258	0.0155	0.0599	0.0011	542.9	12.8	554.1	18.5	598.2	83.4	2.0	9.2	542.9	12.8
G75	83.0	781.5	0.62	0.0931	0.0012	0.8609	0.0233	0.0655	0.0014	573.7	14.3	630.6	23.7	789.8	91.3	9.0	27.4	573.7	14.3
G107	169.6	1550.2	0.60	0.0995	0.0013	0.8993	0.0192	0.0659	0.0012	611.7	14.8	651.3	21.1	803.2	87.1	6.1	23.8	611.7	14.8
G51	283.9	2652.0	0.38	0.1029	0.0013	0.9263	0.0166	0.0647	0.0010	631.4	14.7	665.7	18.9	763.0	83.5	5.2	17.2	631.4	14.7
G83	114.8	1104.8	0.20	0.1053	0.0013	0.9655	0.0201	0.0665	0.0012	645.6	15.4	686.1	21.3	823.4	86.7	5.9	21.6	645.6	15.4
G63	68.2	571.1	0.53	0.1086	0.0014	0.9712	0.0231	0.0639	0.0012	664.7	15.9	689.1	23.0	739.0	87.6	3.5	10.0	664.7	15.9
G17	353.1	2372.6	1.27	0.1140	0.0014	1.0596	0.0179	0.0674	0.0010	696.0	15.9	733.6	19.5	848.9	83.6	5.1	18.0	696.0	15.9
G39	65.9	415.0	1.47	0.1147	0.0015	1.0429	0.0262	0.0678	0.0014	700.1	16.8	725.4	24.9	862.1	90.5	3.5	18.8	700.1	16.8
G21	12.4	92.4	0.79	0.1157	0.0016	1.0025	0.0376	0.0662	0.0019	705.5	18.3	705.1	33.4	814.0	99.6	-0.1	13.3	705.5	18.3
G80	245.9	1462.5	1.47	0.1178	0.0015	1.1399	0.0224	0.0698	0.0012	717.6	16.8	772.4	22.2	922.5	87.2	7.1	22.2	717.6	16.8
G87	33.3	197.0	1.53	0.1198	0.0016	1.0477	0.0325	0.0658	0.0016	729.4	18.3	727.8	29.3	798.7	94.1	-0.2	8.7	729.4	18.3
G110	242.8	1530.3	1.27	0.1209	0.0015	1.1415	0.0248	0.0670	0.0012	735.9	17.6	773.2	23.6	836.5	87.8	4.8	12.0	735.9	17.6
G62	311.8	1510.4	2.57	0.1212	0.0015	1.0879	0.0212	0.0657	0.0011	737.5	17.1	747.5	21.7	797.8	85.2	1.3	7.6	737.5	17.1
G19	211.3	1390.6	1.10	0.1218	0.0015	1.1433	0.0191	0.0673	0.0010	740.6	16.8	774.1	20.0	846.5	83.4	4.3	12.5	740.6	16.8
G20	299.7	1680.5	1.79	0.1223	0.0015	1.1514	0.0191	0.0675	0.0010	743.8	16.9	777.9	20.0	854.5	83.4	4.4	13.0	743.8	16.9
G89	109.1	681.6	1.24	0.1234	0.0016	1.1594	0.0257	0.0684	0.0012	749.9	17.8	781.7	24.1	880.1	88.5	4.1	14.8	749.9	17.8
G42	50.0	304.0	1.40	0.1235	0.0016	1.0584	0.0317	0.0659	0.0015	750.9	18.5	733.0	28.7	804.2	93.1	-2.4	6.6	750.9	18.5
G32	66.5	479.3	0.66	0.1236	0.0015	1.1095	0.0220	0.0669	0.0011	751.0	17.3	757.9	22.0	834.7	85.7	0.9	10.0	751.0	17.3
G100	118.7	897.3	0.48	0.1242	0.0016	1.1323	0.0235	0.0656	0.0011	754.6	17.9	768.8	22.9	792.7	86.2	1.8	4.8	754.6	17.9
G33	68.0	451.8	0.91	0.1247	0.0015	1.1220	0.0231	0.0675	0.0011	757.3	17.5	764.0	22.6	853.9	86.5	0.9	11.3	757.3	17.5
G31	57.7	443.1	0.37	0.1254	0.0015	1.1224	0.0226	0.0670	0.0011	761.8	17.5	764.1	22.3	838.7	85.9	0.3	9.2	761.8	17.5
G52	198.3	925.9	2.57	0.1257	0.0016	1.1606	0.0230	0.0666	0.0011	763.4	17.8	782.2	22.3	824.3	85.7	2.4	7.4	763.4	17.8
G34	56.5	399.8	0.66	0.1259	0.0016	1.1395	0.0235	0.0675	0.0011	764.4	17.7	772.3	22.8	851.7	86.5	1.0	10.2	764.4	17.7
G61	115.7	889.7	0.35	0.1263	0.0016	1.1826	0.0246	0.0661	0.0011	766.6	18.0	792.5	22.8	809.9	86.1	3.3	5.3	766.6	18.0
G6	23.8	157.2	0.84	0.1281	0.0017	1.1497	0.0353	0.0681	0.0016	777.0	19.0	777.1	29.8	871.9	94.7	0.0	10.9	777.0	19.0
G56	117.4	758.7	0.89	0.1285	0.0016	1.1652	0.0227	0.0654	0.0011	779.1	18.1	784.4	22.2	786.9	84.9	0.7	1.0	779.1	18.1
G30	35.9	250.2	0.62	0.1292	0.0016	1.1306	0.0265	0.0651	0.0012	783.1	18.4	768.0	24.4	778.9	87.4	-2.0	-0.5	783.1	18.4
G46	80.6	634.8	0.18	0.1297	0.0016	1.1954	0.0233	0.0671	0.0011	785.9	18.1	798.5	22.3	840.3	85.4	1.6	6.5	785.9	18.1
G2	82.7	582.8	0.54	0.1297	0.0016	1.1904	0.0218	0.0673	0.0010	786.0	17.8	796.1	21.5	848.0	84.6	1.3	7.3	786.0	17.8
G111	85.3	579.3	0.68	0.1297	0.0017	1.1969	0.0270	0.0664	0.0012	786.1	18.8	799.1	24.8	820.3	88.0	1.6	4.2	786.1	18.8
G13	124.0	816.6	0.80	0.1304	0.0016	1.1889	0.0211	0.0678	0.0010	790.3	17.9	795.4	21.2	861.8	84.3	0.6	8.3	790.3	17.9
G102	100.4	658.2	0.78	0.1315	0.0017	1.2086	0.0263	0.0668	0.0012	796.1	18.9	804.6	24.4	831.5	87.6	1.0	4.3	796.1	18.9
G92	165.4	1006.6	1.09	0.1315	0.0016	1.2117	0.0243	0.0665	0.0011	796.3	18.7	806.0	23.1	823.4	86.0	1.2	3.3	796.3	18.7
G54	99.3	746.4	0.28	0.1316	0.0016	1.2196	0.0237	0.0663	0.0011	796.8	18.5	809.6	22.4	814.3	85.1	1.6	2.1	796.8	18.5
G8	76.1	585.7	0.21	0.1316	0.0016	1.2331	0.0245	0.0685	0.0011	796.9	18.1	815.7	22.6	884.3	86.1	2.3	9.9	796.9	18.1
G45	90.4	420.3	2.32	0.1318	0.0017	1.1601	0.0280	0.0662	0.0013	798.0	18.8	782.0	25.3	811.1	88.5	-2.0	1.6	798.0	18.8
G98	93.0	682.1	0.37	0.1318	0.0017	1.2271	0.0261	0.0662	0.0012	798.2	18.8	813.0	23.9	813.3	86.8	1.8	1.9	798.2	18.8
G71	66.9	426.1	0.88	0.1324	0.0017	1.2147	0.0267	0.0674	0.0012	801.6	18.9	807.4	24.4	848.9	87.7	0.7	5.6	801.6	18.9
G68	273.4	2100.2	0.19	0.1330	0.0016	1.2311	0.0228	0.0663	0.0010	804.9	18.5	814.8	22.0	816.8	84.6	1.2	1.5	804.9	18.5
G50	59.2	436.6	0.31	0.1332	0.0017	1.2027	0.0250	0.0666	0.0011	806.2	18.8	801.8	23.3	826.2	86.2	-0.5	2.4	806.2	18.8
G95	146.2	1103.0	0.22	0.1339	0.0017	1.2226	0.0262	0.0662	0.0012	810.3	19.1	811.0	24.2	813.3	87.0	0.1	0.4	810.3	19.1
G38	107.8	674.5	0.81	0.1343	0.0016	1.2291	0.0231	0.0664	0.0010	812.3	18.6	813.9	22.1	818.1	84.6	0.2	0.7	812.3	18.6
G27	131.6	881.5	0.62	0.1345	0.0017	1.2211	0.0263	0.0658	0.0011	813.7	18.8	810.3	23.6	801.3	86.2	-0.4	-1.5	813.7	18.8
G82	122.3	855.2	0.42	0.1359	0.0017	1.2445	0.0250	0.0658	0.0011	821.5	19.2	820.9	23.4	801.3	85.7	-0.1	-2.5	821.5	19.2
G85	44.7	299.3	0.57	0.1360	0.0018	1.2207	0.0382	0.0668	0.0016	822.2	20.4	810.1	30.9	830.0	94.4	-1.5	0.9	822.2	20.4
G94	478.0	2633.3	1.35	0.1361	0.0017	1.2549	0.0252	0.0666	0.0011	822.8	19.3	825.6	23.6	825.6	86.2	0.3	0.3	822.8	19.3
G5	136.7	894.3	0.66	0.1362	0.0017	1.2670	0.0260	0.0674	0.0011	823.1	18.7	831.1	23.2	850.8	86.2	1.0	3.3	823.1	18.7
G99	85.8	410.3	2.01	0.1363	0.0017	1.2284	0.0280	0.0667	0.0012	823.8	19.6	813.6	25.4	826.9	88.2	-1.3	0.4	823.8	19.6
G73	46.4	236.1	1.70	0.1367	0.0018	1.2921	0.0336	0.0703	0.0014	825.9	19.8	842.2	27.8	937.7	92.1	1.9	11.9	825.9	19.8
G57	268.6	1806.2	0.46	0.1375	0.0017	1.5334	0.0298	0.0781	0.0012	830.6	19.2	943.8	24.3	1149.7	89.0	12.0	27.8	830.6	19.2
G81	50.4	341.9	0.47	0.1382	0.0017	1.2482	0.0291	0.0666	0.0012	834.4	19.7	822.6	25.5	823.7	88.2	-1.4	-1.3	834.4	19.7
G49	149.2	906.0	0.87	0.1387	0.0017	1.2674	0.0242	0.0664	0.0010	837.5	19.2	831.2	22.6	818.7	84.8	-0.8	-2.3	837.5	19.2
G84	79.8	413.3	1.56	0.1390	0.0018	1.2911	0.0308	0.0678	0.0013	839.2	19.9	841.8	26.1	860.9	89.1	0.3	2.5	839.2	19.9
G29	130.6	745.3	1.10	0.1393	0.0017	1.2723	0.0230	0.0668	0.0010	840.6	19.1	833.4	22.0	832.5	84.2	-0.9	-1.0	840.6	19.1
G76	92.8	443.1	1.9																

Table 2. U-Pb zircon ages of Zanskar River sands

G86	194.3	1227.5	0.58	0.1439	0.0018	1.3179	0.0256	0.0660	0.0011	866.5	20.1	853.6	23.5	807.6	85.2	-1.5	-7.3	866.5	20.1
G53	126.2	468.2	3.12	0.1450	0.0018	1.3978	0.0337	0.0718	0.0014	872.6	20.5	888.0	27.1	980.6	90.8	1.7	11.0	872.6	20.5
G64	49.6	305.1	0.53	0.1497	0.0019	1.3695	0.0342	0.0678	0.0013	899.0	21.3	875.9	27.4	862.1	89.6	-2.6	-4.3	899.0	21.3
G24	123.9	778.0	0.12	0.1653	0.0020	1.6220	0.0320	0.0707	0.0011	986.0	22.2	978.8	24.7	949.6	86.4	-0.7	-3.8	949.6	86.4
G9	30.8	149.6	0.77	0.1751	0.0022	1.7534	0.0500	0.0735	0.0015	1040.0	24.2	1028.4	31.2	1026.4	93.6	-1.1	-1.3	1026.4	93.6
G106	93.7	488.7	0.79	0.1658	0.0021	1.6570	0.0414	0.0740	0.0014	988.7	23.6	992.2	29.8	1042.6	92.5	0.4	5.2	1042.6	92.5
G78	91.7	427.9	0.55	0.1954	0.0025	2.0536	0.0474	0.0772	0.0014	1150.7	26.5	1133.5	29.7	1126.1	91.2	-1.5	-2.2	1126.1	91.2
G109	42.1	180.0	0.65	0.2067	0.0027	2.2372	0.0589	0.0806	0.0016	1210.9	28.5	1192.8	33.4	1211.5	95.1	-1.5	0.0	1211.5	95.1
G26	184.9	881.5	0.13	0.2147	0.0026	2.4625	0.0416	0.0836	0.0012	1253.8	27.4	1261.1	26.4	1282.8	87.2	0.6	2.3	1282.8	87.2
G28	80.1	234.4	1.09	0.2717	0.0033	3.5995	0.0770	0.0985	0.0015	1549.3	33.7	1549.4	31.2	1595.2	91.7	0.0	2.9	1595.2	91.7
G88	127.1	414.4	0.34	0.2912	0.0036	4.0070	0.0842	0.1026	0.0017	1647.3	36.2	1635.6	33.5	1671.5	93.9	-0.7	1.4	1671.5	93.9
G40	160.8	441.9	0.79	0.3076	0.0038	4.4347	0.0993	0.1078	0.0017	1728.9	37.4	1718.8	33.0	1763.2	93.1	-0.6	1.9	1763.2	93.1
G105	84.1	258.4	0.74	0.2928	0.0037	4.5702	0.1133	0.1167	0.0021	1655.3	37.2	1743.9	36.8	1905.7	98.0	5.1	13.1	1905.7	98.0
G43	868.2	2264.5	0.01	0.3960	0.0048	8.5538	0.1438	0.1582	0.0022	2150.6	44.2	2291.7	33.3	2436.3	92.5	6.2	11.7	2436.3	92.5
G44	84.6	158.4	0.32	0.4902	0.0062	12.0256	0.3333	0.1862	0.0029	2571.6	53.2	2606.4	37.4	2709.1	96.3	1.3	5.1	2709.1	96.3
G36	36.9	43.8	0.74	0.6562	0.0084	22.7902	0.8017	0.2615	0.0040	3252.5	65.3	3218.0	39.0	3255.6	97.2	-1.1	0.1	3255.6	97.2
G104	61.2	466.5	2.30	0.0903	0.0013	0.9058	0.0334	0.0747	0.0022	557.5	15.1	654.8	32.0	1059.9	106.0	14.9	47.4	557.5	15.1
G14	97.3	1112.9	0.38	0.0835	0.0010	0.8005	0.0152	0.0691	0.0011	517.1	12.0	597.1	18.1	900.8	86.4	13.4	42.6	517.1	12.0
G18	189.5	2114.2	0.22	0.0921	0.0011	0.8677	0.0150	0.0676	0.0010	567.8	13.1	634.3	17.8	856.0	84.1	10.5	33.7	567.8	13.1

Sample 12072401 Pishu

Grain No.	Pb (ppm)	U (ppm)	Atomic Th/U	Ratios				Ages (Ma)					% concord. (206/238)	% concord. (206/238)	Best Age (Ma)	± 2σ			
				$^{206}\text{Pb}/^{238}\text{U}$	± 1 σ	$^{207}\text{Pb}/^{235}\text{U}$	± s.e.	$^{207}\text{Pb}/^{206}\text{Pb}$	± s.e.	$^{206}\text{Pb}/^{238}\text{U}$	± 2σ	$^{207}\text{Pb}/^{235}\text{U}$	± 2σ	$^{207}\text{Pb}/^{206}\text{Pb}$	± 2σ				
G67	6.5	2082.3	0.01	0.0034	0.0000	0.0224	0.0008	0.0469	0.0016	22.1	0.4	22.5	1.5	42.1	16.8	1.5	47.4	22.14	0.39
G27	1.1	231.4	0.04	0.0049	0.0001	0.0313	0.0033	0.0480	0.0051	31.6	1.4	31.3	6.9	97.3	33.6	-1.1	67.5	31.64	1.41
G44	36.2	948.4	0.11	0.0405	0.0003	0.2988	0.0074	0.0537	0.0012	255.7	3.6	265.4	11.1	358.5	27.6	3.7	28.7	255.68	3.59
G71	5.5	102.4	0.75	0.0462	0.0005	0.3451	0.0160	0.0570	0.0024	291.1	6.2	301.1	23.2	492.7	46.5	3.3	40.9	291.09	6.16
G94	15.4	224.9	1.30	0.0513	0.0004	0.3775	0.0112	0.0540	0.0014	322.2	4.9	325.2	15.5	372.7	24.0	0.9	13.6	322.19	4.91
G66	37.4	657.9	0.34	0.0558	0.0004	0.4327	0.0098	0.0557	0.0011	349.9	4.5	365.1	13.0	440.0	28.5	4.2	20.5	349.91	4.52
G86	22.9	322.3	1.18	0.0558	0.0004	0.4297	0.0116	0.0569	0.0014	350.2	5.0	363.0	15.7	487.3	32.8	3.5	28.1	350.22	5.01
G49	12.3	190.4	0.70	0.0573	0.0006	0.4514	0.0180	0.0574	0.0020	359.1	6.7	378.2	22.9	507.3	41.8	5.1	29.2	359.12	6.71
G41	9.2	135.0	0.70	0.0598	0.0006	0.4828	0.0213	0.0572	0.0022	374.3	7.5	400.0	25.6	500.4	44.0	6.4	25.2	374.29	7.54
G108	208.9	3548.1	0.22	0.0601	0.0004	0.4747	0.0078	0.0553	0.0008	375.9	4.4	394.4	10.1	425.2	17.6	4.7	11.6	375.93	4.38
G95	19.6	259.0	1.03	0.0604	0.0005	0.4527	0.0161	0.0559	0.0017	377.8	6.4	379.2	20.7	448.4	29.9	0.4	15.8	377.75	6.44
G8	29.7	451.3	0.52	0.0611	0.0004	0.4699	0.0104	0.0554	0.0011	382.1	5.0	391.1	13.2	427.6	27.5	2.3	10.6	382.13	4.98
G11	3.1	41.0	0.81	0.0645	0.0011	0.4801	0.0380	0.0560	0.0038	402.9	13.0	398.1	47.6	450.4	64.0	-1.2	10.5	402.93	12.96
G43	99.5	1505.1	0.04	0.0715	0.0004	0.5513	0.0098	0.0561	0.0009	444.9	5.3	445.8	12.3	457.5	25.7	0.2	2.8	444.89	5.29
G10	69.0	1029.7	0.06	0.0716	0.0004	0.5504	0.0095	0.0562	0.0009	445.5	5.3	445.3	11.8	460.3	25.2	-0.1	3.2	445.49	5.29
G26	34.4	509.7	0.05	0.0724	0.0005	0.5345	0.0119	0.0548	0.0011	450.8	5.9	434.8	14.7	405.3	26.9	-3.7	-11.2	450.78	5.89
G24	71.8	869.4	0.73	0.0727	0.0005	0.5724	0.0110	0.0581	0.0010	452.2	5.5	459.5	13.3	533.5	27.9	1.6	15.3	452.16	5.53
G42	30.2	326.6	1.11	0.0734	0.0005	0.5730	0.0139	0.0575	0.0012	456.3	6.1	460.0	16.5	510.4	30.9	0.8	10.6	456.31	6.13
G18	55.5	759.8	0.12	0.0747	0.0005	0.7123	0.0156	0.0703	0.0013	464.5	6.1	546.1	16.8	935.7	36.7	15.0	50.4	464.47	6.12
G64	87.4	924.3	1.10	0.0747	0.0005	0.5733	0.0110	0.0564	0.0010	464.5	5.6	460.1	13.8	466.6	27.0	-0.9	0.5	464.47	5.64
G6	163.6	2351.0	0.04	0.0751	0.0004	0.5816	0.0084	0.0559	0.0007	467.0	5.3	465.5	10.5	448.0	23.4	-0.3	-4.3	467.05	5.28
G93	70.3	1007.5	0.02	0.0758	0.0005	0.5741	0.0104	0.0564	0.0009	470.8	5.6	460.7	12.8	466.6	19.3	-2.2	-0.9	470.76	5.63
G15	43.2	591.1	0.15	0.0761	0.0005	0.5963	0.0111	0.0576	0.0009	472.6	5.8	474.9	13.4	514.6	27.2	0.5	8.2	472.62	5.75
G47	84.8	1200.8	0.02	0.0767	0.0005	0.6063	0.0118	0.0572	0.0010	476.3	5.7	481.2	14.0	500.4	27.6	1.0	4.8	476.34	5.75
G22	67.9	832.1	0.45	0.0767	0.0005	0.5870	0.0103	0.0558	0.0009	476.5	5.6	469.0	12.5	442.4	25.1	-1.6	-7.7	476.51	5.63
G19	146.2	2064.2	0.03	0.0767	0.0005	0.5993	0.0090	0.0567	0.0008	476.6	5.4	476.8	11.1	481.4	24.3	0.0	1.0	476.63	5.39
G4	79.8	867.0	0.90	0.0770	0.0005	0.6122	0.0105	0.0573	0.0009	478.1	5.6	484.9	12.4	504.3	26.0	1.4	5.2	478.13	5.63
G103	135.1	1862.2	0.08	0.0772	0.0005	0.6022	0.0093	0.0554	0.0008	479.4	5.4	478.6	11.2	429.6	17.1	-0.2	-11.6	479.39	5.39
G37	56.0	739.9	0.08	0.0801	0.0005	0.6405	0.0141	0.0578	0.0011	496.8	6.3	502.6	15.8	523.7	29.4	1.2	5.1	496.84	6.33
G98	71.9	723.9	0.27	0.0988	0.0007	0.9139	0.0254	0.0660	0.0015	607.2	8.7	659.1	22.5	806.1	32.1	7.9	24.7	607.20	8.68
G104</td																			

Table 2. U-Pb zircon ages of Zanskar River sands

G61	137.5	792.9	1.38	0.1256	0.0008	1.1668	0.0252	0.0675	0.0012	762.5	9.4	785.2	21.0	852.3	34.9	2.9	10.5	762.54	9.39
G73	13.0	88.6	0.76	0.1268	0.0012	1.1313	0.0455	0.0647	0.0020	769.8	13.4	768.4	34.5	763.3	46.9	-0.2	-0.9	769.81	13.39
G17	58.4	458.5	0.25	0.1275	0.0008	1.1759	0.0220	0.0670	0.0010	773.4	9.1	789.4	18.2	836.8	31.6	2.0	7.6	773.36	9.15
G80	44.6	215.7	2.28	0.1276	0.0010	1.2330	0.0380	0.0721	0.0017	773.9	11.4	815.7	28.8	988.8	44.5	5.1	21.7	773.87	11.43
G99	53.1	346.2	0.91	0.1276	0.0008	1.1313	0.0235	0.0649	0.0011	774.1	9.4	768.4	19.3	772.4	25.4	-0.7	-0.2	774.10	9.38
G21	73.2	597.1	0.12	0.1280	0.0009	1.2435	0.0269	0.0702	0.0012	776.7	9.7	820.5	20.6	933.3	34.9	5.3	16.8	776.67	9.71
G101	57.3	388.5	0.68	0.1283	0.0008	1.1498	0.0228	0.0646	0.0010	778.3	9.3	777.2	18.6	760.7	24.5	-0.1	-2.3	778.27	9.26
G46	22.1	148.2	0.72	0.1303	0.0010	1.1724	0.0326	0.0664	0.0014	789.3	11.0	787.8	25.3	817.8	38.4	-0.2	3.5	789.35	10.95
G31	19.4	122.9	0.95	0.1303	0.0010	1.2327	0.0362	0.0669	0.0015	789.6	11.3	815.6	26.1	833.7	39.4	3.2	5.3	789.58	11.29
G100	362.0	2020.1	1.45	0.1318	0.0008	1.2049	0.0187	0.0650	0.0009	798.1	8.8	802.9	16.1	775.0	22.0	0.6	-3.0	798.07	8.77
G81	142.9	999.0	0.53	0.1322	0.0008	1.1793	0.0235	0.0666	0.0012	800.3	9.5	791.0	20.9	826.5	34.1	-1.2	3.2	800.29	9.45
G84	69.4	400.7	1.28	0.1323	0.0009	1.3202	0.0308	0.0722	0.0014	801.0	10.1	854.6	24.0	992.4	38.9	6.3	19.3	800.97	10.13
G88	69.4	520.6	0.28	0.1323	0.0009	1.2500	0.0281	0.0677	0.0013	801.1	9.9	823.4	22.9	858.8	36.5	2.7	6.7	801.14	9.91
G78	197.6	1342.4	0.61	0.1335	0.0008	1.2145	0.0228	0.0672	0.0011	807.7	9.3	807.3	20.1	843.4	33.3	-0.1	4.2	807.69	9.33
G9	81.4	419.4	1.73	0.1336	0.0009	1.2247	0.0264	0.0669	0.0011	808.4	10.0	811.9	20.5	835.3	33.4	0.4	3.2	808.37	10.01
G12	99.4	558.5	1.32	0.1344	0.0008	1.2205	0.0227	0.0665	0.0010	812.7	9.5	810.0	18.4	820.6	31.1	-0.3	1.0	812.69	9.55
G70	63.4	345.8	1.41	0.1349	0.0009	1.2293	0.0269	0.0677	0.0013	816.0	10.0	814.0	22.2	859.1	35.4	-0.2	5.0	815.99	10.00
G75	75.6	513.9	0.53	0.1352	0.0009	1.2440	0.0270	0.0670	0.0012	817.2	10.0	820.7	22.1	838.7	35.1	0.4	2.6	817.24	9.99
G83	112.9	895.9	0.03	0.1353	0.0009	1.2328	0.0255	0.0663	0.0012	817.8	9.8	815.6	21.7	814.9	34.5	-0.3	-0.4	817.80	9.77
G38	182.9	1079.7	1.08	0.1354	0.0008	1.2338	0.0211	0.0670	0.0010	818.5	9.3	816.1	17.9	837.5	30.7	-0.3	2.3	818.48	9.31
G91	102.0	634.8	0.88	0.1354	0.0008	1.2361	0.0215	0.0661	0.0010	818.7	9.3	817.1	17.5	809.2	23.5	-0.2	-1.2	818.65	9.31
G74	146.1	896.5	0.93	0.1357	0.0009	1.2652	0.0250	0.0678	0.0012	820.2	9.6	830.2	20.8	861.8	34.1	1.2	4.8	820.24	9.65
G85	129.4	939.9	0.32	0.1358	0.0009	1.3753	0.0277	0.0742	0.0013	820.9	9.8	878.4	22.4	1046.9	37.4	6.5	21.6	820.93	9.76
G79	57.3	432.0	0.18	0.1358	0.0009	1.2427	0.0278	0.0671	0.0013	821.1	10.1	820.1	22.7	840.9	35.7	-0.1	2.4	821.10	10.10
G77	90.9	587.5	0.71	0.1359	0.0009	1.2497	0.0262	0.0678	0.0012	821.4	9.9	823.3	21.7	861.2	34.9	0.2	4.6	821.44	9.87
G55	48.6	348.9	0.32	0.1364	0.0009	1.2580	0.0298	0.0692	0.0013	824.4	10.6	827.0	23.3	905.3	36.9	0.3	8.9	824.44	10.55
G58	36.7	188.0	1.50	0.1373	0.0011	1.2719	0.0390	0.0647	0.0015	829.3	12.0	833.3	27.6	765.2	39.3	0.5	-8.4	829.32	12.02
G53	92.7	469.4	1.72	0.1374	0.0009	1.2643	0.0264	0.0680	0.0012	830.0	10.0	829.8	21.2	867.0	34.3	0.0	4.3	830.00	9.98
G39	89.5	567.0	0.72	0.1379	0.0009	1.2668	0.0265	0.0672	0.0011	832.7	10.1	830.9	20.7	843.4	33.5	-0.2	1.3	832.72	10.08
G87	114.9	845.9	0.20	0.1380	0.0009	1.2540	0.0260	0.0668	0.0012	833.2	10.0	825.2	22.1	832.8	34.9	-1.0	-0.1	833.23	9.97
G1	125.0	557.3	2.30	0.1380	0.0008	1.2739	0.0215	0.0665	0.0009	835.5	9.5	834.1	17.3	823.4	15.8	0.1	-1.2	833.51	9.52
G33	51.0	291.6	1.13	0.1381	0.0010	1.2804	0.0348	0.0678	0.0014	833.7	11.4	837.0	25.1	862.4	38.0	0.4	3.3	833.68	11.44
G97	168.6	924.1	1.30	0.1392	0.0008	1.2825	0.0212	0.0666	0.0009	840.0	9.3	838.0	17.1	823.7	23.1	-0.2	-2.0	840.02	9.28
G5	124.1	848.9	0.40	0.1393	0.0008	1.2782	0.0204	0.0670	0.0009	840.7	9.4	836.0	16.8	836.2	29.3	-0.6	-0.5	840.70	9.39
G2	101.8	617.0	0.83	0.1395	0.0008	1.2797	0.0209	0.0674	0.0009	841.7	9.5	836.7	17.1	851.1	29.8	-0.6	1.1	841.72	9.50
G29	102.0	536.8	1.46	0.1395	0.0009	1.2813	0.0240	0.0666	0.0010	841.8	9.8	837.4	19.0	825.6	31.5	-0.5	-2.0	841.83	9.84
G107	144.5	862.9	0.89	0.1402	0.0009	1.2844	0.0227	0.0663	0.0010	845.5	9.6	838.8	17.9	817.1	23.7	-0.8	-3.5	845.51	9.61
G90	96.7	389.1	2.77	0.1404	0.0010	1.3912	0.0343	0.0708	0.0013	847.0	11.1	885.2	23.4	952.8	23.0	4.3	11.1	847.04	11.08
G23	272.6	1726.8	0.66	0.1406	0.0008	1.3202	0.0202	0.0671	0.0009	847.9	9.3	854.6	16.6	841.2	29.2	0.8	-0.8	847.88	9.27
G28	78.3	417.5	1.35	0.1406	0.0009	1.2804	0.0240	0.0662	0.0010	848.1	9.9	837.0	19.0	811.1	31.3	-1.3	-4.6	848.05	9.95
G3	69.1	439.2	0.59	0.1411	0.0009	1.3162	0.0234	0.0665	0.0010	851.0	9.8	852.8	18.0	820.6	30.3	0.2	-3.7	851.05	9.83
G65	74.4	504.9	0.39	0.1412	0.0009	1.2898	0.0275	0.0676	0.0012	851.6	10.3	841.2	22.0	856.3	34.7	-1.2	0.6	851.56	10.28
G34	117.5	786.3	0.42	0.1416	0.0009	1.3332	0.0242	0.0702	0.0011	853.7	9.8	860.3	19.1	933.9	32.5	0.8	8.6	853.70	9.83
G59	107.2	676.6	0.64	0.1419	0.0009	1.2964	0.0262	0.0678	0.0012	855.2	10.2	844.1	21.1	861.5	33.9	-1.3	0.7	855.23	10.16
G68	95.7	559.1	0.97	0.1419	0.0009	1.2958	0.0266	0.0675	0.0012	855.6	10.2	843.9	21.5	852.3	34.2	-1.4	-0.4	855.62	10.16
G76	126.7	785.7	0.68	0.1425	0.0009	1.3105	0.0260	0.0674	0.0012	858.6	10.0	850.4	21.3	850.5	34.0	-1.0	-1.0	858.56	10.04
G63	47.0	312.1	0.43	0.1427	0.0010	1.3258	0.0325	0.0682	0.0013	859.6	11.1	857.1	24.2	875.2	37.1	-0.3	1.8	859.63	11.06
G82	168.2	1064.0	0.58	0.1435	0.0009	1.2912	0.0262	0.0665	0.0012	864.1	10.1	841.8	22.0	822.5	34.4	-2.6	-5.1	864.14	10.15
G106	174.0	1083.3	0.66	0.1437	0.0009	1.4232	0.0260	0.0710	0.0011	865.3	9.9	898.7	19.0	957.7	25.8	3.7	9.7	865.27	9.92
G51	131.1	830.9	0.72	0.1443	0.0009	1.5603	0.0284	0.0790	0.0012	868.9	9.9	954.6	20.9	1172.6	35.9	9.0	25.9	868.93	9.91
G20	44.5	271.7	0.62	0.1469	0.0010	1.4010	0.0298	0.0711	0.0012	883.5	10.8	889.3	21.4	960.9	34.6	0.7	8.1	883.45	10.79
G16	156.7	1069.5	0.19	0.1498	0.0009	1.4218	0.0223	0.0697	0.0009	899.6	10.0	898.1	17.5	918.9	30.2	-0.2	2.1	899.56	9.98
G69	182.0	1007.4	0.84	0.1515	0.0009	1.4682	0.0280	0.0709	0.0012	909.4	10.5	917.4	21.5	954.0	34.6	0.9	4.7	953.95	34.62
G50	93.6	589.9	0.38	0.1526	0.0010	1.4605	0.0277	0.0709	0.0011	915.3	10.6	914.2	21.0	955.7	33.9	-0.1	4.2	955.69	33.93
G62	39.6	206.1	0.87	0.1632	0.0012	1.6358	0.0480	0.0721	0.0016	974.6	13.6	984.1	28.9	989.3	41.6	1.0	1.5	989.33	41.55

Table 2. U-Pb zircon ages of Zanskar River sands

G13	75.9	239.2	0.61	0.2804	0.0019	3.8314	0.0903	0.0977	0.0015	1593.1	18.8	1599.4	26.9	1579.7	38.6	0.4	-0.8	1579.72	38.64
G45	200.4	664.6	0.25	0.2947	0.0018	4.1238	0.0735	0.1008	0.0015	1665.1	17.7	1659.0	25.6	1638.5	37.6	-0.4	-1.6	1638.52	37.59
G32	159.7	367.5	1.56	0.3076	0.0020	4.5068	0.0986	0.1047	0.0016	1728.7	19.5	1732.2	26.9	1708.2	38.7	0.2	-1.2	1708.17	38.67
G96	196.5	479.4	1.49	0.2979	0.0019	4.5776	0.0969	0.1092	0.0015	1680.7	18.8	1745.2	25.7	1786.4	31.2	3.7	5.9	1786.44	31.16
G36	311.2	560.9	0.66	0.4683	0.0028	10.4185	0.1813	0.1635	0.0022	2475.9	24.6	2472.7	27.0	2491.9	38.7	-0.1	0.6	2491.87	38.67
G89	417.3	808.6	0.94	0.4205	0.0026	9.7157	0.1946	0.1678	0.0029	2262.7	23.8	2408.2	34.1	2536.0	46.6	6.0	10.8	2536.02	46.57

Sample 12072504 Lower Stod

Grain No.	Pb (ppm)	U (ppm)	Atomic Th/U	Ratios				Ages (Ma)					% concord. (206/238)	% concord. (206/238)	Best Age (Ma)	± 2σ			
				$^{206}\text{Pb}/^{238}\text{U}$	± 1 σ	$^{207}\text{Pb}/^{235}\text{U}$	± s.e.	$^{207}\text{Pb}/^{206}\text{Pb}$	± s.e.	$^{206}\text{Pb}/^{238}\text{U}$	± 2σ	$^{207}\text{Pb}/^{235}\text{U}$	± 2σ	$^{207}\text{Pb}/^{206}\text{Pb}$	± 2σ				
G71	22.4	8459.9	0.01	0.0029	0.0000	0.0198	0.0004	0.0482	0.0010	18.7	0.3	19.9	0.8	108.6	11.8	6.0	82.8	18.67	0.26
G67	1.0	263.6	0.01	0.0041	0.0001	0.0274	0.0020	0.0469	0.0035	26.5	0.8	27.4	4.0	45.2	14.2	3.3	41.3	26.50	0.77
G68	31.0	552.6	0.70	0.0482	0.0003	0.3513	0.0077	0.0536	0.0011	303.5	4.1	305.7	11.1	352.2	19.3	0.7	13.8	303.52	4.06
G2	60.4	884.0	1.39	0.0509	0.0003	0.3809	0.0072	0.0532	0.0009	319.9	4.0	327.7	9.9	339.0	17.3	2.4	5.6	319.92	4.05
G49	136.0	1764.8	1.87	0.0515	0.0003	0.3898	0.0061	0.0537	0.0007	323.4	3.8	334.2	8.4	358.1	15.9	3.2	9.7	323.42	3.80
G8	105.4	1410.5	1.73	0.0524	0.0003	0.3856	0.0057	0.0522	0.0007	329.5	3.9	331.1	8.0	295.5	14.3	0.5	-11.5	329.48	3.92
G80	62.6	743.5	1.98	0.0559	0.0004	0.4636	0.0085	0.0595	0.0010	350.3	4.4	386.8	11.1	585.8	22.0	9.4	40.2	350.34	4.40
G28	244.7	3010.6	1.73	0.0562	0.0003	0.4300	0.0060	0.0542	0.0007	352.2	4.0	363.1	8.1	381.0	15.3	3.0	7.6	352.17	4.03
G99	60.9	821.2	1.22	0.0575	0.0004	0.4313	0.0077	0.0540	0.0009	360.2	4.5	364.1	10.3	371.0	17.4	1.1	2.9	360.16	4.51
G98	37.9	518.4	1.15	0.0575	0.0004	0.4287	0.0092	0.0534	0.0010	360.4	4.8	362.2	12.0	344.6	18.6	0.5	-4.6	360.40	4.75
G108	3.1	42.3	1.09	0.0588	0.0007	0.4413	0.0220	0.0541	0.0024	368.0	8.2	371.2	28.0	376.9	35.2	0.9	2.4	368.02	8.16
G19	126.9	864.7	5.00	0.0589	0.0004	0.4349	0.0070	0.0528	0.0007	369.1	4.4	366.6	9.3	319.4	15.3	-0.7	-15.6	369.11	4.38
G111	18.2	264.8	0.82	0.0590	0.0004	0.4671	0.0120	0.0573	0.0013	369.7	5.4	389.2	15.3	501.9	25.5	5.0	26.4	369.66	5.36
G60	5.6	82.1	0.77	0.0598	0.0005	0.4968	0.0163	0.0585	0.0017	374.3	6.2	409.5	19.6	548.2	31.7	8.6	31.7	374.29	6.20
G51	72.1	976.6	1.02	0.0599	0.0004	0.4436	0.0071	0.0536	0.0008	375.0	4.5	372.8	9.6	354.7	16.1	-0.6	-5.7	374.96	4.50
G58	13.3	184.0	0.94	0.0600	0.0004	0.4292	0.0109	0.0525	0.0012	375.4	5.4	362.6	14.4	309.0	19.5	-3.5	-21.5	375.44	5.35
G104	11.8	143.6	1.48	0.0602	0.0005	0.4328	0.0131	0.0534	0.0014	376.5	5.8	365.2	17.2	344.6	23.1	-3.1	-9.3	376.54	5.84
G15	57.4	839.8	0.69	0.0605	0.0004	0.4520	0.0071	0.0533	0.0007	378.8	4.5	378.7	9.5	341.2	15.7	0.0	-11.0	378.79	4.50
G91	35.9	471.2	1.06	0.0613	0.0004	0.4573	0.0087	0.0542	0.0009	383.5	4.9	382.4	11.4	377.7	18.1	-0.3	-1.5	383.47	4.86
G30	40.1	591.8	0.53	0.0620	0.0004	0.4681	0.0086	0.0544	0.0009	387.6	4.9	389.9	11.2	386.4	18.0	0.6	-0.3	387.59	4.86
G81	5.8	76.5	0.97	0.0622	0.0006	0.4952	0.0205	0.0572	0.0020	388.9	7.5	408.5	24.6	498.9	35.6	4.8	22.0	388.93	7.53
G64	87.4	1184.8	0.83	0.0623	0.0004	0.4958	0.0082	0.0575	0.0008	389.5	4.7	408.9	10.6	508.8	19.2	4.7	23.5	389.48	4.73
G79	46.6	611.7	0.99	0.0626	0.0004	0.4721	0.0088	0.0537	0.0009	391.2	4.9	392.7	11.2	358.1	17.4	0.4	-9.2	391.18	4.85
G92	11.6	166.0	0.66	0.0626	0.0006	0.4543	0.0158	0.0522	0.0016	391.2	6.7	380.3	19.9	295.9	23.1	-2.9	-32.2	391.24	6.67
G96	2.8	38.5	0.75	0.0635	0.0008	0.5083	0.0297	0.0583	0.0029	396.8	10.2	417.3	35.7	540.3	49.7	4.9	26.6	396.82	10.18
G93	121.4	1768.0	0.21	0.0702	0.0004	0.5655	0.0095	0.0563	0.0008	437.1	5.3	455.1	11.5	465.8	18.6	4.0	6.2	437.12	5.30
G5	139.9	2057.0	0.08	0.0723	0.0004	0.5615	0.0077	0.0546	0.0007	449.9	5.2	452.5	9.6	395.5	15.5	0.6	-13.8	449.94	5.17
G63	48.3	511.0	1.27	0.0724	0.0005	0.5620	0.0106	0.0571	0.0009	450.5	5.7	452.8	12.9	496.6	20.4	0.5	9.3	450.54	5.65
G100	99.5	1232.1	0.56	0.0730	0.0005	0.5760	0.0104	0.0553	0.0009	454.3	5.5	461.9	12.3	423.6	18.5	1.6	-7.3	454.32	5.53
G46	137.4	2029.0	0.03	0.0732	0.0004	0.5683	0.0080	0.0558	0.0007	455.3	5.2	456.9	10.0	442.4	16.5	0.4	-2.9	455.29	5.17
G24	30.0	387.3	0.42	0.0737	0.0005	0.5773	0.0117	0.0568	0.0010	458.6	5.9	462.7	13.9	481.8	21.0	0.9	4.8	458.59	5.88
G88	270.5	2549.4	1.67	0.0743	0.0005	0.5966	0.0093	0.0565	0.0008	462.1	5.4	475.1	11.1	471.7	17.9	2.7	2.0	462.13	5.40
G75	33.5	393.5	0.65	0.0758	0.0005	0.6185	0.0138	0.0578	0.0011	470.9	6.2	488.9	15.5	523.3	23.2	3.7	10.0	470.94	6.23
G18	42.5	514.7	0.37	0.0803	0.0005	0.6339	0.0109	0.0566	0.0008	497.6	6.0	498.5	12.5	474.0	18.7	0.2	-5.0	497.61	5.97
G70	43.0	419.0	0.80	0.0878	0.0006	0.7062	0.0143	0.0581	0.0010	542.7	6.9	542.5	15.3	534.7	21.8	-0.1	-1.5	542.75	6.87
G31	53.2	514.7	0.21	0.1046	0.0007	0.9275	0.0151	0.0641	0.0009	641.0	7.6	666.3	14.7	743.6	22.1	3.8	13.8	641.02	7.59
G11	130.0	1879.2	1.68	0.1064	0.0007	1.0341	0.0159	0.0687	0.0009	651.7	7.6	721.0	14.5	888.8	22.8	9.6	26.7	651.69	7.57
G82	110.0	783.9	1.22	0.1112	0.0007	1.0340	0.0181	0.0659	0.0010	679.6	8.1	720.9	16.3	803.8	24.0	5.7	15.5	679.60	8.12
G12	90.1	558.9	1.61	0.1135	0.0007	1.0324	0.0165	0.0660	0.0009	693.0	8.1	720.1	15.2	804.8	22.4	3.8	13.9	693.04	8.11
G29	561.2	5039.7	0.21	0.1144	0.0007	1.0622	0.0140	0.0656	0.0008	698.0	7.8	734.9	13.4	794.0	20.4	5.0	12.1	698.02	7.75
G65	72.2	530.3	0.80	0.1153	0.0007	1.1137	0.0188	0.0698	0.0010	703.6	8.3	759.9	16.4	921.3	24.6	7.4	23.6	703.57	8.32
G101	109.7	830.5	0.71	0.1159	0.0007	1.0920	0.0199	0.0663	0.0010	706.9	8.5	749.5	17.3	817.1	24.7	5.7	13.5	706.92	8.55
G62	73.9	484.3	1.10	0.1193	0.0008	1.1210	0.0199	0.0678	0.0010	726.5	8.8	763.4	17.1	862.8	24.6	4.8	15.8	726.53	8.75
G59	79.3	499.8	1.24																

Table 2. U-Pb zircon ages of Zanskar River sands

Sample 13071703 Upper Sto

Campbell 1991 - 1993 Upper Oct.										
Grain	Dh	II	Atomic		Ratios		Ages (Ma)	% concord.	% concord.	Rest Age

Table 2. U-Pb zircon ages of Zanskar River sands

Gdz No.	Γ_U (ppm)	Σ (ppm)	$\Delta_{Th/U}$	$^{206}\text{Pb}/^{238}\text{U}$	$^{207}\text{Pb}/^{235}\text{U}$			$^{207}\text{Pb}/^{206}\text{Pb}$			$^{206}\text{Pb}/^{238}\text{U}$	$^{207}\text{Pb}/^{235}\text{U}$			$^{207}\text{Pb}/^{206}\text{Pb}$			$(206/238)$ $(207/235)$	$(206/238)$ $(207/206)$	Dose Rate (Ma)	$\pm 2\sigma$
					$\pm 1\sigma$	$\pm \text{s.e.}$	$\pm 2\sigma$	$\pm \text{s.e.}$	$\pm 2\sigma$	$\pm 2\sigma$		$\pm 1\sigma$	$\pm \text{s.e.}$	$\pm 2\sigma$	$\pm \text{s.e.}$	$\pm 2\sigma$	$\pm 2\sigma$				
G9	3.5	102.8	0.42	0.0316	0.0004	0.2452	0.0090	0.0546	0.0019	200.4	4.9	222.6	14.1	395.9	26.0	10.0	49.4	200.37	4.87		
G54	19.6	483.0	0.23	0.0409	0.0003	0.3391	0.0066	0.0604	0.0010	258.5	3.7	296.5	9.3	619.0	18.8	12.8	58.2	258.53	3.72		
G31	18.9	226.8	2.96	0.0444	0.0004	0.3407	0.0080	0.0560	0.0011	280.2	4.6	297.7	11.2	451.6	18.2	5.9	38.0	280.17	4.57		
G38	9.7	196.6	0.30	0.0488	0.0004	0.3781	0.0080	0.0545	0.0010	307.0	4.5	325.7	10.4	390.1	15.1	5.7	21.3	307.03	4.55		
G27	25.0	465.9	0.56	0.0491	0.0003	0.3621	0.0070	0.0532	0.0009	309.2	4.2	313.8	9.4	338.6	12.8	1.4	8.7	309.24	4.18		
G91	3.3	62.0	0.37	0.0510	0.0007	0.3575	0.0140	0.0520	0.0018	320.5	8.0	310.3	20.1	285.8	21.0	-3.3	-12.1	320.54	7.97		
G102	8.7	176.2	0.15	0.0511	0.0004	0.4011	0.0082	0.0575	0.0010	321.4	4.8	342.4	10.8	510.8	17.0	6.1	37.1	321.39	4.78		
G89	17.4	312.5	0.44	0.0525	0.0004	0.3934	0.0068	0.0544	0.0007	329.7	4.3	336.8	8.7	387.2	12.4	2.1	14.9	329.67	4.29		
G62	3.3	61.2	0.37	0.0526	0.0005	0.3855	0.0118	0.0540	0.0014	330.2	6.6	331.1	16.1	371.5	20.0	0.3	11.1	330.16	6.61		
G1	18.9	326.4	0.60	0.0526	0.0003	0.4590	0.0072	0.0624	0.0008	330.5	3.9	383.5	8.5	687.8	12.0	13.8	51.9	330.53	3.92		
G43	162.3	2277.2	1.36	0.0530	0.0003	0.3944	0.0042	0.0533	0.0003	332.7	3.1	337.6	4.5	341.2	7.3	1.5	2.5	332.67	3.06		
G18	24.6	399.0	0.77	0.0532	0.0003	0.3873	0.0054	0.0540	0.0006	333.8	3.6	332.4	6.7	372.3	10.1	-0.4	10.3	333.83	3.55		
G76	6.5	110.1	0.52	0.0544	0.0004	0.4269	0.0095	0.0562	0.0010	341.4	5.3	361.0	12.0	461.1	17.2	5.4	26.0	341.42	5.26		
G58	60.4	940.7	0.74	0.0560	0.0003	0.4200	0.0050	0.0537	0.0004	351.1	3.5	356.1	5.7	356.4	8.5	1.4	1.5	351.07	3.54		
G81	21.2	368.8	0.32	0.0561	0.0004	0.4100	0.0085	0.0536	0.0009	352.1	5.1	348.9	10.9	356.0	13.7	-0.9	1.1	352.11	5.13		
G3	5.8	97.1	0.46	0.0569	0.0005	0.4219	0.0109	0.0525	0.0011	356.9	6.0	357.4	13.7	308.1	15.1	0.1	-15.8	356.93	5.98		
G2	2.3	35.9	0.64	0.0570	0.0007	0.4265	0.0160	0.0541	0.0018	357.4	8.3	360.7	21.0	373.5	24.0	0.9	4.3	357.36	8.29		
G72	31.3	540.1	0.31	0.0571	0.0003	0.4550	0.0061	0.0576	0.0005	358.0	3.9	380.7	6.9	515.0	11.2	6.0	30.5	357.96	3.90		
G48	6.2	108.5	0.23	0.0576	0.0004	0.4361	0.0093	0.0549	0.0010	360.7	5.2	367.5	11.7	406.5	15.4	1.8	11.3	360.71	5.24		
G25	46.0	694.3	0.77	0.0576	0.0003	0.4265	0.0054	0.0542	0.0005	361.1	3.7	360.7	6.2	377.3	9.1	-0.1	4.3	361.07	3.66		
G109	32.0	480.6	0.72	0.0577	0.0003	0.4271	0.0061	0.0554	0.0006	361.4	4.1	361.1	7.4	427.2	10.8	-0.1	15.4	361.38	4.14		
G8	20.9	288.0	1.06	0.0582	0.0003	0.4264	0.0066	0.0522	0.0006	364.5	4.1	360.6	7.8	293.3	9.6	-1.1	-24.3	364.49	4.14		
G90	7.6	98.7	1.23	0.0583	0.0006	0.5001	0.0131	0.0637	0.0014	365.3	6.7	411.8	16.2	732.7	26.3	11.3	50.1	365.34	6.70		
G19	58.6	809.4	1.05	0.0583	0.0003	0.4375	0.0055	0.0548	0.0005	365.5	3.7	368.5	6.2	402.8	9.4	0.8	9.3	365.46	3.65		
G84	22.8	360.6	0.53	0.0585	0.0004	0.4259	0.0065	0.0548	0.0006	366.5	4.3	360.2	8.0	402.0	11.2	-1.7	8.8	366.50	4.26		
G75	3.9	62.0	0.37	0.0604	0.0007	0.4903	0.0160	0.0590	0.0016	378.1	8.1	405.1	19.9	567.1	27.7	6.7	33.3	378.06	8.15		
G80	6.8	92.2	0.96	0.0604	0.0005	0.4196	0.0111	0.0526	0.0012	378.3	6.6	355.8	14.9	312.4	15.7	-6.3	-21.1	378.30	6.57		
G65	150.7	2047.1	1.13	0.0607	0.0003	0.5119	0.0057	0.0606	0.0004	379.8	3.6	419.7	5.7	623.3	10.0	9.5	39.1	379.82	3.65		
G96	47.8	691.9	0.67	0.0611	0.0003	0.4603	0.0063	0.0545	0.0005	382.1	4.1	384.5	7.1	392.6	9.9	0.6	2.7	382.07	4.13		
G66	9.5	133.0	0.75	0.0618	0.0005	0.4739	0.0101	0.0563	0.0010	386.6	5.7	393.9	12.3	463.0	16.3	1.8	16.5	386.62	5.71		
G50	3.3	53.0	0.29	0.0619	0.0007	0.4767	0.0158	0.0538	0.0015	387.0	8.0	395.8	19.2	361.8	20.7	2.2	-7.0	387.05	8.01		
G88	2.3	28.6	0.91	0.0666	0.0009	0.4548	0.0205	0.0502	0.0020	415.8	11.1	380.7	26.5	203.8	18.1	-9.2	-104.0	415.76	11.12		
G104	150.1	2003.9	0.59	0.0682	0.0004	0.5317	0.0066	0.0565	0.0005	425.3	4.5	433.0	6.9	472.5	9.8	1.8	10.0	425.30	4.47		
G22	86.3	1121.1	0.62	0.0682	0.0003	0.5323	0.0059	0.0565	0.0004	425.4	4.0	433.3	5.9	472.5	8.9	1.8	10.0	425.42	3.98		
G42	22.3	285.6	0.44	0.0738	0.0004	0.5805	0.0082	0.0574	0.0006	458.8	4.9	464.8	8.6	505.8	11.7	1.3	9.3	458.77	4.92		
G52	58.0	786.5	0.19	0.0744	0.0004	0.6813	0.0095	0.0647	0.0006	462.7	5.0	527.6	9.0	765.2	13.9	12.3	39.5	462.67	5.04		
G57	102.2	1221.4	0.42	0.0770	0.0004	0.7134	0.0086	0.0665	0.0005	478.1	4.8	546.7	7.8	823.1	12.3	12.5	41.9	478.13	4.79		
G59	12.8	123.2	1.29	0.0785	0.0005	0.6139	0.0115	0.0571	0.0008	486.9	6.3	486.0	12.2	493.5	14.7	-0.2	1.3	486.86	6.34		
G101	7.0	61.2	1.59	0.0808	0.0008	0.7146	0.0208	0.0629	0.0014	501.1	9.5	547.5	20.8	703.5	26.7	8.5	28.8	501.08	9.54		
G17	31.2	380.2	0.31	0.0813	0.0004	0.6855	0.0089	0.0595	0.0005	503.6	5.1	530.1	8.3	586.9	11.4	5.0	14.2	503.58	5.13		
G24	92.4	1130.8	0.28	0.0814	0.0004	0.6714	0.0074	0.0586	0.0004	504.4	4.6	521.6	6.6	551.9	9.3	3.3	8.6	504.41	4.65		
G111	24.1	250.5	0.82	0.0828	0.0005	0.6551	0.0103	0.0582	0.0007	512.6	6.1	511.6	10.3	535.6	13.0	-0.2	4.5	512.58	6.07		
G105	72.9	826.5	0.44	0.0839	0.0005	0.6689	0.0091	0.0588	0.0005	519.1	5.6	520.0	8.8	558.6	11.5	0.2	7.1	519.06	5.59		
G10	16.9	142.0	1.51	0.0856	0.0006	0.6950	0.0132	0.0579	0.0008	529.6	6.9	535.8	12.9	527.1	15.3	1.2	-0.5	529.64	6.89		
G11	22.5	248.9	0.42	0.0864	0.0005	0.7036	0.0102	0.0582	0.0006	534.4	5.7	540.9	9.5	538.1	12.0	1.2	0.7	534.45	5.70		
G39	59.1	708.2	0.14	0.0869	0.0005	0.7161	0.0089	0.0587	0.0005	537.1	5.3	548.4	8.0	556.0	10.5	2.1	3.4	537.06	5.34		
G49	15.2	142.0	0.96	0.0880	0.0006	0.6866	0.0126	0.0578	0.0008	543.6	6.9	530.7	12.7	520.7	14.8	-2.4	-4.4	543.64	6.87		
G82	45.3	496.1	0.39	0.0882	0.0005	0.7170	0.0098	0.0584	0.0005	544.8	5.8	548.9	9.0	545.9	11.3	0.7	0.2	544.82	5.81		
G107	40.1	453.6																			

Table 2. U-Pb zircon ages of Zanskar River sands

Sample 12072507 Lower Tsarap

Grain No.	Pb (ppm)	U (ppm)	Atomic Th/U	Ratios						Ages (Ma)						% concord. (206/238 207/235)	% concord. (206/238 207/206)	Best Age (Ma)	$\pm 2\sigma$
				$^{206}\text{Pb}/^{238}\text{U}$	$\pm 1\sigma$	$^{207}\text{Pb}/^{235}\text{U}$	$\pm \text{s.e.}$	$^{207}\text{Pb}/^{206}\text{Pb}$	$\pm \text{s.e.}$	$^{206}\text{Pb}/^{238}\text{U}$	$\pm 2\sigma$	$^{207}\text{Pb}/^{235}\text{U}$	$\pm 2\sigma$	$^{207}\text{Pb}/^{206}\text{Pb}$	$\pm 2\sigma$				
G18	7.7	237.0	0.60	0.0273	0.0002	0.007	0.0053	0.0544	0.0014	173.8	2.5	185.7	9.0	385.6	18.0	6.4	54.9	173.82	2.51
G45	77.4	1140.5	1.38	0.0551	0.0003	0.4395	0.0076	0.0586	0.0009	345.5	4.0	369.9	10.4	551.5	15.1	6.6	37.4	345.51	4.03

Table 2. U-Pb zircon ages of Zanskar River sands

G54	119.8	1768.4	1.10	0.0558	0.0003	0.4630	0.0067	0.0599	0.0008	350.2	3.9	386.4	9.2	601.4	13.9	9.4	41.8	350.22	3.91
G118	124.4	1890.6	0.77	0.0562	0.0003	0.4505	0.0072	0.0579	0.0009	352.7	4.0	377.6	9.9	526.7	14.0	6.6	33.0	352.72	4.03
G111	161.5	2561.8	0.81	0.0565	0.0003	0.4475	0.0066	0.0571	0.0008	354.1	3.9	375.5	9.1	495.8	12.5	5.7	28.6	354.06	3.91
G64	56.4	863.6	0.48	0.0601	0.0004	0.4896	0.0083	0.0588	0.0009	376.3	4.4	404.6	10.8	560.8	14.9	7.0	32.9	376.29	4.38
G9	95.3	1357.9	0.89	0.0625	0.0004	0.5175	0.0071	0.0603	0.0008	391.1	4.2	423.5	9.5	614.7	13.4	7.7	36.4	391.05	4.25
G90	66.8	977.1	0.29	0.0678	0.0004	0.5349	0.0089	0.0577	0.0009	422.9	4.8	435.0	11.4	518.8	14.0	2.8	18.5	422.89	4.83
G21	47.9	609.7	0.82	0.0681	0.0004	0.5613	0.0085	0.0602	0.0008	424.9	4.7	452.3	10.8	611.8	14.4	6.1	30.6	424.88	4.71
G24	77.3	903.5	1.50	0.0690	0.0004	0.5854	0.0091	0.0612	0.0009	430.2	4.8	467.9	11.2	646.6	15.2	8.1	33.5	430.19	4.82
G136	43.6	657.0	0.13	0.0695	0.0004	0.5531	0.0102	0.0573	0.0009	433.2	5.1	447.0	12.6	503.5	14.9	3.1	14.0	433.20	5.06
G1	114.5	1457.8	0.72	0.0696	0.0004	0.5340	0.0072	0.0559	0.0007	433.8	4.7	434.5	9.6	448.8	9.0	0.2	3.3	433.81	4.70
G122	125.5	1947.4	0.03	0.0696	0.0004	0.5743	0.0090	0.0603	0.0009	433.9	4.8	460.8	11.4	612.6	15.0	5.8	29.2	433.87	4.82
G126	42.2	564.5	0.47	0.0701	0.0004	0.5748	0.0117	0.0605	0.0011	436.8	5.3	461.1	14.2	622.9	18.5	5.3	29.9	436.82	5.30
G57	88.6	1353.8	0.06	0.0702	0.0004	0.5619	0.0086	0.0581	0.0008	437.6	4.8	452.8	10.9	532.4	13.3	3.3	17.8	437.60	4.82
G55	85.8	1275.5	0.12	0.0705	0.0004	0.5633	0.0083	0.0581	0.0008	439.3	4.8	453.7	10.6	532.8	12.9	3.2	17.5	439.35	4.82
G40	65.9	953.4	0.16	0.0716	0.0004	0.5592	0.0086	0.0565	0.0008	445.5	4.9	451.0	10.9	473.2	12.3	1.2	5.9	445.55	4.93
G19	90.9	1245.8	0.34	0.0716	0.0004	0.5567	0.0077	0.0568	0.0007	445.8	4.8	449.4	10.0	483.0	11.5	0.8	7.7	445.79	4.81
G105	71.4	1023.0	0.18	0.0718	0.0004	0.5501	0.0085	0.0561	0.0008	446.7	4.9	445.1	10.9	457.1	12.1	-0.4	2.3	446.69	4.93
G47	73.7	979.1	0.39	0.0724	0.0004	0.5631	0.0083	0.0568	0.0008	450.4	4.9	453.5	10.7	484.6	12.2	0.7	7.0	450.42	4.93
G58	147.1	2133.1	0.12	0.0731	0.0004	0.5786	0.0082	0.0571	0.0007	454.9	4.9	463.6	10.5	494.6	12.1	1.9	8.0	454.87	4.93
G102	89.8	982.5	1.13	0.0732	0.0004	0.5839	0.0092	0.0573	0.0008	455.1	5.0	467.0	11.3	503.9	13.1	2.5	9.7	455.11	5.05
G61	104.3	1000.7	1.63	0.0734	0.0004	0.5752	0.0086	0.0567	0.0008	456.7	5.0	461.4	10.9	480.3	12.3	1.0	4.9	456.73	5.04
G82	113.2	1529.4	0.28	0.0735	0.0004	0.6101	0.0093	0.0597	0.0008	457.4	5.0	483.6	11.4	591.3	14.2	5.4	22.6	457.45	5.04
G121	112.4	1415.3	0.58	0.0737	0.0004	0.6256	0.0091	0.0617	0.0008	458.4	4.9	493.4	11.3	663.4	14.9	7.1	30.9	458.41	4.92
G123	128.2	1808.3	0.14	0.0738	0.0004	0.5792	0.0085	0.0569	0.0008	458.8	4.9	464.0	10.9	486.5	12.4	1.1	5.7	458.77	4.92
G38	112.2	1634.7	0.05	0.0738	0.0004	0.5723	0.0077	0.0562	0.0007	459.1	4.9	459.5	10.0	461.1	11.0	0.1	0.4	459.07	4.92
G130	83.4	1054.0	0.49	0.0738	0.0004	0.5736	0.0088	0.0568	0.0008	459.1	5.0	460.3	11.3	483.4	12.7	0.3	5.0	459.13	5.04
G144	64.4	605.0	1.68	0.0741	0.0004	0.5761	0.0102	0.0578	0.0009	460.6	5.3	462.0	12.8	521.0	14.9	0.3	11.6	460.57	5.28
G44	558.2	8220.9	0.00	0.0742	0.0004	0.5742	0.0071	0.0564	0.0007	461.4	4.8	460.7	9.5	469.7	10.6	-0.1	1.8	461.41	4.80
G32	77.3	1017.6	0.36	0.0742	0.0004	0.5775	0.0082	0.0568	0.0007	461.6	5.0	462.9	10.5	481.8	11.8	0.3	4.2	461.65	5.04
G31	120.5	1733.3	0.05	0.0744	0.0004	0.5950	0.0084	0.0575	0.0007	462.6	5.0	474.0	10.5	510.4	12.1	2.4	9.4	462.61	5.04
G112	93.9	1147.2	0.55	0.0748	0.0004	0.5776	0.0086	0.0562	0.0008	464.7	5.0	462.9	10.9	460.7	11.9	-0.4	-0.9	464.71	5.04
G56	73.6	899.4	0.59	0.0748	0.0004	0.5925	0.0088	0.0587	0.0008	465.0	5.2	472.5	11.2	556.4	13.4	1.6	16.4	465.01	5.16
G117	73.8	1062.1	0.04	0.0750	0.0004	0.5866	0.0090	0.0574	0.0008	466.1	5.2	468.7	11.4	505.4	13.0	0.6	7.8	466.09	5.16
G51	75.9	1066.2	0.11	0.0750	0.0004	0.5910	0.0086	0.0577	0.0008	466.2	5.0	471.5	10.9	517.6	12.6	1.1	9.9	466.21	5.04
G39	51.4	715.1	0.12	0.0754	0.0005	0.6025	0.0101	0.0583	0.0009	468.8	5.4	478.8	12.2	540.7	14.3	2.1	13.3	468.85	5.39
G88	49.1	568.5	0.73	0.0757	0.0005	0.6050	0.0104	0.0581	0.0009	470.4	5.4	480.4	12.5	533.9	14.5	2.1	11.9	470.41	5.39
G8	82.1	973.0	0.63	0.0758	0.0004	0.5876	0.0083	0.0560	0.0007	470.9	5.2	469.3	10.4	453.2	11.2	-0.3	-3.9	470.88	5.15
G79	95.3	1191.1	0.45	0.0758	0.0004	0.5960	0.0089	0.0572	0.0008	471.0	5.2	474.7	11.1	497.3	12.5	0.8	5.3	471.00	5.15
G97	54.5	717.1	0.25	0.0762	0.0005	0.6110	0.0103	0.0580	0.0009	473.1	5.4	484.2	12.4	529.4	14.3	2.3	10.6	473.10	5.39
G86	33.3	429.4	0.29	0.0763	0.0005	0.6528	0.0123	0.0620	0.0010	474.1	5.6	510.2	14.1	674.8	18.1	7.1	29.7	474.12	5.63
G106	189.6	2174.9	0.72	0.0765	0.0004	0.6027	0.0084	0.0568	0.0007	475.3	5.0	478.9	10.6	484.9	11.8	0.8	2.0	475.26	5.03
G92	75.3	960.9	0.29	0.0771	0.0005	0.6523	0.0104	0.0610	0.0009	479.0	5.4	509.9	12.3	639.9	15.4	6.1	25.2	478.97	5.39
G36	81.9	1043.2	0.32	0.0774	0.0005	0.6409	0.0099	0.0601	0.0008	480.5	5.4	502.9	11.8	606.5	14.4	4.5	20.8	480.47	5.39
G52	116.8	1571.3	0.06	0.0793	0.0004	0.6188	0.0084	0.0566	0.0007	491.6	5.3	489.1	10.5	474.4	11.3	-0.5	-3.6	491.64	5.26
G137	45.4	532.8	0.53	0.0797	0.0005	0.6127	0.0105	0.0568	0.0009	494.5	5.6	485.3	12.8	485.3	13.7	-1.9	-1.9	494.51	5.61
G69	56.5	746.1	0.10	0.0799	0.0005	0.6379	0.0107	0.0572	0.0009	495.3	5.6	501.0	12.5	498.1	13.6	1.1	0.6	495.35	5.61
G109	45.0	528.0	0.31	0.0842	0.0005	0.6959	0.0128	0.0596	0.0010	521.3	6.1	536.3	14.3	589.1	16.3	2.8	11.5	521.26	6.06
G91	43.5	422.0	0.97	0.0847	0.0005	0.6958	0.0130	0.0593	0.0010	523.9	6.2	536.3	14.4	579.2	16.2	2.3	9.5	523.94	6.18
G11	56.6	606.4	0.38	0.0887	0.0005	0.7721	0.0114	0.0632	0.0008	547.7	6.0	580.9	12.6	713.3	15.2	5.7	23.2	547.67	6.04
G71	13.0	100.6	1.80	0.0887	0.0008	0.7606	0.0262	0.0603	0.0017	547.9	8.9	574.3	25.1	615.4	27.6	4.6	11.0	547.90	8.88
G131	73.4	870.4	0.05	0.0905	0.0005	0.7363	0.0113	0.0588	0.0008	558.6	6.0	560.3	12.9	559.0	13.9	0.3	0.1	558.55	6.03
G20	95.0	986.5	0.37	0.0936	0.0005	0.7734	0.0106	0.0596	0.0007	576.9	6.1	581.7	12.0	588.7	13.0	0.8	2.0	576.85	6.13
G150	65.5	667.8	0.35	0.0948	0.0006	0.8408	0.0148	0.0636	0.0010	584.0	6.6	619.6	15.2	728.4	17.9	5.7	19.8	583.98	6.59
G37	152.3	1580.7	0.18	0.0989	0.0006	0.8721	0.0123	0.0643	0.0008	608.1	6.6	636.7	13.1	751.2	15.3	4.5	19.0	608.14	6.57
G132	127.2	1266.7	0.26	0.0999	0.0006	0.8359	0.0127	0.0611	0.0008	613.6	6.6	616.9	13.8	642.4	15.0	0.5	4.5	613.65	6.56
G70																			

Table 2. U-Pb zircon ages of Zanskar River sands

G128	443.2	2222.2	1.74	0.1373	0.0008	1.2644	0.0181	0.0668	0.0009	829.5	8.6	829.9	16.0	831.5	16.7	0.0	0.2	829.55	8.62
G6	264.0	1665.8	0.57	0.1447	0.0008	1.3814	0.0183	0.0695	0.0008	871.2	9.0	881.0	15.4	913.0	16.1	1.1	4.6	871.19	9.01
G34	20.9	83.7	2.64	0.1453	0.0011	1.4629	0.0421	0.0723	0.0015	874.4	12.2	915.2	26.6	993.0	28.4	4.5	11.9	874.39	12.16
G84	100.0	503.7	1.43	0.1461	0.0008	1.3974	0.0227	0.0694	0.0010	878.8	9.4	887.9	17.6	909.5	18.4	1.0	3.4	878.84	9.45
G94	38.8	218.1	0.94	0.1463	0.0009	1.4287	0.0299	0.0721	0.0012	880.2	10.5	901.0	21.1	988.8	22.6	2.3	11.0	880.19	10.46
G104	25.9	133.7	1.28	0.1470	0.0010	1.4122	0.0339	0.0688	0.0013	884.0	11.0	894.1	22.9	893.0	23.5	1.1	1.0	884.01	11.02
G124	30.0	170.8	0.86	0.1482	0.0009	1.3997	0.0286	0.0688	0.0011	890.6	10.3	888.8	20.7	893.9	21.2	-0.2	0.4	890.64	10.33
G103	47.3	294.4	0.38	0.1542	0.0009	1.4987	0.0281	0.0694	0.0011	924.2	10.4	929.9	19.7	909.8	20.1	0.6	-1.6	909.76	20.10
G135	72.7	382.9	0.64	0.1686	0.0010	1.6529	0.0279	0.0708	0.0010	1004.3	10.8	990.7	19.5	951.4	19.5	-1.4	-5.6	951.36	19.53
G99	91.5	569.2	0.31	0.1584	0.0009	1.5981	0.0255	0.0713	0.0010	948.0	10.1	969.5	18.1	965.5	18.7	2.2	1.8	965.45	18.69
G134	57.0	293.1	0.91	0.1616	0.0010	1.5792	0.0294	0.0715	0.0011	965.8	10.8	962.1	20.4	972.3	21.0	-0.4	0.7	972.31	20.98
G145	73.9	406.5	0.59	0.1650	0.0010	1.6229	0.0271	0.0720	0.0010	984.7	10.5	979.1	19.4	985.7	20.0	-0.6	0.1	985.66	19.96
G101	104.4	678.6	0.15	0.1585	0.0009	1.5627	0.0237	0.0721	0.0010	948.2	10.0	955.5	17.8	989.6	18.6	0.8	4.2	989.61	18.56
G16	82.3	474.0	0.49	0.1623	0.0009	1.6280	0.0236	0.0722	0.0009	969.7	10.2	981.1	17.0	991.9	17.5	1.2	2.2	991.87	17.51
G43	97.5	532.1	0.74	0.1590	0.0009	1.5909	0.0253	0.0725	0.0010	951.3	10.2	966.7	17.9	1000.8	18.6	1.6	5.0	1000.85	18.58
G63	70.1	395.0	0.45	0.1664	0.0010	1.6545	0.0256	0.0726	0.0009	992.4	10.5	991.3	18.0	1002.8	18.4	-0.1	1.0	1002.81	18.41
G133	19.8	93.9	1.19	0.1628	0.0011	1.6663	0.0396	0.0727	0.0013	972.4	12.0	995.8	24.0	1005.6	24.7	2.3	3.3	1005.60	24.73
G115	77.0	440.3	0.41	0.1656	0.0010	1.6556	0.0265	0.0730	0.0010	988.0	10.5	991.7	18.8	1015.1	19.5	0.4	2.7	1015.06	19.48
G4	179.5	841.3	1.07	0.1701	0.0010	1.7111	0.0230	0.0738	0.0009	1012.4	10.5	1012.7	16.8	1036.6	17.2	0.0	2.3	1036.55	17.22
G87	46.6	257.9	0.61	0.1622	0.0010	1.6166	0.0309	0.0739	0.0011	968.8	11.0	976.7	20.5	1037.4	21.4	0.8	6.6	1037.37	21.44
G5	93.7	518.6	0.43	0.1696	0.0010	1.7291	0.0261	0.0739	0.0009	1009.7	10.7	1019.4	17.8	1039.0	18.3	0.9	2.8	1039.01	18.28
G74	54.2	346.4	0.30	0.1528	0.0009	1.5282	0.0266	0.0741	0.0011	916.8	10.2	941.8	19.0	1045.3	20.4	2.7	12.3	1045.28	20.39
G12	37.7	207.3	0.70	0.1587	0.0009	1.6291	0.0281	0.0746	0.0010	949.5	10.5	981.5	18.9	1057.2	20.1	3.3	10.2	1057.20	20.05
G107	18.1	89.8	0.73	0.1744	0.0012	1.8589	0.0502	0.0748	0.0014	1036.3	13.5	1066.6	26.6	1062.6	27.1	2.8	2.5	1062.59	27.10
G15	118.7	610.4	0.65	0.1729	0.0010	1.7725	0.0245	0.0748	0.0009	1027.9	10.7	1035.4	17.1	1063.4	17.6	0.7	3.3	1063.40	17.59
G148	60.5	312.6	0.56	0.1757	0.0011	1.8344	0.0363	0.0764	0.0012	1043.7	11.8	1057.9	22.2	1106.6	23.1	1.3	5.7	1106.62	23.07
G89	17.6	93.9	0.70	0.1632	0.0012	1.7109	0.0503	0.0772	0.0016	974.5	13.5	1012.6	28.4	1125.8	30.1	3.8	13.4	1125.84	30.12
G29	41.2	185.7	1.05	0.1786	0.0011	1.9235	0.0379	0.0783	0.0012	1059.5	12.1	1089.3	21.5	1153.7	22.3	2.7	8.2	1153.73	22.34
G96	103.5	517.2	0.47	0.1867	0.0011	2.0672	0.0313	0.0794	0.0010	1103.3	11.4	1138.0	19.1	1181.4	19.9	3.0	6.6	1181.38	19.85
G110	44.0	182.3	0.67	0.2120	0.0013	2.4514	0.0472	0.0821	0.0012	1239.6	13.6	1257.8	22.7	1248.6	22.9	1.4	0.7	1248.62	22.90
G46	126.3	586.8	0.73	0.1856	0.0010	2.1310	0.0303	0.0832	0.0010	1097.7	11.3	1158.9	18.5	1272.7	19.5	5.3	13.8	1272.74	19.53
G75	99.4	403.1	0.35	0.2354	0.0013	2.8658	0.0451	0.0873	0.0011	1362.6	14.0	1373.0	20.9	1366.9	21.0	0.8	0.3	1366.90	21.01
G149	65.6	270.1	0.45	0.2278	0.0014	2.8001	0.0518	0.0894	0.0013	1323.2	14.3	1355.6	23.7	1413.2	24.3	2.4	6.4	1413.17	24.26
G76	62.6	243.1	0.29	0.2512	0.0015	3.1940	0.0602	0.0947	0.0013	1444.5	15.6	1455.7	23.3	1522.9	23.6	0.8	5.1	1522.91	23.55
G85	334.7	896.0	1.29	0.2799	0.0016	3.7910	0.0535	0.0985	0.0012	1590.7	15.6	1590.8	21.5	1595.2	21.5	0.0	0.3	1595.16	21.51
G10	64.4	223.5	0.60	0.2575	0.0015	3.6348	0.0585	0.1000	0.0012	1477.2	15.3	1557.2	21.5	1624.1	21.8	5.1	9.0	1624.08	21.84
G73	37.0	106.0	0.99	0.2786	0.0019	3.9474	0.1048	0.1001	0.0016	1584.4	19.3	1623.5	28.3	1625.9	28.1	2.4	2.6	1625.94	28.15
G62	90.4	294.4	1.01	0.2477	0.0015	3.4820	0.0615	0.1013	0.0013	1426.6	15.1	1523.1	22.7	1648.6	23.3	6.3	13.5	1648.62	23.31
G120	288.2	981.8	0.15	0.2948	0.0016	4.1819	0.0588	0.1045	0.0013	1665.3	16.2	1670.5	22.5	1704.7	22.6	0.3	2.3	1704.65	22.62
G108	297.2	921.0	0.62	0.2890	0.0016	4.1888	0.0617	0.1045	0.0013	1636.4	16.1	1671.8	22.5	1705.0	22.6	2.1	4.0	1705.00	22.62
G139	42.7	144.5	0.57	0.2640	0.0017	3.7438	0.0836	0.1050	0.0016	1510.4	17.1	1580.8	26.9	1715.0	27.4	4.5	11.9	1715.02	27.44
G49	206.0	661.1	0.54	0.2799	0.0016	4.0774	0.0595	0.1069	0.0013	1590.8	15.8	1649.8	21.6	1747.1	21.9	3.6	8.9	1747.05	21.87
G53	240.2	690.8	0.57	0.3102	0.0017	4.7020	0.0654	0.1090	0.0013	1741.5	16.9	1767.6	21.7	1782.1	21.6	1.5	2.3	1782.10	21.64
G50	350.8	1029.1	0.28	0.3258	0.0018	4.9784	0.0660	0.1106	0.0013	1817.9	17.4	1815.7	21.5	1809.1	21.3	-0.1	-0.5	1809.13	21.30
G83	179.1	655.7	0.87	0.2573	0.0015	3.7742	0.0577	0.1128	0.0014	1475.8	15.0	1587.3	22.3	1845.0	23.2	7.0	20.0	1845.01	23.2
G78	268.3	683.3	0.90	0.3260	0.0018	5.8391	0.0829	0.1287	0.0015	1818.7	17.6	1952.2	22.8	2079.6	23.1	6.8	12.5	2079.61	23.08
G119	216.8	490.2	0.34	0.4091	0.0023	7.8168	0.1149	0.1402	0.0018	2210.8	20.9	2210.1	24.8	2229.1	24.6	0.0	0.8	2229.06	24.57
G147	5.2	10.8	1.04	0.3628	0.0046	6.3971	0.4011	0.1499	0.0041	1995.5	43.6	2031.9	54.5	2345.0	52.4	1.8	14.9	2345.01	52.42
G95	521.7	1326.8	0.37	0.3688	0.0020	7.8045	0.1082	0.1528	0.0018	2023.7	19.1	2208.7	23.8	2377.5	24.0	8.4	14.9	2377.50	24.01
G3	248.6	500.3	0.24	0.4631	0.0026	10.2048	0.1495	0.1601	0.0018	2453.1	23.0	2453.5	23.6	2456.4	23.1	0.0	0.1	2456.40	23.06
G146	379.2	545.6	1.64	0.4714	0.0026	10.5159	0.1605	0.1610	0.0021	2489.9	23.1	2481.3	26.4	2466.3	26.2	-0.3	-1.0	2466.29	26.17
G27	123.5	242.4	0.94	0.4136	0.0024	9.1298	0.1525	0.1610	0.0019	2231.2	21.8	2351.1	24.2	2466.6	23.9	5.1	9.5	2466.61	23.87
G14	120.0	222.2	0.78	0.4464	0.0025	9.7440	0.1493	0.1617	0.0019	2379.2	22.6	2410.9	23.8	2473.5	23.3	1.3	3.8	2473.51	23.34
G22	542.2	1137.1	0.16	0.4581	0.0025	10.2242	0.1298	0.1621	0.0018	2431.2	22.2	2455.3	23.0	2477.7	22.6	1.0	1.9	2477.68	

Table 2. U-Pb zircon ages of Zanskar River sands

G100	-1.3	6.1	0.23	0.0939	0.0025	45.0084	4.9649	2.0809	0.0651	578.7	29.1	3887.7	80.0	6248.2	65.3	85.1	90.7
G30	8.9	721.8	0.02	0.0129	0.0001	0.1217	0.0038	0.0672	0.0020	82.9	1.4	116.6	6.8	844.3	36.5	28.9	90.2
G60	4.2	49.3	0.99	0.0782	0.0010	3.8431	0.1540	0.3802	0.0090	485.2	12.1	1601.8	44.1	3832.4	49.0	69.7	87.3
G13	72.4	1100.0	0.08	0.0746	0.0004	2.8444	0.0370	0.2767	0.0032	463.7	5.0	1367.3	19.2	3344.6	24.4	66.1	86.1
G116	168.0	2227.6	0.53	0.0692	0.0004	0.9965	0.0140	0.1049	0.0014	431.2	4.7	702.0	14.3	1712.4	23.2	38.6	74.8
G67	1.0	16.9	0.13	0.0583	0.0011	0.6729	0.0560	0.0819	0.0057	365.3	13.6	522.5	58.0	1242.4	101.4	30.1	70.6
G25	95.4	973.7	1.71	0.0723	0.0004	0.9247	0.0131	0.0934	0.0012	450.1	4.9	664.8	13.5	1496.2	21.5	32.3	69.9
G138	22.0	208.6	0.89	0.0875	0.0006	1.0776	0.0218	0.0915	0.0015	540.6	6.6	742.5	19.2	1456.4	28.0	27.2	62.9
G28	154.8	1084.4	0.54	0.1271	0.0007	1.7339	0.0236	0.0998	0.0012	771.3	8.1	1021.2	17.0	1620.4	21.2	24.5	52.4
G41	162.8	1994.6	0.49	0.0711	0.0004	0.6744	0.0096	0.0695	0.0009	443.0	4.8	523.4	11.5	914.2	17.3	15.4	51.5
G23	11.7	82.4	0.72	0.1272	0.0009	1.6580	0.0394	0.0943	0.0017	772.1	10.2	992.6	23.9	1513.1	29.4	22.2	49.0
G7	1.5	11.5	0.28	0.1210	0.0020	1.4491	0.1148	0.0856	0.0048	736.5	23.5	909.5	69.6	1328.0	84.5	19.0	44.5
G26	11.1	77.7	0.78	0.1224	0.0010	1.3244	0.0418	0.0788	0.0018	744.4	11.4	856.4	28.5	1165.9	34.1	13.1	36.1
G141	73.5	736.0	0.23	0.1021	0.0006	0.9936	0.0180	0.0718	0.0011	626.5	7.1	700.5	17.1	978.9	21.5	10.6	36.0
G17	35.6	367.3	0.60	0.0848	0.0005	0.7740	0.0127	0.0656	0.0009	524.9	5.9	582.1	13.5	793.0	17.5	9.8	33.8
G42	1.9	18.9	0.21	0.0969	0.0018	0.9511	0.0842	0.0690	0.0047	595.9	21.2	678.7	68.6	898.7	83.0	12.2	33.7
G35	14.1	118.2	1.14	0.0948	0.0007	0.9089	0.0270	0.0683	0.0016	583.7	8.7	656.5	23.8	878.3	29.6	11.1	33.5
G48	140.8	389.6	0.14	0.3782	0.0021	12.3415	0.1741	0.2378	0.0027	2067.7	19.7	2630.7	24.0	3105.6	24.1	21.4	33.4
G140	88.3	903.5	0.32	0.0949	0.0006	0.8944	0.0155	0.0683	0.0010	584.5	6.6	648.7	15.7	876.2	19.8	9.9	33.3
G81	50.1	260.0	0.54	0.1796	0.0012	2.4797	0.0548	0.0980	0.0015	1064.6	12.8	1266.1	24.3	1586.4	27.0	15.9	32.9
G33	435.3	1099.3	0.62	0.3703	0.0020	8.7494	0.1170	0.1712	0.0019	2030.8	19.2	2312.2	23.0	2569.6	23.1	12.2	21.0
G80	550.0	1438.9	0.10	0.3890	0.0021	8.9062	0.1190	0.1660	0.0020	2118.0	19.8	2328.4	23.7	2517.5	23.8	9.0	15.9

Sample 14080401 Zara

Grain No.	Pb (ppm)	U (ppm)	Atomic Th/U	Ratios				Ages (Ma)					% concord. (206/238)	% concord. (206/238) / 207(235)	Best Age (Ma)	± 2σ	
				$^{206}\text{Pb}/^{238}\text{U}$	± 1 σ	$^{207}\text{Pb}/^{235}\text{U}$	± s.e.	$^{207}\text{Pb}/^{206}\text{Pb}$	± s.e.	$^{206}\text{Pb}/^{238}\text{U}$	± 2σ	$^{207}\text{Pb}/^{235}\text{U}$	± 2σ	$^{207}\text{Pb}/^{206}\text{Pb}$	± 2σ		
G100	12.0	297.3	0.34	0.0395	0.0005	0.2772	0.0076	0.0509	0.0014	249.8	6.3	248.5	13.3	236.8	11.5	-0.5	-5.5
G34	92.4	1521.6	1.06	0.0498	0.0006	0.3726	0.0078	0.0543	0.0011	313.0	7.5	321.6	13.2	384.3	13.2	2.7	18.5
G55	45.0	723.2	0.51	0.0582	0.0007	0.4579	0.0107	0.0571	0.0013	364.4	8.9	382.8	16.9	496.2	18.3	4.8	26.6
G24	99.5	1263.0	1.09	0.0633	0.0008	0.4782	0.0078	0.0548	0.0009	395.5	9.1	396.8	12.9	404.9	10.5	0.3	2.3
G69	50.3	784.6	0.23	0.0651	0.0008	0.4969	0.0091	0.0554	0.0010	406.3	9.4	409.6	14.5	428.4	12.5	0.8	5.2
G87	72.3	959.9	0.74	0.0657	0.0008	0.5085	0.0095	0.0562	0.0010	410.1	9.6	417.4	14.8	458.7	13.3	1.7	10.6
G39	48.7	524.7	1.66	0.0661	0.0008	0.5052	0.0097	0.0555	0.0010	412.5	9.7	415.2	15.2	430.8	13.2	0.7	4.3
G68	33.3	376.1	1.36	0.0665	0.0008	0.5018	0.0106	0.0547	0.0011	415.1	9.9	412.9	16.4	401.2	13.8	-0.5	-3.5
G61	20.6	249.2	0.99	0.0675	0.0008	0.5153	0.0120	0.0554	0.0013	420.8	10.1	422.0	18.0	428.8	16.0	0.3	1.9
G38	18.0	246.1	0.54	0.0675	0.0009	0.5072	0.0120	0.0545	0.0013	421.3	10.3	416.6	18.1	390.9	15.1	-1.1	-7.8
G64	29.9	349.4	1.16	0.0679	0.0009	0.5285	0.0135	0.0565	0.0014	423.6	10.5	430.8	20.0	470.5	19.2	1.7	10.0
G33	22.8	284.8	0.77	0.0696	0.0009	0.5354	0.0117	0.0558	0.0012	433.6	10.4	435.4	17.6	445.2	15.5	0.4	2.6
G22	12.1	145.5	0.91	0.0697	0.0009	0.5219	0.0153	0.0543	0.0016	434.4	11.1	426.4	22.5	383.9	18.8	-1.9	-13.1
G12	24.5	320.4	0.58	0.0701	0.0009	0.5335	0.0113	0.0552	0.0012	436.9	10.4	434.1	17.1	419.5	14.3	-0.6	-4.1
G89	22.8	260.8	1.09	0.0702	0.0009	0.5425	0.0157	0.0561	0.0016	437.2	11.2	440.1	22.7	455.9	21.2	0.7	4.1
G16	23.4	331.1	0.30	0.0703	0.0009	0.5436	0.0115	0.0561	0.0012	438.1	10.5	440.8	17.2	455.1	15.2	0.6	3.7
G90	45.0	559.4	0.74	0.0704	0.0009	0.5414	0.0109	0.0558	0.0011	438.5	10.4	439.4	16.4	444.8	14.1	0.2	1.4
G79	32.9	418.3	0.63	0.0708	0.0009	0.5438	0.0113	0.0558	0.0011	440.7	10.5	440.9	17.1	442.8	14.7	0.1	0.5
G125	32.3	388.1	0.82	0.0711	0.0009	0.5530	0.0125	0.0564	0.0013	442.7	10.6	447.0	18.4	469.7	16.7	1.0	5.7
G99	11.0	142.9	0.51	0.0713	0.0009	0.5382	0.0154	0.0547	0.0016	444.2	11.3	437.2	22.4	401.2	19.0	-1.6	-10.7
G77	36.7	404.1	1.17	0.0716	0.0009	0.5550	0.0116	0.0563	0.0012	445.5	10.6	448.3	17.3	463.0	15.2	0.6	3.8
G123	37.4	453.0	0.74	0.0720	0.0009	0.5484	0.0120	0.0553	0.0012	448.0	10.7	443.9	17.9	423.6	14.9	-0.9	-5.8
G37	15.0	178.9	0.81	0.0723	0.0009	0.5584	0.0141	0.0560	0.0014	450.2	11.1	450.5	20.4	452.0	18.2	0.1	0.4
G122	10.6	108.6	1.41	0.0727	0.0010	0.5756	0.0176	0.0575	0.0018	452.2	11.7	461.6	24.9	509.6	24.7	2.0	11.3
G105	30.9	374.7	0.70	0.0728	0.0009	0.5525	0.0122	0.0550	0.0012	453.2	10.8	446.6	18.0	413.4	14.7	-1.5	-9.6
G81	30.2	368.5	0.67	0.0730	0.0009	0.5820	0.0124	0.0578	0.0012	454.1	10.8	465.7	18.1	523.7	17.1	2.5	13.3
G83	18.5	225.2	0.68	0.0730	0.0009	0.5729	0.0137	0.0569	0.0014	454.1	11.1	459.9	19.9	489.2	18.4	1.2	7.2
G130	18.8	230.5	0.64	0.0730	0.0010	0.5806	0.0161	0.0577	0.0016	454.4	11.4	464.8	22.9	517.6	22.5	2.2	12.2
G05	54.5	582.6	1.15	0.0744	0.0009	0.5699	0.0104	0.0556	0.0010	462.7	10.8	458.0	15.8	434.8	12.5	-1.0	-6.4
G120	16.2	206.5	0.41	0.0746	0.0010	0.6117	0.0172	0.0595	0.0017	463.5	11.8	484.6	24.0	586.9	25.2	4.4	21.0
G128	10.7	118.4	0.84	0.0772	0.0011	0.6050	0.0215	0.0569	0.0021	479.3	13.0	480.4	29.6	486.5	27.9	0.2	1.5
G109	14.7	158.4	0.87	0.0783	0.0010	0.5994	0.0159	0.0555	0.0015	486.1	12.1	476.9	22.4	433.6	18.7	-1.9	-12.1
G106	43.8	523.4	0.47	0.0791	0.0010	0.6330	0										

Table 2. U-Pb zircon ages of Zanskar River sands

G49	6.5	60.5	0.26	0.1054	0.0014	0.8694	0.0274	0.0599	0.0019	645.9	16.8	635.2	32.6	598.2	28.7	-1.7	-8.0	645.86	16.80
G95	45.9	373.4	0.77	0.1066	0.0013	0.8984	0.0196	0.0612	0.0013	652.8	15.4	650.9	23.8	645.2	20.5	-0.3	-1.2	652.80	15.38
G15	128.1	1235.9	0.15	0.1072	0.0013	0.1032	0.0154	0.0685	0.0010	656.6	14.8	710.5	19.0	884.9	16.9	7.6	25.8	656.64	14.79
G92	10.0	73.9	0.78	0.1145	0.0016	0.9974	0.0311	0.0632	0.0020	699.0	18.2	702.5	34.7	714.3	32.1	0.5	2.1	699.00	18.16
G46	50.8	453.5	0.12	0.1165	0.0014	1.0293	0.0179	0.0641	0.0011	710.4	16.2	718.6	21.2	744.6	17.6	1.1	4.6	710.39	16.17
G65	25.8	209.6	0.33	0.1199	0.0015	1.0828	0.0243	0.0655	0.0015	730.1	17.4	745.0	26.9	790.4	24.3	2.0	7.6	730.10	17.38
G35	20.6	156.7	0.47	0.1235	0.0015	1.0936	0.0232	0.0642	0.0013	750.7	17.7	750.3	25.8	749.5	22.1	-0.1	-0.2	750.68	17.67
G124	12.9	87.2	0.89	0.1235	0.0016	1.0981	0.0294	0.0645	0.0017	750.8	18.6	752.4	31.7	757.7	28.6	0.2	0.9	750.85	18.59
G14	11.9	76.5	1.12	0.1245	0.0018	1.2084	0.0403	0.0704	0.0024	756.2	20.5	804.5	40.8	940.9	41.5	6.0	19.6	756.18	20.52
G48	12.2	77.0	1.06	0.1269	0.0017	1.1591	0.0295	0.0662	0.0017	770.4	18.9	781.5	31.1	814.0	28.4	1.4	5.4	770.39	18.88
G102	25.0	129.5	1.95	0.1271	0.0016	1.1370	0.0268	0.0649	0.0015	771.5	18.4	771.1	28.8	770.4	25.3	-0.1	-0.1	771.47	18.42
G19	34.7	217.6	1.10	0.1275	0.0016	1.1619	0.0224	0.0661	0.0012	773.6	17.8	782.8	24.4	809.5	20.9	1.2	4.4	773.59	17.84
G30	26.7	177.1	0.83	0.1292	0.0016	1.1901	0.0240	0.0668	0.0013	783.4	18.2	796.0	25.7	831.5	22.4	1.6	5.8	783.41	18.15
G62	5.4	36.5	0.79	0.1311	0.0021	1.3057	0.0548	0.0723	0.0031	793.9	24.1	848.2	52.5	993.8	54.2	6.4	20.1	793.85	24.05
G129	10.2	96.6	1.68	0.1312	0.0017	1.1879	0.0303	0.0657	0.0017	794.9	19.4	795.0	31.5	796.2	28.1	0.0	0.2	794.88	19.38
G107	24.5	147.8	1.05	0.1330	0.0017	1.2036	0.0273	0.0657	0.0015	804.9	19.0	802.3	28.5	795.6	24.7	-0.3	-1.2	804.90	19.00
G56	21.8	113.5	1.75	0.1334	0.0018	1.2212	0.0331	0.0664	0.0018	807.5	20.1	810.3	33.7	818.7	30.5	0.4	1.4	807.46	20.13
G60	114.7	757.9	0.60	0.1365	0.0016	1.2996	0.0212	0.0691	0.0011	825.0	18.4	845.5	22.5	900.2	18.7	2.4	8.4	825.01	18.38
G131	26.2	172.7	0.58	0.1389	0.0017	1.4004	0.0313	0.0732	0.0016	838.2	19.7	889.1	30.1	1018.9	28.5	5.7	17.7	838.16	19.70
G11	64.3	398.3	0.72	0.1423	0.0018	1.3163	0.0259	0.0671	0.0013	857.4	19.8	852.9	26.3	841.2	22.0	-0.5	-1.9	857.43	19.75
G132	21.9	122.8	0.96	0.1473	0.0019	1.4304	0.0338	0.0705	0.0017	885.7	21.0	901.7	31.8	942.1	28.7	1.8	6.0	885.70	21.01
G01	125.2	757.0	0.44	0.1569	0.0019	1.5051	0.0230	0.0696	0.0010	939.2	20.6	932.5	22.7	916.6	17.3	-0.7	-2.5	916.58	17.35
G10	12.2	69.9	0.48	0.1635	0.0021	1.5787	0.0386	0.0701	0.0017	975.9	23.5	961.9	34.2	930.1	29.6	-1.5	-4.9	930.11	29.56
G58	55.8	320.4	0.64	0.1556	0.0019	1.5040	0.0266	0.0701	0.0012	932.4	21.0	932.0	25.6	931.3	20.9	0.0	-0.1	931.28	20.87
G25	99.9	567.0	0.60	0.1589	0.0019	1.5411	0.0243	0.0703	0.0011	950.8	21.0	946.9	23.5	938.3	18.3	-0.4	-1.3	938.29	18.28
G21	43.6	259.9	0.64	0.1501	0.0018	1.4570	0.0260	0.0704	0.0012	901.5	20.4	912.8	25.5	940.3	21.2	1.2	4.1	940.33	21.25
G32	24.8	138.9	0.49	0.1664	0.0021	1.6168	0.0323	0.0705	0.0014	992.4	22.8	976.8	29.1	942.1	24.0	-1.6	-5.3	942.08	24.04
G71	49.3	244.3	0.90	0.1683	0.0020	1.6343	0.0303	0.0705	0.0013	1002.5	22.5	983.5	27.4	942.1	22.1	-1.9	-6.4	942.08	22.13
G17	105.4	551.0	1.15	0.1514	0.0018	1.4735	0.0233	0.0706	0.0011	908.8	20.2	919.6	23.2	945.9	18.5	1.2	3.9	945.85	18.48
G50	60.4	318.6	0.66	0.1695	0.0020	1.6512	0.0284	0.0707	0.0012	1009.6	22.5	990.0	25.9	947.3	20.4	-2.0	-6.6	947.30	20.40
G70	58.0	369.8	0.29	0.1565	0.0019	1.5357	0.0305	0.0712	0.0014	937.0	21.5	944.8	28.3	963.4	24.1	0.8	2.7	963.45	24.12
G28	78.2	445.0	0.70	0.1547	0.0018	1.5230	0.0246	0.0714	0.0011	927.0	20.5	939.7	23.9	969.7	19.2	1.3	4.4	969.74	19.24
G111	108.9	573.7	0.77	0.1626	0.0020	1.6045	0.0298	0.0716	0.0013	971.1	21.7	971.9	27.1	974.6	22.6	0.1	0.4	974.59	22.58
G43	38.8	213.6	0.88	0.1526	0.0019	1.5101	0.0308	0.0718	0.0014	915.5	21.3	934.5	28.8	980.0	25.2	2.0	6.6	979.99	25.22
G23	31.5	161.1	0.95	0.1623	0.0020	1.6074	0.0308	0.0719	0.0013	969.4	22.1	973.1	27.9	981.7	23.5	0.4	1.2	981.69	23.47
G134	35.2	206.9	0.35	0.1643	0.0020	1.6294	0.0348	0.0720	0.0015	980.7	22.6	981.6	30.7	984.5	26.5	0.1	0.4	984.53	26.46
G101	13.7	67.6	0.81	0.1736	0.0023	1.7413	0.0441	0.0728	0.0018	1031.6	24.9	1024.0	36.7	1008.4	32.3	-0.8	-2.3	1008.39	32.31
G47	67.5	397.4	0.34	0.1656	0.0020	1.6625	0.0300	0.0728	0.0013	987.9	22.2	994.3	26.9	1008.9	22.3	0.6	2.1	1008.95	22.31
G117	68.6	381.4	0.53	0.1654	0.0020	1.6606	0.0321	0.0728	0.0014	986.9	22.2	993.6	28.4	1009.2	24.1	0.7	2.2	1009.23	24.06
G06	19.5	94.3	1.27	0.1599	0.0020	1.6066	0.0363	0.0729	0.0016	956.1	22.7	972.8	32.2	1010.9	28.6	1.7	5.4	1010.90	28.63
G84	49.9	240.3	0.95	0.1712	0.0021	1.7240	0.0367	0.0730	0.0015	1018.9	23.6	1017.5	31.4	1015.1	26.9	-0.1	-0.4	1015.06	26.89
G94	78.3	473.1	0.10	0.1727	0.0021	1.7458	0.0328	0.0734	0.0013	1026.9	23.1	1025.6	28.3	1023.6	23.6	-0.1	-0.3	1023.64	23.56
G74	27.6	135.3	0.69	0.1791	0.0022	1.8193	0.0366	0.0737	0.0015	1062.2	24.3	1052.4	30.5	1032.7	25.5	-0.9	-2.9	1032.72	25.51
G113	62.4	309.3	1.12	0.1611	0.0021	1.6456	0.0390	0.0741	0.0017	962.7	22.9	987.9	33.8	1044.7	30.6	2.5	7.9	1044.74	30.63
G98	46.9	203.4	1.02	0.1862	0.0023	1.9175	0.0385	0.0747	0.0015	1100.8	24.9	1087.2	31.0	1060.7	25.9	-1.2	-3.8	1060.71	25.90
G121	84.0	441.5	0.45	0.1788	0.0022	1.8441	0.0355	0.0748	0.0014	1060.3	23.7	1061.3	29.4	1064.2	24.7	0.1	0.4	1064.21	24.67
G135	70.6	360.5	0.48	0.1819	0.0023	1.8813	0.0394	0.0750	0.0015	1077.5	24.5	1074.5	31.8	1069.6	27.1	-0.3	-0.7	1069.57	27.14
G72	72.5	341.3	0.70	0.1863	0.0022	1.9283	0.0335	0.0751	0.0013	1101.1	24.3	1091.0	27.6	1071.4	22.2	-0.9	-2.8	1071.45	22.21
G67	88.1	482.9	0.40	0.1762	0.0021	1.8368	0.0314	0.0756	0.0012	1046.0	23.1	1058.7	26.7	1085.6	21.9	1.2	3.6	1085.56	21.86
G108	113.1	652.4	0.12	0.1791	0.0022	1.8725	0.0340	0.0759	0.0013	1061.8	23.6	1071.4	28.2	1091.6	23.5	0.9	2.7	1091.64	23.45
G29	24.0	116.6	1.03	0.1664	0.0022	1.7474	0.0450	0.0762	0.0020	992.4	24.5	1026.2	37.4	1099.3	34.6	3.3	9.7	1099.28	34.56
G86	24.0	104.1	0.67	0.1991	0.0026	2.0920	0.0540	0.0762	0.0020	1170.3	28.4	1146.2	39.9	1101.4	34.7	-2.1	-6.3	1101.38	34.74
G97	174.4	851.8	0.74	0.1767	0.0021	1.8580	0.0331	0.0763	0.0013	1049.1	23.2	1066.3	27.7	1102.2	23.1	1.6	4.8	1102.17	23.10
G114	9.3	51.2	0.30	0.1767	0.0024	1.8737	0.0536	0.0769	0.0022	1048.8	26.5	1071.8	42.1	1119.6	39.0	2.1	6.3	1119.63	38.97
G66	30.7	123.7	1.23	0.1912	0.0024	2.0453	0.0401	0.0776	0.0015										

Table 2. U-Pb zircon ages of Zanskar River sands

G78	87.6	289.3	0.64	0.2678	0.0032	3.5651	0.0605	0.0966	0.0016	1529.8	32.7	1541.8	32.1	1558.7	25.9	0.8	1.9	1558.69	25.91
G26	115.5	402.8	0.36	0.2722	0.0032	3.6380	0.0549	0.0970	0.0014	1551.8	32.6	1557.9	29.5	1566.4	22.7	0.4	0.9	1566.44	22.72
G115	149.1	606.1	0.09	0.2538	0.0031	3.3998	0.0616	0.0972	0.0017	1457.9	31.5	1504.3	33.3	1571.1	28.0	3.1	7.2	1571.08	27.96
G31	61.7	186.5	0.82	0.2796	0.0034	3.7603	0.0612	0.0976	0.0015	1589.2	33.9	1584.3	31.4	1578.0	24.8	-0.3	-0.7	1578.00	24.79
G75	48.9	128.6	1.40	0.2812	0.0034	3.8342	0.0695	0.0989	0.0017	1597.3	34.6	1600.0	34.5	1604.0	28.4	0.2	0.4	1604.05	28.36
G93	53.5	163.8	0.58	0.2924	0.0036	4.1279	0.0793	0.1024	0.0019	1653.7	36.1	1659.8	36.7	1668.3	30.7	0.4	0.9	1668.25	30.71
G40	88.6	247.4	1.03	0.2881	0.0034	4.0741	0.0644	0.1026	0.0015	1632.2	34.4	1649.1	31.3	1671.0	24.6	1.0	2.3	1670.96	24.61
G104	75.9	210.1	0.82	0.3032	0.0037	4.3412	0.0795	0.1039	0.0018	1707.1	36.4	1701.2	35.4	1694.6	29.2	-0.3	-0.7	1694.57	29.19
G07	66.3	189.6	0.70	0.3034	0.0036	4.3550	0.0691	0.1041	0.0016	1708.0	36.0	1703.8	31.8	1698.8	24.9	-0.2	-0.5	1698.82	24.87
G08	70.0	197.2	0.51	0.3218	0.0039	4.7377	0.0747	0.1068	0.0016	1798.5	37.6	1773.9	32.2	1745.3	25.0	-1.4	-3.0	1745.34	24.97
G44	23.8	61.4	1.13	0.3054	0.0038	4.5681	0.0873	0.1085	0.0020	1718.1	37.9	1743.5	37.6	1774.4	31.4	1.5	3.2	1774.38	31.38
G09	240.6	700.0	0.41	0.3192	0.0038	4.7827	0.0692	0.1087	0.0015	1785.7	36.7	1781.9	30.1	1777.4	22.7	-0.2	-0.5	1777.41	22.70
G03	82.5	252.3	0.86	0.2792	0.0034	4.1836	0.0704	0.1087	0.0018	1587.2	34.3	1670.8	33.2	1777.6	27.2	5.0	10.7	1777.58	27.17
G36	40.0	128.6	0.41	0.2935	0.0037	4.4876	0.0850	0.1109	0.0021	1659.0	36.8	1728.7	37.1	1814.4	31.2	4.0	8.6	1814.38	31.25
G82	91.6	236.8	0.70	0.3332	0.0040	5.2275	0.0889	0.1138	0.0019	1853.9	38.8	1857.1	34.6	1861.3	27.9	0.2	0.4	1861.28	27.88
G112	57.8	116.6	0.85	0.4027	0.0049	7.2287	0.1356	0.1302	0.0024	2181.6	45.4	2140.1	39.2	2101.1	32.3	-1.9	-3.8	2101.07	32.29
G116	56.6	119.3	0.80	0.3920	0.0048	7.2177	0.1366	0.1336	0.0025	2132.1	44.6	2138.7	39.5	2145.7	32.9	0.3	0.6	2145.69	32.88
G45	54.4	93.9	1.00	0.4554	0.0055	10.0920	0.1624	0.1607	0.0025	2419.3	49.0	2443.2	36.2	2463.5	28.4	1.0	1.8	2463.46	28.45
G18	76.8	107.7	2.30	0.4394	0.0054	9.7428	0.1575	0.1608	0.0025	2348.0	48.3	2410.8	36.4	2464.4	28.7	2.6	4.7	2464.40	28.66
G42	388.3	906.1	0.10	0.4249	0.0050	9.4211	0.1383	0.1608	0.0022	2282.6	45.2	2379.9	33.2	2464.5	25.4	4.1	7.4	2464.51	25.44
G63	102.9	190.9	0.82	0.4444	0.0054	9.8621	0.1597	0.1610	0.0025	2370.5	47.8	2422.0	36.1	2465.9	28.5	2.1	3.9	2465.87	28.53
G103	145.2	192.3	2.28	0.4609	0.0056	10.2327	0.1805	0.1611	0.0027	2443.5	49.2	2456.0	38.6	2467.0	31.5	0.5	1.0	2467.03	31.50
G80	81.7	135.7	1.17	0.4592	0.0056	10.2717	0.1735	0.1623	0.0026	2435.9	49.1	2459.6	37.4	2479.7	30.0	1.0	1.8	2479.66	30.05
G04	226.1	440.1	0.37	0.4663	0.0055	10.4786	0.1500	0.1630	0.0022	2467.4	48.4	2478.0	33.0	2486.9	24.7	0.4	0.8	2486.92	24.70
G59	233.5	415.7	0.98	0.4457	0.0053	10.0405	0.1543	0.1634	0.0024	2376.1	47.2	2438.5	34.6	2491.4	26.9	2.6	4.6	2491.36	26.92
G118	134.0	231.4	0.71	0.4777	0.0058	10.7900	0.1972	0.1639	0.0029	2517.2	50.4	2505.2	39.7	2496.2	32.7	-0.5	-0.8	2496.19	32.75
G133	59.0	96.6	1.29	0.4553	0.0058	10.4010	0.2135	0.1658	0.0033	2418.7	51.1	2471.1	44.1	2515.3	37.5	2.1	3.8	2515.28	37.48
G73	109.3	177.6	0.67	0.5041	0.0061	11.6851	0.1895	0.1682	0.0026	2631.5	51.9	2579.5	36.6	2539.3	28.8	-2.0	-3.6	2539.31	28.83
G27	370.8	646.6	0.96	0.4700	0.0056	11.3018	0.1653	0.1744	0.0024	2483.6	48.8	2548.4	33.8	2600.5	25.7	2.5	4.5	2600.51	25.68
G127	48.2	88.1	0.57	0.4760	0.0061	11.8463	0.2400	0.1806	0.0036	2510.0	52.8	2592.3	44.2	2658.0	37.4	3.2	5.6	2658.02	37.43
G88	72.0	110.4	0.77	0.5241	0.0064	13.1822	0.2278	0.1825	0.0030	2716.7	54.1	2692.8	38.9	2675.4	31.3	-0.9	-1.5	2675.45	31.30
G76	128.4	193.6	1.00	0.5345	0.0065	16.9115	0.2761	0.2296	0.0036	2760.2	54.2	2929.8	37.7	3049.0	30.0	5.8	9.5	3048.98	30.01
G110	146.5	232.3	0.16	0.5878	0.0071	18.8884	0.3332	0.2331	0.0040	2980.5	57.6	3036.1	40.2	3073.7	32.8	1.8	3.0	3073.73	32.82
G13	150.1	212.7	0.36	0.6346	0.0075	23.6373	0.3397	0.2702	0.0036	3167.9	59.3	3253.6	34.9	3307.0	26.2	2.6	4.2	3306.95	26.16
G57	29.4	230.1	0.83	0.1111	0.0015	1.1674	0.0291	0.0762	0.0019	679.1	16.8	785.4	30.8	1100.9	33.5	13.5	38.3	679.13	16.83
G119	10.3	117.0	0.95	0.0723	0.0010	0.6248	0.0188	0.0627	0.0019	449.9	11.7	492.8	25.9	698.4	30.6	8.7	35.6	449.94	11.66
G20	39.5	529.6	0.56	0.0688	0.0008	0.5123	0.0097	0.0540	0.0010	428.7	10.0	420.0	15.2	372.7	11.5	-2.1	-15.0	428.74	10.01
G02	22.2	212.7	1.04	0.0851	0.0011	0.6522	0.0158	0.0556	0.0013	526.3	12.8	509.8	21.8	436.8	17.1	-3.2	-20.5	526.25	12.83

Sample 13072301 Toze Lungpa

Grain No.	Pb (ppm)	U (ppm)	Atomic Th/U	Ratios				Ages (Ma)					% concord. (206/238)	% concord. (206/238)	Best Age (Ma)	± 2σ			
				206Pb/238U	± 1 σ	207Pb/235U	± s.e.	207Pb/206Pb	± s.e.	206Pb/238U	± 2σ	207Pb/235U	± 2σ	207Pb/206Pb	± 2σ				
G104	12.1	336.5	0.97	0.0293	0.0004	0.2375	0.0045	0.0562	0.0010	186.4	4.4	216.3	8.1	461.5	20.5	13.9	59.6	186.35	4.38
G10	20.8	661.4	0.20	0.0322	0.0004	0.2224	0.0040	0.0513	0.0009	204.2	4.7	203.9	7.7	254.3	14.7	-0.1	19.7	204.18	4.75
G75	17.7	473.8	0.70	0.0329	0.0004	0.2177	0.0040	0.0484	0.0008	208.4	5.0	200.0	7.6	116.9	11.0	-4.2	-78.2	208.36	4.99
G66	17.1	523.5	0.23	0.0330	0.0004	0.2323	0.0039	0.0511	0.0008	209.2	4.9	212.1	7.4	244.9	13.9	1.4	14.6	209.23	4.87
G7	27.7	858.8	0.15	0.0336	0.0004	0.2471	0.0036	0.0523	0.0007	213.1	4.7	224.2	6.9	299.0	14.2	4.9	28.7	213.10	4.74
G40	15.5	451.2	0.20	0.0351	0.0004	0.2520	0.0047	0.0517	0.0009	222.6	5.2	228.2	8.5	273.5	15.5	2.4	18.6	222.64	5.23
G29	146.7	2430.9	0.33	0.0598	0.0007	0.4820	0.0060	0.0588	0.0007	374.1	8.0	399.4	10.4	559.0	16.9	6.3	33.1	374.10	8.03
G17	16.3	196.9	1.00	0.0661	0.0008	0.5385	0.0105	0.0578	0.0010	412.8	9.6	437.4	14.5	522.9	21.1	5.6	21.1	412.80	9.55
G11	23.0	258.1	1.23	0.0682	0.0008	0.5887	0.0111	0.0617	0.0010	425.3	9.8	470.0	15.0	664.8	23.1	9.5	36.0	425.30	9.78
G4	54.0	767.8	0.32	0.0689	0.0008	0.5614	0.0074	0.0584	0.0008	429.5	9.2	452.5	11.7	546.3	17.3	5.1	21.4	429.46	9.17
G92	44.8	604.0	0.43	0.0702	0.0008	0.5666	0.0089	0.0589	0.0008	437.6	10.0	455.8	13.4	564.1	19.2	4.0	22.4	437.60</td	

Table 2. U-Pb zircon ages of Zanskar River sands

G57	24.5	195.8	2.44	0.0743	0.0009	0.6141	0.0124	0.0592	0.0010	462.1	10.9	486.1	16.2	573.4	22.4	4.9	19.4	462.13	10.92
G25	27.9	329.9	0.68	0.0746	0.0009	0.6016	0.0100	0.0577	0.0008	463.8	10.3	478.2	13.9	519.5	19.0	3.0	10.7	463.81	10.32
G18	30.6	372.9	0.53	0.0753	0.0009	0.5915	0.0090	0.0577	0.0008	468.1	10.2	471.9	13.3	518.8	18.1	0.8	9.8	468.07	10.19
G59	90.9	659.7	1.72	0.0753	0.0009	0.6162	0.0096	0.0586	0.0008	468.2	10.6	487.4	13.7	553.4	18.8	3.9	15.4	468.25	10.55
G34	35.3	468.9	0.39	0.0754	0.0009	0.7153	0.0115	0.0676	0.0009	468.3	10.4	547.9	15.0	856.3	23.2	14.5	45.3	468.31	10.43
G87	10.1	95.4	1.39	0.0775	0.0010	0.6309	0.0143	0.0574	0.0011	481.4	12.0	496.7	17.8	506.2	22.6	3.1	4.9	481.36	11.97
G102	6.9	69.5	1.04	0.0777	0.0000	0.6793	0.0000	0.0611	0.0000	482.4	0.0	526.3	0.0	644.2	7.3	8.4	25.1	482.38	0.00
G26	25.9	289.0	0.69	0.0797	0.0009	0.7183	0.0112	0.0628	0.0009	494.4	10.9	549.6	14.7	700.4	21.0	10.1	29.4	494.39	10.87
G70	951.7	12925.6	0.00	0.0802	0.0014	0.6659	0.0286	0.0602	0.0021	497.1	16.4	518.2	31.9	610.1	39.7	4.1	18.5	497.14	16.35
G98	19.8	247.7	0.24	0.0804	0.0010	0.6885	0.0126	0.0613	0.0010	498.7	11.8	531.9	16.3	649.4	22.2	6.2	23.2	498.69	11.81
G76	47.1	477.1	0.98	0.0809	0.0009	0.6251	0.0095	0.0573	0.0008	501.7	11.2	493.1	14.0	501.2	17.8	-1.7	-0.1	501.67	11.21
G47	80.2	1031.5	0.12	0.0816	0.0009	0.6977	0.0094	0.0613	0.0007	505.7	11.0	537.4	13.6	650.5	18.7	5.9	22.3	505.73	10.97
G2	1.9	23.7	0.04	0.0835	0.0013	0.6727	0.0272	0.0595	0.0020	516.9	15.9	522.4	30.6	585.4	37.0	1.0	11.7	516.92	15.95
G64	27.0	297.9	0.49	0.0838	0.0010	0.7304	0.0119	0.0597	0.0008	518.5	11.7	556.8	15.1	591.6	19.8	6.9	12.4	518.53	11.66
G41	27.9	332.6	0.26	0.0842	0.0010	0.6997	0.0113	0.0590	0.0008	521.4	11.7	538.6	15.0	567.8	19.4	3.2	8.2	521.38	11.65
G93	32.9	403.2	0.16	0.0857	0.0010	0.7407	0.0115	0.0633	0.0009	530.1	12.1	562.8	15.6	717.7	21.1	5.8	26.1	530.12	12.11
G49	132.9	1611.8	0.09	0.0875	0.0010	0.6933	0.0092	0.0580	0.0007	540.7	11.7	534.8	13.6	529.8	17.0	-1.1	-2.1	540.73	11.74
G95	31.4	336.5	0.44	0.0887	0.0011	0.7972	0.0134	0.0650	0.0009	547.8	12.7	595.3	16.7	775.6	22.6	8.0	29.4	547.78	12.67
G44	210.7	2238.4	0.35	0.0919	0.0010	0.7821	0.0098	0.0617	0.0007	566.5	12.2	586.7	14.1	664.4	18.2	3.4	14.7	566.47	12.16
G69	25.0	262.6	0.25	0.0963	0.0011	0.8832	0.0148	0.0653	0.0009	592.8	13.4	642.7	17.4	783.1	22.7	7.8	24.3	592.81	13.41
G27	382.7	2912.4	1.39	0.1050	0.0012	0.9983	0.0119	0.0687	0.0007	643.5	13.4	703.0	15.6	890.9	20.1	8.5	27.8	643.47	13.42
G101	35.5	358.5	0.07	0.1053	0.0013	0.9610	0.0162	0.0667	0.0009	645.3	14.8	683.8	18.5	827.2	23.2	5.6	22.0	645.34	14.81
G88	49.3	455.1	0.24	0.1102	0.0013	0.1030	0.0154	0.0685	0.0009	674.1	15.0	719.4	17.9	882.2	22.3	6.3	23.6	674.08	14.98
G22	27.5	248.2	0.22	0.1110	0.0013	0.1043	0.0175	0.0683	0.0010	678.6	14.9	724.5	18.8	878.9	23.6	6.3	22.8	678.55	14.85
G80	23.9	200.8	0.38	0.1141	0.0014	1.0757	0.0189	0.0671	0.0010	696.7	15.9	741.6	19.5	841.5	23.7	6.0	17.2	696.69	15.85
G42	33.3	284.1	0.30	0.1148	0.0013	1.1031	0.0174	0.0701	0.0009	700.3	15.3	754.8	18.5	929.8	23.1	7.2	24.7	700.28	15.27
G39	47.3	386.7	0.43	0.1148	0.0013	1.1240	0.0167	0.0691	0.0009	700.3	15.2	764.9	17.9	902.3	22.2	8.4	22.4	700.28	15.15
G24	89.8	818.0	0.09	0.1157	0.0013	1.0734	0.0144	0.0685	0.0008	705.5	14.9	740.4	17.0	884.0	20.9	4.7	20.2	705.48	14.91
G89	41.5	348.6	0.28	0.1176	0.0014	1.0833	0.0168	0.0665	0.0009	716.5	16.0	745.2	18.5	821.2	21.9	3.9	12.8	716.50	16.04
G6	138.9	1078.4	0.51	0.1194	0.0013	1.1763	0.0148	0.0714	0.0008	727.0	15.0	789.6	17.0	967.5	21.1	7.9	24.9	726.99	14.97
G32	84.8	738.6	0.08	0.1215	0.0014	1.1076	0.0148	0.0654	0.0008	739.4	15.6	757.0	17.1	787.9	20.0	2.3	6.1	739.42	15.63
G1	107.8	785.5	0.59	0.1220	0.0013	1.0936	0.0144	0.0647	0.0007	741.9	15.3	750.3	16.7	764.9	12.3	1.1	3.0	741.89	15.28
G12	82.6	654.7	0.30	0.1225	0.0014	1.2925	0.0172	0.0721	0.0008	745.0	15.5	842.4	17.7	989.0	21.7	11.6	24.7	744.99	15.51
G13	97.6	794.9	0.20	0.1253	0.0014	1.2614	0.0162	0.0734	0.0008	760.7	15.8	828.5	17.8	1024.5	21.7	8.2	25.7	760.71	15.81
G15	109.9	794.3	0.55	0.1253	0.0014	1.2549	0.0167	0.0716	0.0008	761.0	15.9	825.6	17.9	973.7	21.6	7.8	21.8	761.00	15.93
G38	141.6	1115.9	0.23	0.1285	0.0014	1.3131	0.0171	0.0731	0.0008	779.2	16.3	851.5	18.1	1017.3	21.7	8.5	23.4	779.19	16.34
G16	92.3	519.6	1.45	0.1298	0.0014	1.3085	0.0178	0.0743	0.0009	786.8	16.4	849.4	18.6	1048.3	22.4	7.4	24.9	786.84	16.43
G51	109.8	870.4	0.13	0.1305	0.0015	1.2763	0.0173	0.0711	0.0008	790.7	16.9	835.2	18.6	961.2	21.8	5.3	17.7	790.72	16.88
G71	17.6	116.9	0.61	0.1342	0.0016	1.2859	0.0253	0.0687	0.0011	811.7	18.6	839.5	22.4	890.3	25.6	3.3	8.8	811.72	18.64
G84	98.4	752.9	0.09	0.1377	0.0016	1.3893	0.0195	0.0727	0.0009	831.8	18.1	884.4	19.6	1005.6	22.6	6.0	17.3	831.76	18.13
G21	90.7	659.7	0.23	0.1390	0.0015	1.3411	0.0175	0.0696	0.0008	839.0	17.4	863.7	18.3	915.4	20.8	2.9	8.3	839.01	17.43
G97	76.2	403.2	1.35	0.1392	0.0017	1.3591	0.0210	0.0711	0.0009	840.0	18.7	871.5	20.4	958.9	23.2	3.6	12.4	840.02	18.67
G63	200.2	1502.6	0.09	0.1393	0.0016	1.4488	0.0185	0.0745	0.0008	840.6	17.8	909.4	18.9	1054.8	21.9	7.6	20.3	840.65	17.77
G43	101.3	756.8	0.10	0.1398	0.0016	1.3687	0.0185	0.0697	0.0008	843.8	17.8	875.6	18.8	920.4	21.3	3.6	8.3	843.76	17.76
G82	55.0	348.6	0.71	0.1400	0.0016	1.4301	0.0220	0.0731	0.0009	844.8	18.5	901.6	20.6	1016.4	23.6	6.3	16.9	844.83	18.55
G8	71.2	509.7	0.23	0.1406	0.0016	1.3852	0.0197	0.0715	0.0009	848.0	17.6	882.7	19.2	972.3	22.2	3.9	12.8	848.00	17.63
G86	31.3	225.6	0.19	0.1406	0.0017	1.4306	0.0244	0.0719	0.0010	848.1	19.0	901.8	21.4	982.3	24.5	6.0	13.7	848.05	18.99
G36	108.5	803.1	0.12	0.1409	0.0016	1.3355	0.0177	0.0686	0.0008	849.6	17.7	861.3	18.5	887.0	20.7	1.4	4.2	849.64	17.74
G65	73.4	486.5	0.42	0.1420	0.0016	1.3696	0.0196	0.0701	0.0008	856.1	18.4	876.0	19.5	931.3	21.9	2.3	8.1	856.07	18.40
G74	24.1	134.6	1.02	0.1440	0.0017	1.4649	0.0272	0.0737	0.0011	867.4	19.6	916.0	22.8	1033.8	26.1	5.3	16.1	867.41	19.61
G19	28.6	187.0	0.42	0.1445	0.0018	1.4100	0.0299	0.0693	0.0011	870.1	19.7	893.1	23.6	908.0	26.5	2.6	4.2	870.12	19.71
G91	13.3	79.4	0.72	0.1453	0.0019	1.4612	0.0339	0.0743	0.0013	874.5	21.2	914.5	26.3	1049.6	30.0	4.4	16.7	874.45	21.16
G99	91.9	642.6	0.11	0.1489	0.0018	1.4431	0.0207	0.0708	0.0009	894.8	19.6	907.0	20.3	952.5	22.3	1.3	6.1	894.79	19.64
G37	25.0	171.5	0.15	0.1496	0.0018	1.5707	0.0300	0.0715	0.0010	898.7	20.0	958.7	22.7	971.2	25.5	6.3	7.5	898.72	19.96
G33	40.2	222.3	0.39	0.1719	0.0020	1.7956	0.0288	0.0737	0.0009	1022.7	21.7</td								

Table 2. U-Pb zircon ages of Zanskar River sands

G48	76.8	410.4	0.40	0.1781	0.0020	2.0112	0.0288	0.0812	0.0010	1056.3	22.1	1119.3	22.0	1226.5	23.9	5.6	13.9	1226.53	23.94
G50	69.7	228.4	0.33	0.2948	0.0034	4.2117	0.0610	0.1035	0.0012	1665.7	33.4	1676.3	26.4	1686.9	26.1	0.6	1.3	1686.92	26.05
G94	68.4	230.6	0.52	0.2725	0.0032	3.9588	0.0633	0.1063	0.0013	1553.3	32.6	1625.8	27.7	1736.9	27.8	4.5	10.6	1736.91	27.79
G53	32.9	128.5	0.04	0.2593	0.0030	3.8261	0.0583	0.1065	0.0013	1486.2	30.4	1598.2	26.4	1739.7	26.8	7.0	14.6	1739.67	26.83
G45	111.7	314.4	0.78	0.2978	0.0034	4.7648	0.0746	0.1114	0.0013	1680.6	33.9	1778.7	27.2	1822.4	27.0	5.5	7.8	1822.38	27.05
G20	338.6	1143.5	0.43	0.2741	0.0030	4.2685	0.0516	0.1114	0.0012	1561.7	30.4	1687.3	25.0	1822.5	25.2	7.4	14.3	1822.54	25.22
G35	101.9	309.4	0.64	0.2896	0.0033	4.6379	0.0677	0.1138	0.0013	1639.4	32.7	1756.1	26.6	1861.6	26.6	6.6	11.9	1861.60	26.62
G46	95.8	248.2	0.85	0.3235	0.0037	5.6932	0.0866	0.1240	0.0014	1806.8	35.9	1930.3	27.8	2015.0	27.3	6.4	10.3	2014.99	27.34
G72	174.7	381.7	0.56	0.4071	0.0047	8.7691	0.1267	0.1557	0.0018	2201.8	42.8	2314.3	29.3	2409.2	28.1	4.9	8.6	2409.16	28.11
G100	50.6	78.3	0.84	0.5349	0.0067	15.6263	0.3583	0.2184	0.0028	2762.2	56.4	2854.2	34.3	2968.6	31.9	3.2	7.0	2968.56	31.93
G30	57.9	690.6	0.25	0.0861	0.0010	0.8222	0.0113	0.0683	0.0008	532.5	11.5	609.3	15.0	876.8	21.4	12.6	39.3	532.55	11.51
G90	49.0	511.3	0.39	0.0924	0.0011	0.9147	0.0145	0.0703	0.0009	569.4	13.0	659.6	17.2	936.3	23.6	13.7	39.2	569.42	12.98
G73	97.5	787.7	0.11	0.1299	0.0015	1.4708	0.0203	0.0814	0.0010	787.1	17.0	918.5	19.8	1230.2	24.1	14.3	36.0	787.12	17.00
G31	18.2	151.1	0.81	0.1033	0.0012	1.0500	0.0204	0.0717	0.0011	633.7	14.5	728.9	20.2	976.0	26.9	13.1	35.1	633.66	14.49
G96	15.6	115.8	1.07	0.1143	0.0015	1.1867	0.0252	0.0749	0.0013	697.4	16.8	794.4	23.0	1065.8	29.3	12.2	34.6	697.44	16.78
G67	114.5	1171.6	0.36	0.0955	0.0011	0.9019	0.0120	0.0688	0.0008	587.8	12.8	652.8	15.7	891.2	21.1	10.0	34.0	587.81	12.83
G5	89.8	1171.6	0.10	0.0819	0.0009	0.7289	0.0092	0.0648	0.0007	507.6	10.6	555.9	13.4	766.2	19.4	8.7	33.8	507.57	10.61
G52	41.4	359.6	0.56	0.1022	0.0012	0.9710	0.0150	0.0695	0.0009	627.3	13.8	689.0	17.5	913.3	23.1	9.0	31.3	627.29	13.80
G54	126.0	989.0	0.64	0.1159	0.0013	1.1642	0.0157	0.0733	0.0009	706.9	15.1	783.9	17.7	1023.1	22.2	9.8	30.9	706.92	15.14

Sample 13072302 Gata

Grain No.	Pb (ppm)	U (ppm)	Atomic Th/U	Ratios				Ages (Ma)					% concord. (206/238)		% concord. (206/238)		Best Age (Ma)	± 2σ	
				$^{206}\text{Pb}/^{238}\text{U}$	± 1 σ	$^{207}\text{Pb}/^{235}\text{U}$	± s.e.	$^{207}\text{Pb}/^{206}\text{Pb}$	± s.e.	$^{206}\text{Pb}/^{238}\text{U}$	± 2σ	$^{207}\text{Pb}/^{235}\text{U}$	± 2σ	$^{207}\text{Pb}/^{206}\text{Pb}$	± 2σ				
G82	137.8	2113.9	0.28	0.0649	0.0008	0.5818	0.0123	0.0649	0.0012	405.2	9.9	465.6	16.6	772.1	20.3	13.0	47.5	405.24	9.93
G75	42.1	591.1	0.10	0.0759	0.0010	0.5965	0.0167	0.0576	0.0014	471.7	11.9	475.0	20.6	513.8	19.5	0.7	8.2	471.66	11.86
G92	36.0	317.9	1.57	0.0807	0.0011	0.6368	0.0201	0.0590	0.0016	500.1	12.9	500.3	24.0	567.8	23.6	0.0	11.9	500.12	12.88
G17	17.3	153.0	1.43	0.0820	0.0012	0.6392	0.0258	0.0562	0.0019	508.0	13.8	501.8	28.9	461.5	25.5	-1.2	-10.1	508.05	13.82
G56	30.3	311.5	0.82	0.0822	0.0011	0.6410	0.0194	0.0571	0.0015	509.1	13.0	502.9	22.9	495.0	20.4	-1.2	-2.9	509.12	12.99
G117	27.1	286.0	0.75	0.0826	0.0012	0.6613	0.0252	0.0589	0.0019	511.7	13.9	515.4	28.3	562.3	27.9	0.7	9.0	511.68	13.93
G29	109.9	1247.8	0.45	0.0828	0.0010	0.6481	0.0125	0.0574	0.0009	512.9	12.3	507.3	16.5	505.8	13.5	-1.1	-1.4	512.93	12.26
G110	21.6	235.0	0.61	0.0829	0.0011	0.6390	0.0226	0.0572	0.0017	513.4	13.6	501.7	26.2	497.3	23.7	-2.3	-3.2	513.41	13.57
G39	13.4	122.0	1.23	0.0837	0.0012	0.6618	0.0301	0.0566	0.0021	517.9	14.8	515.7	32.6	476.0	29.2	-0.4	-8.8	517.93	14.75
G125	52.7	601.1	0.40	0.0838	0.0011	0.6542	0.0178	0.0575	0.0013	518.6	13.0	511.1	21.5	509.6	19.0	-1.5	-1.8	518.59	12.97
G34	13.7	147.5	0.57	0.0845	0.0012	0.6717	0.0267	0.0578	0.0019	522.6	14.3	521.8	29.4	523.3	27.5	-0.2	0.1	522.63	14.27
G70	45.3	470.0	0.59	0.0852	0.0011	0.6878	0.0179	0.0596	0.0013	527.3	13.1	531.5	21.2	587.6	19.9	0.8	10.3	527.26	13.07
G66	24.2	249.6	0.66	0.0858	0.0012	0.6989	0.0231	0.0597	0.0016	530.7	13.8	538.1	25.6	593.1	25.0	1.4	10.5	530.71	13.77
G43	14.9	163.9	0.40	0.0863	0.0012	0.7022	0.0268	0.0595	0.0019	533.6	14.4	540.1	29.0	586.2	28.4	1.2	9.0	533.56	14.36
G42	47.1	573.8	0.10	0.0864	0.0011	0.6949	0.0164	0.0585	0.0012	534.0	13.1	535.8	19.7	548.5	17.3	0.3	2.6	534.03	13.05
G84	41.8	461.8	0.37	0.0874	0.0011	0.6942	0.0185	0.0582	0.0013	540.2	13.4	535.3	21.6	537.3	19.1	-0.9	-0.5	540.20	13.40
G102	9.1	92.0	0.66	0.0883	0.0014	0.7177	0.0359	0.0616	0.0025	545.6	16.2	549.3	38.2	661.3	40.4	0.7	17.5	545.59	16.23
G1	111.2	1104.8	0.69	0.0888	0.0011	0.7158	0.0138	0.0593	0.0010	548.4	13.0	548.2	17.4	578.9	14.3	0.0	5.3	548.44	13.03
G101	36.7	398.9	0.21	0.0933	0.0012	0.7565	0.0213	0.0598	0.0014	575.1	14.4	572.0	23.7	597.4	21.6	-0.5	3.7	575.08	14.39
G108	28.8	279.6	0.60	0.0934	0.0013	0.7225	0.0229	0.0584	0.0015	575.7	14.7	552.1	25.8	545.5	22.7	-4.3	-5.5	575.73	14.74
G28	44.1	459.9	0.25	0.0970	0.0013	0.8668	0.0290	0.0651	0.0017	596.9	15.5	633.8	28.3	778.9	29.5	5.8	23.4	596.92	15.51
G120	8.8	96.5	0.07	0.0973	0.0015	0.7846	0.0380	0.0612	0.0024	598.3	17.4	588.1	38.6	647.3	38.1	-1.7	7.6	598.33	17.39
G45	91.2	725.0	0.32	0.1238	0.0016	1.1436	0.0261	0.0691	0.0013	752.2	18.0	774.2	24.4	902.9	22.3	2.8	16.7	752.23	18.01
G111	121.7	866.1	0.75	0.1249	0.0016	1.1078	0.0286	0.0669	0.0014	758.7	18.5	757.1	26.7	834.0	24.3	-0.2	9.0	758.71	18.45
G118	89.8	643.0	0.49	0.1303	0.0017	1.3081	0.0406	0.0737	0.0018	789.3	19.8	849.3	31.8	1033.3	31.6	7.1	23.6	789.35	19.85
G54	55.0	363.4	0.77	0.1305	0.0017	1.1759	0.0304	0.0653	0.0013	790.8	19.0	789.4	26.2	783.4	22.5	-0.2	-0.9	790.77	19.05
G72	127.1	832.5	0.74	0.1330	0.0017	1.2840	0.0268	0.0703	0.0012	805.0	19.0	838.6	24.1	936.8	21.2	4.0	14.1	805.01	19.00
G55	11.1	69.2	1.30	0.1334	0.0020	1.3684	0.0672	0.0768	0.0027	807.0	23.2	875.5	46.0	1115.7	48.6	7.8	27.7	807.01	23.21
G62	132.7	1023.7	0.34	0.1334	0.0017	1.3783	0.0270	0.0732	0.0012	807.5	18.9	879.7	23.6	1018.1	21.0	8.2	20.7	807.46	18.88
G80	13.0	95.6	0.32	0.1346	0.0021	1.312													

Table 2. U-Pb zircon ages of Zanskar River sands

G8	18.3	118.4	0.36	0.1492	0.0021	1.4232	0.0528	0.0709	0.0019	896.2	23.0	898.7	36.4	954.0	33.8	0.3	6.1	896.20	23.00
G21	96.7	603.8	0.46	0.1493	0.0019	1.4432	0.0300	0.0709	0.0012	896.9	20.9	907.0	24.6	955.4	20.5	1.1	6.1	896.93	20.87
G115	17.6	120.2	0.15	0.1500	0.0022	1.4418	0.0648	0.0693	0.0023	901.1	24.6	906.5	42.8	906.5	39.6	0.6	0.6	906.49	39.59
G33	67.0	425.3	0.36	0.1514	0.0019	1.4338	0.0334	0.0695	0.0012	908.8	21.4	903.2	26.3	912.4	22.0	-0.6	0.4	912.43	21.95
G52	42.9	210.4	0.95	0.1675	0.0022	1.5531	0.0456	0.0695	0.0015	998.4	24.2	951.7	31.6	914.5	26.5	-4.9	-9.2	914.51	26.47
G116	60.1	366.1	0.32	0.1598	0.0021	1.4868	0.0397	0.0697	0.0015	955.7	23.0	925.0	30.3	920.1	25.8	-3.3	-3.9	920.12	25.80
G98	145.2	977.3	0.15	0.1529	0.0019	1.4634	0.0311	0.0699	0.0012	917.0	21.5	915.4	26.0	925.7	21.7	-0.2	0.9	925.71	21.66
G13	70.4	403.5	0.52	0.1603	0.0020	1.4977	0.0340	0.0700	0.0012	958.6	22.4	929.4	26.4	927.2	21.5	-3.1	-3.4	927.18	21.49
G122	31.2	172.1	0.69	0.1586	0.0022	1.5077	0.0519	0.0700	0.0018	949.0	23.9	933.5	35.7	928.4	31.7	-1.7	-2.2	928.35	31.75
G126	24.7	122.0	0.94	0.1659	0.0023	1.5791	0.0616	0.0702	0.0020	989.3	25.5	962.0	39.5	933.6	35.1	-2.8	-6.0	933.62	35.08
G114	39.2	226.8	0.38	0.1653	0.0022	1.5412	0.0471	0.0707	0.0016	986.3	24.2	947.0	33.5	947.3	29.1	-4.2	-4.1	947.30	29.05
G91	65.5	405.3	0.25	0.1609	0.0021	1.5963	0.0401	0.0709	0.0014	961.5	22.9	968.8	28.9	955.4	24.5	0.8	-0.6	955.40	24.55
G49	52.5	313.3	0.19	0.1698	0.0022	1.6334	0.0413	0.0710	0.0013	1011.0	23.9	983.2	28.9	957.1	23.9	-2.8	-5.6	957.13	23.86
G103	64.4	289.6	1.17	0.1749	0.0023	1.6576	0.0492	0.0711	0.0016	1039.1	25.2	992.5	33.1	960.9	28.1	-4.7	-8.1	960.86	28.06
G85	12.9	73.8	0.47	0.1630	0.0024	1.6071	0.0753	0.0715	0.0024	973.4	26.6	973.0	45.1	972.6	41.6	0.0	-0.1	972.60	41.58
G14	71.2	383.4	0.73	0.1609	0.0020	1.5719	0.0369	0.0718	0.0013	961.9	22.5	959.2	27.1	978.9	22.7	-0.3	1.7	978.86	22.70
G106	36.1	205.8	0.32	0.1714	0.0024	1.6447	0.0649	0.0718	0.0020	1020.0	26.4	987.5	40.3	981.1	36.0	-3.3	-4.0	981.13	36.01
G124	74.1	492.7	0.05	0.1597	0.0021	1.5376	0.0389	0.0718	0.0015	955.1	22.8	945.5	29.8	981.4	25.9	-1.0	2.7	981.41	25.85
G27	96.9	654.8	0.26	0.1524	0.0019	1.4822	0.0300	0.0719	0.0012	914.2	21.3	923.1	24.8	983.4	20.6	1.0	7.0	983.39	20.60
G76	124.0	732.3	0.36	0.1626	0.0020	1.5552	0.0338	0.0719	0.0012	971.4	22.6	952.6	26.7	984.2	22.2	-2.0	1.3	984.24	22.18
G11	70.9	427.2	0.44	0.1558	0.0020	1.5309	0.0345	0.0721	0.0012	933.3	21.9	942.9	26.3	989.0	22.2	1.0	5.6	989.05	22.19
G36	91.6	629.3	0.12	0.1526	0.0019	1.4859	0.0304	0.0722	0.0012	915.5	21.3	924.6	24.9	991.9	20.8	1.0	7.7	991.87	20.80
G64	93.5	653.9	0.03	0.1528	0.0019	1.4945	0.0348	0.0722	0.0013	916.4	21.6	928.2	27.1	991.9	23.4	1.3	7.6	991.87	23.43
G113	77.8	405.3	0.81	0.1652	0.0021	1.5854	0.0407	0.0723	0.0015	985.8	23.6	964.5	30.3	993.3	26.1	-2.2	0.7	993.27	26.06
G131	55.8	339.7	0.19	0.1662	0.0022	1.6300	0.0451	0.0723	0.0016	990.9	23.9	981.8	31.9	994.1	27.8	-0.9	0.3	994.12	27.82
G63	185.1	1020.1	0.57	0.1632	0.0020	1.6280	0.0315	0.0724	0.0011	974.7	22.5	981.1	25.1	998.3	20.3	0.6	2.4	998.33	20.29
G26	97.2	619.3	0.22	0.1576	0.0020	1.5496	0.0317	0.0725	0.0012	943.6	21.8	950.3	25.2	998.6	20.8	0.7	5.5	998.61	20.81
G10	20.7	120.2	0.72	0.1504	0.0021	1.4731	0.0532	0.0725	0.0019	903.1	23.0	919.4	35.9	1001.1	33.6	1.8	9.8	1001.13	33.63
G41	96.6	465.4	0.91	0.1709	0.0021	1.6729	0.0370	0.0725	0.0012	1017.0	23.6	998.3	27.0	1001.1	22.0	-1.9	-1.6	1001.13	22.05
G25	19.3	85.6	1.25	0.1723	0.0024	1.7274	0.0705	0.0730	0.0021	1024.9	26.5	1018.8	40.6	1014.5	36.7	-0.6	-1.0	1014.51	36.65
G57	37.3	232.2	0.41	0.1518	0.0020	1.4928	0.0425	0.0731	0.0016	911.1	22.2	927.4	30.6	1017.6	27.7	1.8	10.5	1017.56	27.70
G77	48.7	222.2	1.17	0.1693	0.0022	1.6625	0.0480	0.0734	0.0016	1008.0	24.4	994.3	32.1	1024.5	28.1	-1.4	1.6	1024.47	28.07
G112	54.0	303.3	0.33	0.1727	0.0022	1.7072	0.0473	0.0735	0.0016	1026.8	24.6	1011.2	32.0	1026.4	27.7	-1.5	0.0	1026.39	27.72
G68	41.1	260.5	0.30	0.1560	0.0020	1.5622	0.0434	0.0736	0.0015	934.3	22.5	955.4	30.5	1031.3	27.4	2.2	9.4	1031.34	27.37
G6	230.1	1347.0	0.31	0.1675	0.0021	1.7270	0.0317	0.0738	0.0011	998.2	22.7	1018.6	24.3	1035.5	19.3	2.0	3.6	1035.46	19.29
G121	109.0	560.1	0.59	0.1754	0.0022	1.7681	0.0431	0.0739	0.0014	1041.6	24.6	1033.8	30.2	1039.8	25.6	-0.8	-0.2	1039.83	25.63
G47	85.0	445.4	0.34	0.1843	0.0023	1.8564	0.0419	0.0746	0.0013	1090.5	25.3	1065.7	28.1	1058.8	22.8	-2.3	-3.0	1058.82	22.83
G100	156.2	1059.2	0.04	0.1570	0.0020	1.6431	0.0374	0.0748	0.0014	940.1	22.2	986.9	27.8	1063.1	24.4	4.7	11.6	1063.13	24.42
G24	90.1	505.5	0.63	0.1585	0.0020	1.6584	0.0363	0.0751	0.0013	948.4	22.1	992.7	26.3	1072.0	22.5	4.5	11.5	1071.98	22.49
G3	78.4	407.1	0.38	0.1841	0.0023	1.8607	0.0408	0.0753	0.0012	1089.4	25.0	1067.2	27.4	1076.0	22.1	-2.1	-1.3	1075.99	22.14
G19	68.8	383.4	0.14	0.1836	0.0023	1.9126	0.0430	0.0753	0.0013	1086.5	25.1	1085.5	27.8	1076.3	22.7	-0.1	-1.0	1076.25	22.67
G40	132.4	795.1	0.29	0.1632	0.0020	1.7109	0.0334	0.0754	0.0012	974.4	22.4	1012.6	25.2	1079.5	20.9	3.8	9.7	1079.45	20.91
G35	55.9	269.6	0.62	0.1843	0.0024	1.9137	0.0492	0.0757	0.0014	1090.6	25.6	1085.9	30.2	1086.4	25.3	-0.4	-0.4	1086.35	25.32
G58	67.3	415.3	0.13	0.1669	0.0021	1.8678	0.0456	0.0757	0.0014	995.1	23.3	1069.7	28.2	1088.2	24.3	7.0	8.6	1088.21	24.26
G90	40.0	199.5	0.45	0.1871	0.0025	1.9788	0.0608	0.0758	0.0017	1105.4	26.7	1108.3	34.5	1089.3	29.9	0.3	-1.5	1089.26	29.90
G109	148.6	868.0	0.16	0.1775	0.0022	1.8397	0.0405	0.0759	0.0014	1053.1	24.5	1059.7	28.9	1093.2	24.4	0.6	3.7	1093.23	24.44
G50	35.9	152.1	0.94	0.1922	0.0025	1.9410	0.0617	0.0760	0.0017	1133.2	27.5	1095.3	35.1	1096.1	30.3	-3.5	-3.4	1096.12	30.26
G12	166.5	654.8	1.49	0.1830	0.0023	1.8929	0.0375	0.0761	0.0012	1083.3	24.7	1078.6	26.2	1096.4	20.9	-0.4	1.2	1096.39	20.91
G65	33.0	175.8	0.17	0.1902	0.0025	1.9567	0.0597	0.0768	0.0017	1122.6	27.1	1100.7	34.2	1116.8	29.6	-2.0	-0.5	1116.78	29.55
G18	66.2	318.8	0.59	0.1863	0.0024	1.8639	0.0439	0.0771	0.0013	1101.0	25.5	1068.4	29.0	1123.3	24.1	-3.1	2.0	1123.26	24.08
G132	44.6	213.1	0.41	0.1968	0.0000	2.0138	0.0000	0.0773	0.0000	1157.8	0.0	1120.2	0.0	1128.2	0.5	-3.4	-2.6	1128.17	0.46
G74	51.7	265.0	0.48	0.1815	0.0024	1.9403	0.0615	0.0774	0.0017	1075.3	26.2	1095.1	34.8	1130.7	31.0	1.8	4.9	1130.74	30.96
G107	26.7	123.9	0.51	0.1979	0.0027	2.0316	0.0729	0.0774	0.0019	1164.2	29.0	1126.1	39.3	1131.0	34.7	-3.4	-2.9	1131.00	34.66
G20	78.5	318.8	1.05	0.1959	0.0025	2.0257	0.0485	0.0775	0.0014	1153.1	26.6	1124.2	29.5	1134.9	24.3	-2.6	-1.6	1134.86	24.25
G48	36.8	188.5	0.17	0.1976	0.0026	2.09													

Table 2. U-Pb zircon ages of Zanskar River sands

G96	55.6	240.4	0.45	0.2161	0.0028	2.4717	0.0693	0.0835	0.0017	1261.2	29.7	1263.8	34.5	1280.7	29.6	0.2	1.5	1280.70	29.57
G46	105.4	439.9	0.50	0.2207	0.0028	2.5343	0.0551	0.0840	0.0014	1285.5	29.2	1281.9	29.7	1292.1	24.0	-0.3	0.5	1292.09	23.96
G32	74.1	322.4	0.54	0.2163	0.0027	2.4618	0.0572	0.0846	0.0014	1262.5	28.8	1260.9	30.4	1306.6	25.0	-0.1	3.4	1306.62	24.95
G88	59.5	231.3	0.41	0.2408	0.0031	2.8470	0.0786	0.0871	0.0017	1391.1	32.3	1368.0	34.9	1361.8	29.2	-1.7	-2.1	1361.82	29.22
G81	88.6	345.2	0.47	0.2360	0.0030	2.8047	0.0675	0.0876	0.0015	1366.0	31.2	1356.8	32.4	1373.9	26.8	-0.7	0.6	1373.95	26.76
G129	74.1	314.2	0.33	0.2273	0.0030	2.7458	0.0831	0.0886	0.0019	1320.3	31.4	1340.9	37.7	1396.0	33.2	1.5	5.4	1395.96	33.16
G71	154.5	628.4	0.21	0.2443	0.0030	2.8859	0.0593	0.0889	0.0014	1409.1	31.5	1378.2	30.6	1401.1	24.4	-2.2	-0.6	1401.14	24.40
G73	61.3	198.5	0.42	0.2859	0.0037	3.9407	0.1078	0.1013	0.0018	1621.1	36.8	1622.1	35.9	1648.6	29.7	0.1	1.7	1648.62	29.74
G86	138.9	463.6	0.51	0.2709	0.0034	3.7472	0.0823	0.1033	0.0017	1545.3	34.5	1581.5	33.3	1684.6	27.4	2.3	8.3	1684.60	27.35
G2	20.0	92.0	2.00	0.3064	0.0040	4.4223	0.1525	0.1046	0.0020	1722.7	39.9	1716.5	39.0	1706.6	32.7	-0.4	-0.9	1706.59	32.70
G130	153.6	452.7	0.51	0.3054	0.0039	4.3168	0.1058	0.1048	0.0019	1718.1	38.4	1696.6	37.2	1710.1	31.1	-1.3	-0.5	1710.11	31.09
G95	66.6	172.1	0.73	0.3269	0.0043	4.6140	0.1457	0.1052	0.0021	1823.2	41.6	1751.8	39.6	1717.8	33.1	-4.1	-6.1	1717.81	33.06
G60	207.8	704.0	0.48	0.2732	0.0034	4.0368	0.0784	0.1090	0.0016	1557.0	34.3	1641.6	31.5	1782.8	25.3	5.2	12.7	1782.77	25.27
G61	1116.8	1766.9	4.46	0.2826	0.0035	4.2744	0.0742	0.1096	0.0016	1604.5	35.0	1688.4	30.9	1793.3	24.3	5.0	10.5	1793.27	24.26
G89	110.8	322.4	0.23	0.3335	0.0042	5.1707	0.1241	0.1153	0.0019	1855.4	40.7	1847.8	35.8	1884.9	29.1	-0.4	1.6	1884.89	29.13
G69	202.3	619.3	0.32	0.3125	0.0039	5.2346	0.1127	0.1230	0.0019	1752.9	38.3	1858.3	33.8	2000.6	27.3	5.7	12.4	2000.63	27.31
G59	105.1	253.2	0.44	0.3750	0.0047	6.4729	0.1572	0.1269	0.0020	2052.8	44.3	2042.2	35.3	2055.0	28.0	-0.5	0.1	2055.05	27.96
G23	363.1	742.3	0.67	0.4133	0.0051	8.2587	0.1620	0.1448	0.0020	2230.0	46.4	2259.8	33.2	2284.8	25.1	1.3	2.4	2284.81	25.06
G123	231.4	466.3	0.25	0.4606	0.0058	9.7505	0.2280	0.1588	0.0028	2442.4	51.4	2411.5	39.6	2442.9	32.5	-1.3	0.0	2442.92	32.45
G128	204.9	385.3	0.52	0.4632	0.0059	9.9470	0.2410	0.1621	0.0029	2453.8	51.8	2429.9	40.3	2477.5	33.3	-1.0	1.0	2477.48	33.28
G105	77.9	159.4	0.22	0.4610	0.0059	10.4876	0.3060	0.1696	0.0030	2443.9	52.4	2478.8	40.6	2553.2	33.4	1.4	4.3	2553.21	33.37
G7	91.0	186.7	0.71	0.4185	0.0053	9.7511	0.2464	0.1730	0.0025	2253.6	47.8	2411.5	35.4	2587.0	27.5	6.5	12.9	2586.98	27.51
G83	77.1	131.2	0.42	0.5120	0.0066	12.1414	0.3659	0.1763	0.0029	2665.1	56.1	2615.4	39.5	2618.2	31.7	-1.9	-1.8	2618.18	31.65
G15	541.6	1083.8	0.32	0.4637	0.0057	11.5136	0.1930	0.1787	0.0023	2455.8	49.9	2565.7	33.0	2640.7	24.6	4.3	7.0	2640.75	24.55
G5	317.5	567.4	0.47	0.4922	0.0060	11.9942	0.2240	0.1813	0.0024	2580.2	52.2	2604.0	33.6	2664.7	25.0	0.9	3.2	2664.71	24.98
G104	108.1	156.7	0.32	0.5783	0.0074	15.0883	0.4439	0.1939	0.0033	2941.8	60.6	2820.8	40.7	2775.5	32.9	-4.3	-6.0	2775.53	32.87
G127	56.6	95.6	0.38	0.5284	0.0070	13.9350	0.4889	0.2011	0.0038	2734.5	59.0	2745.3	44.2	2835.1	36.9	0.4	3.5	2835.06	36.86
G22	272.8	399.8	0.54	0.5800	0.0072	18.5942	0.3794	0.2303	0.0030	2948.7	58.3	3021.0	34.7	3054.1	25.9	2.4	3.5	3054.13	25.86
G4	19.3	148.5	1.39	0.0962	0.0013	0.9661	0.0346	0.0753	0.0021	592.0	15.8	686.5	31.9	1076.0	37.8	13.8	45.0	592.04	15.76
G97	27.2	272.3	0.35	0.0975	0.0014	0.7515	0.0272	0.0577	0.0017	599.9	15.9	569.1	29.0	518.0	24.5	-5.4	-15.8	599.92	15.86

Sample 14080609 Yunanm

Grain No.	Pb (ppm)	U (ppm)	Atomic Th/U	Ratios				Ages (Ma)				% concord. (206/238)		% concord. (206/238)		Best Age (Ma)	$\pm 2\sigma$		
				$^{206}\text{Pb}/^{238}\text{U}$	$\pm 1\sigma$	$^{207}\text{Pb}/^{235}\text{U}$	$\pm \text{s.e.}$	$^{207}\text{Pb}/^{206}\text{Pb}$	$\pm \text{s.e.}$	$^{206}\text{Pb}/^{238}\text{U}$	$\pm 2\sigma$	$^{207}\text{Pb}/^{235}\text{U}$	$\pm 2\sigma$	$^{207}\text{Pb}/^{206}\text{Pb}$	$\pm 2\sigma$				
G26	141.4	2026.5	0.20	0.0712	0.0009	0.5892	0.0092	0.0601	0.0009	443.3	10.2	470.3	14.2	605.4	13.4	5.7	26.8	443.32	10.23
G103	41.3	471.5	1.09	0.0727	0.0009	0.5694	0.0124	0.0568	0.0012	452.5	11.1	457.6	18.3	483.8	16.4	1.1	6.5	452.52	11.06
G93	49.1	546.0	1.09	0.0742	0.0009	0.5846	0.0117	0.0572	0.0011	461.3	11.2	467.4	17.3	498.1	15.3	1.3	7.4	461.29	11.16
G114	20.7	268.0	0.36	0.0752	0.0010	0.5859	0.0142	0.0566	0.0014	467.1	11.8	468.2	20.4	474.4	18.1	0.2	1.5	467.11	11.75
G15	78.9	965.3	0.34	0.0798	0.0010	0.6513	0.0113	0.0592	0.0010	494.7	11.5	509.2	16.4	575.6	14.5	2.8	14.0	494.75	11.46
G78	24.7	227.3	1.36	0.0799	0.0010	0.6308	0.0151	0.0573	0.0014	495.7	12.3	496.6	21.1	501.2	18.7	0.2	1.1	495.70	12.30
G17	37.9	403.2	0.73	0.0823	0.0010	0.6534	0.0131	0.0576	0.0011	509.8	12.2	510.6	18.5	514.6	15.7	0.1	0.9	509.84	12.15
G95	27.2	262.6	1.01	0.0839	0.0011	0.6494	0.0153	0.0561	0.0013	519.6	12.8	508.1	21.2	457.1	17.1	-2.3	-13.7	519.60	12.85
G74	9.3	104.4	0.45	0.0842	0.0012	0.6667	0.0207	0.0575	0.0018	520.8	13.8	518.7	27.7	510.0	25.0	-0.4	-2.1	520.85	13.79
G53	134.1	1269.4	1.06	0.0849	0.0010	0.6800	0.0111	0.0581	0.0009	525.5	12.2	526.8	16.1	532.8	12.7	0.2	1.4	525.48	12.24
G33	54.2	585.1	0.58	0.0851	0.0011	0.7091	0.0151	0.0605	0.0013	526.2	12.7	544.2	20.5	620.8	19.4	3.3	15.2	526.20	12.71
G50	60.8	497.6	1.73	0.0854	0.0011	0.6879	0.0131	0.0584	0.0011	528.2	12.5	531.6	18.3	546.3	15.5	0.6	3.3	528.22	12.47
G32	44.3	185.8	1.78	0.0855	0.0011	0.6800	0.0168	0.0577	0.0014	529.1	13.1	526.8	22.7	517.2	19.8	-0.4	-2.3	529.11	13.06
G68	9.3	77.6	1.61	0.0857	0.0014	0.7002	0.0331	0.0593	0.0028	530.1	16.6	538.9	42.3	577.0	42.2	1.6	8.1	530.06	16.63
G99	35.5	389.3	0.46	0.0857	0.0011	0.6670	0.0140	0.0564	0.0012	530.2	12.8	518.9	19.5	469.7	15.3	-2.2	-12.9	530.23	12.82
G21	8.5	81.4	0.96	0.0858	0.0012	0.6921	0.0235	0.0585	0.0020	530.5	14.2	534.0	30.7	550.0	29.0	0.7	3.5	530.53	14.25
G47	54.2	542.9	0.77	0.0861	0.0011	0.6938	0.0128	0.0585	0.0010	532.5	12.6	535.1	18.0	546.7	15.0	0.5	2.6	532.49	12.58
G5	10.3	103.7	0.73	0.0866	0.0012	0.6917	0.0222	0.0580	0.0019	535.3	14.1	533.8	29.1	527.9	26.6	-0.3</			

Table 2. U-Pb zircon ages of Zanskar River sands

G34	116.9	924.6	0.36	0.1250	0.0015	1.2508	0.0211	0.0726	0.0012	759.2	17.4	823.8	22.7	1002.8	20.4	7.8	24.3	759.16	17.42
G124	102.4	853.1	0.08	0.1268	0.0016	1.1551	0.0227	0.0661	0.0012	769.8	18.3	779.6	24.6	808.3	20.9	1.3	4.8	769.81	18.31
G19	26.6	174.3	0.88	0.1270	0.0016	1.1425	0.0245	0.0653	0.0014	770.7	18.3	773.7	26.5	783.1	22.9	0.4	1.6	770.73	18.30
G45	26.5	149.0	1.49	0.1286	0.0017	1.1780	0.0280	0.0665	0.0016	779.7	19.1	790.4	29.5	821.2	26.4	1.4	5.1	779.70	19.08
G104	85.8	688.0	0.15	0.1288	0.0016	1.2679	0.0253	0.0714	0.0014	780.9	18.6	831.4	26.2	969.5	24.1	6.1	19.4	780.90	18.62
G25	48.9	343.3	0.57	0.1295	0.0016	1.1534	0.0207	0.0646	0.0011	784.7	18.0	778.8	22.9	762.6	18.4	-0.8	-2.9	784.73	18.04
G80	61.4	367.1	1.07	0.1324	0.0016	1.2141	0.0223	0.0665	0.0012	801.5	18.7	807.1	23.8	822.8	19.7	0.7	2.6	801.54	18.67
G76	241.0	1915.2	0.09	0.1327	0.0016	1.2623	0.0198	0.0690	0.0010	803.5	18.3	828.9	21.4	898.1	17.3	3.1	10.5	803.48	18.32
G84	27.6	168.2	0.92	0.1363	0.0018	1.1931	0.0279	0.0635	0.0015	823.5	20.0	797.4	29.1	725.4	23.8	-3.3	-13.5	823.54	19.97
G125	56.3	388.6	0.34	0.1400	0.0018	1.2950	0.0250	0.0671	0.0012	844.5	19.9	843.5	25.6	841.5	21.1	-0.1	-0.4	844.49	19.91
G118	51.2	363.2	0.34	0.1407	0.0018	1.3756	0.0286	0.0709	0.0014	848.8	20.2	878.6	27.9	954.5	24.8	3.4	11.1	848.85	20.23
G113	68.1	462.3	0.36	0.1426	0.0018	1.3657	0.0257	0.0695	0.0012	859.1	20.1	874.3	25.5	913.3	21.5	1.7	5.9	859.12	20.09
G81	61.1	182.0	4.25	0.1428	0.0018	1.4442	0.0316	0.0734	0.0016	860.6	20.8	907.4	30.0	1023.6	27.6	5.2	15.9	860.65	20.76
G30	57.4	291.0	1.19	0.1530	0.0019	1.4307	0.0276	0.0678	0.0013	917.9	21.2	901.8	26.9	863.4	21.8	-1.8	-6.3	863.36	21.78
G59	151.8	1052.8	0.22	0.1454	0.0018	1.4739	0.0244	0.0735	0.0012	875.4	19.9	919.7	24.0	1028.0	20.2	4.8	14.9	875.35	19.92
G37	13.9	90.6	0.42	0.1458	0.0020	1.5308	0.0399	0.0762	0.0020	877.3	22.3	942.8	36.2	1099.5	35.1	6.9	20.2	877.32	22.28
G94	35.9	193.5	0.96	0.1517	0.0019	1.4289	0.0295	0.0683	0.0014	910.3	21.5	901.1	28.3	878.9	23.6	-1.0	-3.6	878.88	23.58
G91	100.9	709.5	0.15	0.1462	0.0018	1.3662	0.0232	0.0678	0.0011	879.6	20.1	874.5	23.6	862.1	18.5	-0.6	-2.0	879.63	20.13
G122	76.2	505.3	0.31	0.1470	0.0019	1.3818	0.0292	0.0682	0.0014	884.1	21.1	881.2	28.4	874.6	23.9	-0.3	-1.1	884.07	21.13
G18	164.0	1133.4	0.19	0.1484	0.0018	1.5818	0.0255	0.0773	0.0012	892.2	20.1	963.1	24.2	1129.2	20.8	7.4	21.0	892.21	20.10
G127	36.9	228.1	0.51	0.1497	0.0019	1.3858	0.0304	0.0672	0.0014	899.1	21.6	882.9	29.4	843.0	24.4	-1.8	-6.7	899.11	21.64
G116	99.4	698.8	0.08	0.1497	0.0019	1.4224	0.0261	0.0689	0.0012	899.5	20.9	898.4	25.5	896.0	20.7	-0.1	-0.4	899.51	20.86
G56	33.1	167.4	0.91	0.1637	0.0021	1.5604	0.0335	0.0691	0.0015	977.5	23.2	954.6	30.4	902.6	25.1	-2.4	-8.3	902.62	25.08
G27	97.5	626.6	0.34	0.1509	0.0018	1.4404	0.0226	0.0693	0.0010	905.8	20.3	905.9	22.8	906.5	17.7	0.0	0.1	906.49	17.66
G110	28.7	183.5	0.26	0.1551	0.0020	1.4858	0.0335	0.0695	0.0015	929.4	22.4	924.6	31.0	913.6	26.5	-0.5	-1.7	913.62	26.53
G85	107.4	724.1	0.08	0.1559	0.0019	1.4997	0.0248	0.0698	0.0011	934.0	21.2	930.3	24.0	921.9	18.8	-0.4	-1.3	921.89	18.75
G101	130.5	672.7	1.00	0.1558	0.0019	1.5024	0.0259	0.0700	0.0011	933.4	21.4	931.3	24.8	926.9	19.6	-0.2	-0.7	926.89	19.64
G36	83.4	534.5	0.18	0.1593	0.0019	1.5413	0.0265	0.0702	0.0011	952.9	21.6	947.0	25.0	933.9	19.8	-0.6	-2.0	933.92	19.84
G16	49.7	273.4	0.79	0.1556	0.0019	1.5060	0.0269	0.0702	0.0012	932.4	21.2	932.8	25.6	934.5	20.9	0.0	0.2	934.50	20.88
G82	46.8	241.9	0.84	0.1625	0.0021	1.5767	0.0313	0.0704	0.0014	970.8	22.7	961.1	28.5	939.5	23.5	-1.0	-3.3	939.46	23.51
G87	43.3	251.9	0.51	0.1583	0.0020	1.5378	0.0291	0.0705	0.0013	947.3	22.0	945.6	27.1	942.1	22.3	-0.2	-0.6	942.08	22.30
G12	131.5	793.3	0.49	0.1537	0.0018	1.4930	0.0226	0.0705	0.0010	921.4	20.5	927.5	22.4	943.0	17.3	0.7	2.3	942.95	17.25
G121	22.1	237.3	1.57	0.1502	0.0019	1.4660	0.0299	0.0708	0.0014	902.1	21.4	916.5	28.2	951.6	24.3	1.6	5.2	951.64	24.25
G67	45.9	273.4	0.36	0.1621	0.0020	1.5816	0.0291	0.0708	0.0013	968.2	22.3	963.0	26.8	951.6	21.8	-0.5	-1.7	951.64	21.81
G123	70.4	443.9	0.27	0.1560	0.0020	1.5235	0.0286	0.0708	0.0013	934.6	21.7	939.9	26.7	952.8	22.0	0.6	1.9	952.80	21.99
G120	26.4	138.2	0.87	0.1580	0.0021	1.5432	0.0348	0.0708	0.0016	945.8	22.8	947.8	31.5	952.8	27.2	0.2	0.7	952.80	27.22
G105	43.0	235.7	0.83	0.1549	0.0020	1.5149	0.0348	0.0710	0.0016	928.1	22.6	936.4	31.9	956.3	27.9	0.9	2.9	956.26	27.93
G52	147.1	963.7	0.17	0.1578	0.0019	1.5538	0.0247	0.0714	0.0011	944.4	21.3	952.0	23.7	970.0	18.5	0.8	2.6	970.03	18.54
G44	143.8	712.6	0.97	0.1663	0.0020	1.6387	0.0281	0.0715	0.0012	991.9	22.4	985.2	25.6	970.9	20.3	-0.7	-2.2	970.89	20.29
G41	52.7	291.8	0.53	0.1658	0.0021	1.6350	0.0301	0.0716	0.0013	988.8	22.7	983.8	27.3	973.2	22.2	-0.5	-1.6	973.17	22.22
G106	49.9	278.0	0.35	0.1726	0.0022	1.7052	0.0325	0.0717	0.0013	1026.5	23.7	1010.5	28.2	976.3	22.8	-1.6	-5.1	976.30	22.76
G39	77.9	452.3	0.46	0.1607	0.0020	1.5912	0.0262	0.0718	0.0011	960.7	21.7	966.8	24.5	981.1	19.4	0.6	2.1	981.13	19.44
G3	83.4	460.0	1.04	0.1529	0.0019	1.5192	0.0268	0.0721	0.0012	917.4	20.8	938.2	25.5	987.9	21.4	2.2	7.1	987.92	21.38
G62	29.4	133.6	1.05	0.1768	0.0023	1.7563	0.0412	0.0721	0.0017	1049.4	25.3	1029.5	34.4	987.9	29.3	-1.9	-6.2	987.92	29.27
G7	115.3	653.5	0.41	0.1675	0.0020	1.6643	0.0270	0.0721	0.0011	998.4	22.3	995.0	24.7	988.5	19.3	-0.3	-1.0	988.48	19.28
G20	101.5	411.6	1.87	0.1649	0.0020	1.6444	0.0297	0.0724	0.0013	983.9	22.4	987.4	26.7	995.8	21.9	0.4	1.2	995.80	21.93
G66	182.5	943.0	0.96	0.1641	0.0020	1.6366	0.0264	0.0724	0.0011	979.2	22.0	984.4	24.4	996.4	19.1	0.5	1.7	996.36	19.12
G107	37.2	216.6	0.66	0.1505	0.0019	1.5044	0.0327	0.0725	0.0015	904.0	21.7	932.2	30.2	1000.0	26.8	3.0	9.6	1000.01	26.85
G31	69.3	364.8	0.54	0.1738	0.0021	1.7390	0.0289	0.0726	0.0011	1032.7	23.2	1023.1	25.6	1003.1	20.0	-0.9	-3.0	1003.09	20.01
G51	108.5	497.6	1.12	0.1724	0.0021	1.7316	0.0282	0.0729	0.0011	1025.3	23.0	1020.4	25.1	1010.1	19.5	-0.5	-1.5	1010.06	19.50
G29	24.1	98.3	1.64	0.1725	0.0023	1.7337	0.0438	0.0729	0.0018	1025.9	25.2	1021.1	36.6	1011.5	32.1	-0.5	-1.4	1011.45	32.15
G77	73.8	357.1	0.70	0.1798	0.0022	1.8434	0.0318	0.0744	0.0012	1065.6	24.2	1061.1	26.8	1052.3	21.3	-0.4	-1.3	1052.34	21.31
G8	35.4	164.3	0.61	0.1938	0.0024	1.9992	0.0406	0.0749	0.0015	1141.8	26.4	1115.3	31.7	1064.7	26.1	-2.4	-7.2	1064.75	26.08
G55	75.1	370.1	0.73	0.1783	0.0022	1.8444	0.0310	0.0750	0.0012	1057.8	23.9	1061.4	26.4	1069.3	21.0	0.3	1.1	1069.31	20.97
G46	98.4	452.3	0.90	0.1806	0.0022	1.8752	0.0303	0.0753	0.0011	1									

Table 2. U-Pb zircon ages of Zanskar River sands

G111	27.0	134.4	0.50	0.1855	0.0026	2.0089	0.0563	0.0785	0.0022	1097.1	28.3	1118.5	42.5	1160.6	38.7	1.9	5.5	1160.57	38.75
G86	203.1	1024.4	0.38	0.1887	0.0023	2.1177	0.0335	0.0814	0.0012	1114.2	24.8	1154.6	26.2	1231.6	20.9	3.5	9.5	1231.60	20.86
G79	91.7	401.6	0.46	0.2119	0.0026	2.4000	0.0396	0.0822	0.0013	1239.0	27.6	1242.6	28.3	1249.1	22.2	0.3	0.8	1249.09	22.22
G73	45.0	177.4	0.79	0.2156	0.0027	2.4879	0.0453	0.0837	0.0015	1258.6	28.5	1268.5	31.1	1285.8	25.4	0.8	2.1	1285.82	25.44
G70	114.0	479.2	0.81	0.2078	0.0026	2.4506	0.0409	0.0856	0.0013	1216.9	27.2	1257.6	28.7	1328.3	23.2	3.2	8.4	1328.26	23.21
G64	32.8	121.3	0.51	0.2473	0.0034	3.0444	0.0766	0.0893	0.0022	1424.3	35.0	1418.8	43.7	1411.0	38.2	-0.4	-0.9	1411.03	38.24
G6	204.3	746.4	0.51	0.2497	0.0030	3.0911	0.0445	0.0898	0.0012	1436.7	30.5	1430.5	27.3	1421.9	20.3	-0.4	-1.0	1421.92	20.27
G23	87.6	289.5	1.11	0.2375	0.0030	2.9763	0.0558	0.0909	0.0017	1373.6	31.0	1401.6	33.5	1444.9	28.0	2.0	4.9	1444.93	27.97
G72	176.7	661.2	0.40	0.2502	0.0030	3.1856	0.0492	0.0924	0.0013	1439.2	31.2	1453.7	29.0	1475.2	22.2	1.0	2.4	1475.21	22.23
G115	126.0	418.5	1.03	0.2384	0.0030	3.0566	0.0537	0.0930	0.0015	1378.5	30.8	1421.9	31.7	1487.9	25.9	3.1	7.4	1487.89	25.86
G102	335.8	1560.4	0.02	0.2287	0.0028	2.9948	0.0492	0.0950	0.0015	1327.7	29.4	1406.3	29.9	1527.9	24.3	5.6	13.1	1527.88	24.28
G71	177.4	566.7	1.47	0.2350	0.0029	3.1047	0.0495	0.0958	0.0014	1360.7	29.9	1433.8	29.6	1544.4	23.7	5.1	11.9	1544.44	23.68
G42	180.2	530.6	0.83	0.2832	0.0034	3.8334	0.0582	0.0982	0.0014	1607.5	34.3	1599.8	29.8	1590.0	22.6	-0.5	-1.1	1590.03	22.58
G83	95.7	293.3	0.44	0.3002	0.0037	4.1006	0.0708	0.0991	0.0016	1692.4	37.0	1654.4	33.5	1606.9	26.4	-2.3	-5.3	1606.87	26.38
G61	59.3	179.7	0.37	0.3094	0.0038	4.3059	0.0722	0.1010	0.0016	1737.6	37.5	1694.5	33.1	1642.0	25.8	-2.5	-5.8	1642.02	25.79
G28	234.9	788.6	0.19	0.2944	0.0035	4.1503	0.0593	0.1023	0.0013	1663.6	35.0	1664.3	29.0	1665.7	21.4	0.0	0.1	1665.72	21.45
G63	71.4	197.4	0.56	0.3214	0.0040	4.6545	0.0806	0.1051	0.0017	1796.6	39.0	1759.1	34.5	1715.4	27.3	-2.1	-4.7	1715.37	27.27
G60	84.2	209.6	0.66	0.3468	0.0043	5.4410	0.0921	0.1138	0.0018	1919.1	41.3	1891.3	34.7	1861.4	27.3	-1.5	-3.1	1861.44	27.28
G112	56.3	104.4	0.62	0.4575	0.0058	9.9137	0.1754	0.1572	0.0026	2428.6	51.1	2426.8	38.7	2425.7	30.9	-0.1	-0.1	2425.66	30.86
G14	55.2	102.9	0.85	0.4380	0.0056	9.5908	0.1659	0.1589	0.0026	2341.7	50.1	2396.3	38.5	2443.7	30.7	2.3	4.2	2443.67	30.70
G69	183.4	316.4	0.73	0.4763	0.0058	10.7227	0.1620	0.1633	0.0023	2511.0	50.5	2499.4	34.3	2490.3	25.8	-0.5	-0.8	2490.32	25.80
G22	29.3	49.1	1.14	0.4521	0.0061	10.1879	0.2008	0.1635	0.0032	2404.7	54.2	2452.0	43.6	2492.0	35.9	1.9	3.5	2491.97	35.88
G97	308.3	698.8	0.21	0.4270	0.0052	9.6971	0.1563	0.1647	0.0025	2292.2	47.3	2406.4	35.7	2504.9	27.9	4.7	8.5	2504.90	27.86
G88	288.3	592.1	0.13	0.4702	0.0058	11.2336	0.1770	0.1733	0.0025	2484.6	50.4	2542.7	35.5	2589.8	27.3	2.3	4.1	2589.77	27.33
G2	115.8	227.3	0.40	0.4614	0.0056	11.1037	0.1683	0.1746	0.0025	2445.9	49.7	2531.9	34.9	2602.2	26.6	3.4	6.0	2602.23	26.62
G57	662.4	1496.7	0.13	0.4386	0.0053	10.8791	0.1575	0.1799	0.0024	2344.5	47.1	2512.8	33.2	2652.1	24.9	6.7	11.6	2652.13	24.89
G96	340.5	548.3	0.58	0.5217	0.0064	13.3752	0.2097	0.1860	0.0027	2706.4	53.9	2706.5	35.7	2706.9	27.3	0.0	0.0	2706.93	27.33
G109	466.5	743.3	0.20	0.5702	0.0070	16.7444	0.2716	0.2130	0.0032	2908.7	57.3	2920.3	37.1	2928.7	28.8	0.4	0.7	2928.66	28.80
G10	104.4	132.8	0.49	0.6405	0.0077	21.9196	0.3134	0.2483	0.0033	3191.1	60.8	3180.2	34.7	3173.8	25.6	-0.3	-0.5	3173.83	25.57
G43	51.1	59.9	0.87	0.6522	0.0082	23.6625	0.3635	0.2632	0.0038	3236.8	63.6	3254.6	37.0	3266.0	27.9	0.5	0.9	3265.96	27.92
G98	72.0	556.0	0.69	0.7271	0.0089	30.5792	0.4819	0.3051	0.0044	3522.7	66.4	3505.6	37.4	3496.2	28.6	-0.5	-0.8	3496.16	28.61
G48	8.4	81.4	1.31	0.0771	0.0012	0.6959	0.0292	0.0655	0.0028	478.7	14.5	536.3	37.8	790.1	46.8	10.7	39.4	478.73	14.48
G117	114.8	1451.4	0.26	0.0792	0.0010	0.7196	0.0133	0.0659	0.0012	491.2	11.7	550.4	18.2	804.2	19.4	10.8	38.9	491.23	11.71
G126	84.5	584.4	0.46	0.1401	0.0018	1.6435	0.0301	0.0851	0.0015	845.4	19.8	987.0	27.0	1317.4	25.7	14.4	35.8	845.40	19.79
G75	32.7	246.5	0.51	0.1264	0.0016	1.0584	0.0234	0.0607	0.0013	767.3	18.4	733.0	26.2	630.0	20.2	-4.7	-21.8	767.30	18.43

TABLES

Table 1. Sample locations for Zanskar River sediments.

Table 2. Bulk petrography of Zanskar River sediments.

Table 3. Major and trace element geochemistry of Zanskar River sediments.

Table 4. Nd and Sr isotope geochemistry of Zanskar River sediments.

Table S1. U-Pb zircon ages of Zanskar River sediments.